Myelin is remodeled cell-autonomously by oligodendroglial macroautophagy

Etan Aber

Submitted in partial fulfillment of the
requirements for the degree of
Doctor of Philosophy
under the Executive Committee
of the Graduate School of Arts and Sciences

COLUMBIA UNIVERSITY

2018

ABSTRACT

Myelin is remodeled cell-autonomously by oligodendroglial macroautophagy

Etan Aber

Myelination of axons in the CNS by oligodendrocytes (OLs) is critical for the rapid and reliable conduction of action potentials down neuronal axons, as evidenced by the severe disabilities associated with myelin loss in multiple sclerosis and other diseases of myelin. The specification, differentiation, and maturation of OLs along with myelin formation by OLs have been thoroughly characterized. How myelin is turned over, however remains unclear.

It is unsurprising that little is known about myelin turnover considering that for decades following their discovery, myelin and OLs were considered static elements in the adult nervous system. Recent evidence, however, shows that myelin in the CNS is actually plastic. Moreover, myelin remodeling in humans has been suggested to be mediated by mature OLs. As mature OLs have limited capacity to generate new myelin sheaths, we must ask whether mature OLs can remodel the myelin at preexisting myelin sheaths. One intriguing but unproven possibility is that myelin at individual internodes may be remodeled cell-autonomously by mature OLs to modulate neuronal circuit function.

Macroautophagy (MA) is responsible for the lysosome-mediated elimination of cytosolic proteins, lipids, and organelles. MA achieves this by capturing cargo in bulk or selectively in a transient, multilamellar structure known as an autophagosome (AP). In this study, we used a combination of *in vivo* and cellular approaches to test the hypothesis that MA in OLs may be important for myelin remodeling in the adult CNS.

We establish that myelin of individual internodes is remodeled, and does so through the coordinated efforts of endocytosis and MA. We found that autophagy protein Atg7 is essential for myelin remodeling *in vivo:* loss of Atg7 in OLs leads to an age-dependent increase of myelin at the internode and the formation of aberrant myelin structures, most notably myelin outfoldings. In addition, we find that MA has the potential to occur throughout the mature OL, and examination of OLs in culture suggests that formation of a mature AP structure, the amphisome, is required to facilitate the efficient degradation of myelin-containing endocytic structures. Together, we propose that myelin is a dynamic structure that is regularly remodeled through the cooperative efforts of MA and endocytosis. These findings raise the possibility that myelin remodeling is involved in neural plasticity and the tuning of neural circuits.

Table of Contents

List of Figures

Chapter 1

Chapter 2

Chapter 3

Acknowledgments

I would like to begin by thanking my advisor, Dr. Ai Yamamoto, for being a far better mentor than I could have ever imagined was possible. Nothing presented here would have been remotely close to possible without her fantastic guidance and mentorship. I have learned so many invaluable lessons from the endless hours of meetings, presentation rehearsals, casual conversations, and other time together. Ai's enormous breadth of knowledge and tireless passion for her work is just inspiring. Ai has always pushed me to improve and ingrained in me an unflagging perseverance in the face of adversity. Perhaps most of all, I would like to thank Ai for always making science fun and making fun of everything else.

I'd like to thank my thesis committee members, Drs. James Goldman, Clarissa Waites, and Dritan Agalliu, for thoughtful discussions and suggestions that helped to shape this project. I would like to an extend a special thanks to Dr. Brain Popko for serving as outside examiner.

I also thank Tim Davies, Julie Canman, Kristy Brown, Thong Ma, Youngjoo Yang, Julian Smith, and Dritan Agalliu for their contributions to this work. I'd also like to thank the members of the Yamamoto lab for their friendship and guidance throughout my doctoral work.

I am also grateful for my wonderful classmates in the Columbia MD-PhD program, who have been with me through the best and worst of times. Thanks for planning so many wonderful brunches (I wish I had been at more of them) and thanks for always commiserating with me. Most of all, thanks for being my community throughout this otherwise isolating process.

I'd also like to thank my parents for their unconditional love and support. They have always urged me to pursue my passions and do the things I love. I greatly appreciate their constant encouragement to give everything 110% and for sharing with me a love for science and a thirst for knowledge. They also gave me an extraordinary older brother, Daniel, who always pushed me to

try to keep up with him. I also credit him for my impeccable sense of humor. I would also like to thank my parents-in-law, for always being so caring and supportive.

To Katie, my awesome and loving wife, thank you for always being the best part of my day. Thank you for keeping me sane and happy for all these years. Thank you for hanging out in lab with me on so many nights and weekends. I will always have fond memories of immunopanning until 3 AM with you. Being with you makes doing the mundane absolutely sublime.

Lastly, I would like to thank the many teachers and friends who have influenced me in too many ways to count. Thank you all very much.

Chapter 1.

Oligodendrocyte Biology

1.1 Introduction

The functions of the CNS ranging from essential biological functions like breathing to higher order functions like thought and introspection are achieved by the coordinated efforts of highly specified cell types, including the well-studied neurons, and a lesser-studied broad class of cells known as glia. Glia make up the majority of the cells in the brain, but until recently they were understood to be passive supporting players of the CNS (Azevedo et al., 2009; Baumann and Pham-Dinh, 2001). In recent years, it has become increasingly clear that glia not only perform many other essential tasks, including facilitating the development, operation, and modification of neural circuitry, but are active players in these functions.

There are several glial cell types that are identified by their morphology, location, and function. In mammals, glia include astrocytes, microglia, NG2 cells (also known as oligodendrocyte progenitor cells (OPCs)), and oligodendrocytes (OLs) (Zuchero and Barres, 2015). OLs, and the related Schwann cells of the peripheral nervous system, ensure rapid and

reliable electrical neural communication (Zuchero and Barres, 2015). OLs and Schwann cells achieve this by ensheathing axons with a lipid-rich membrane called myelin, which decreases capacitance and increases resistance of the axonal membrane, thereby speeding up the conduction of action potentials (Castelfranco and Hartline, 2015) (Figure 1.1). Given that the conduction

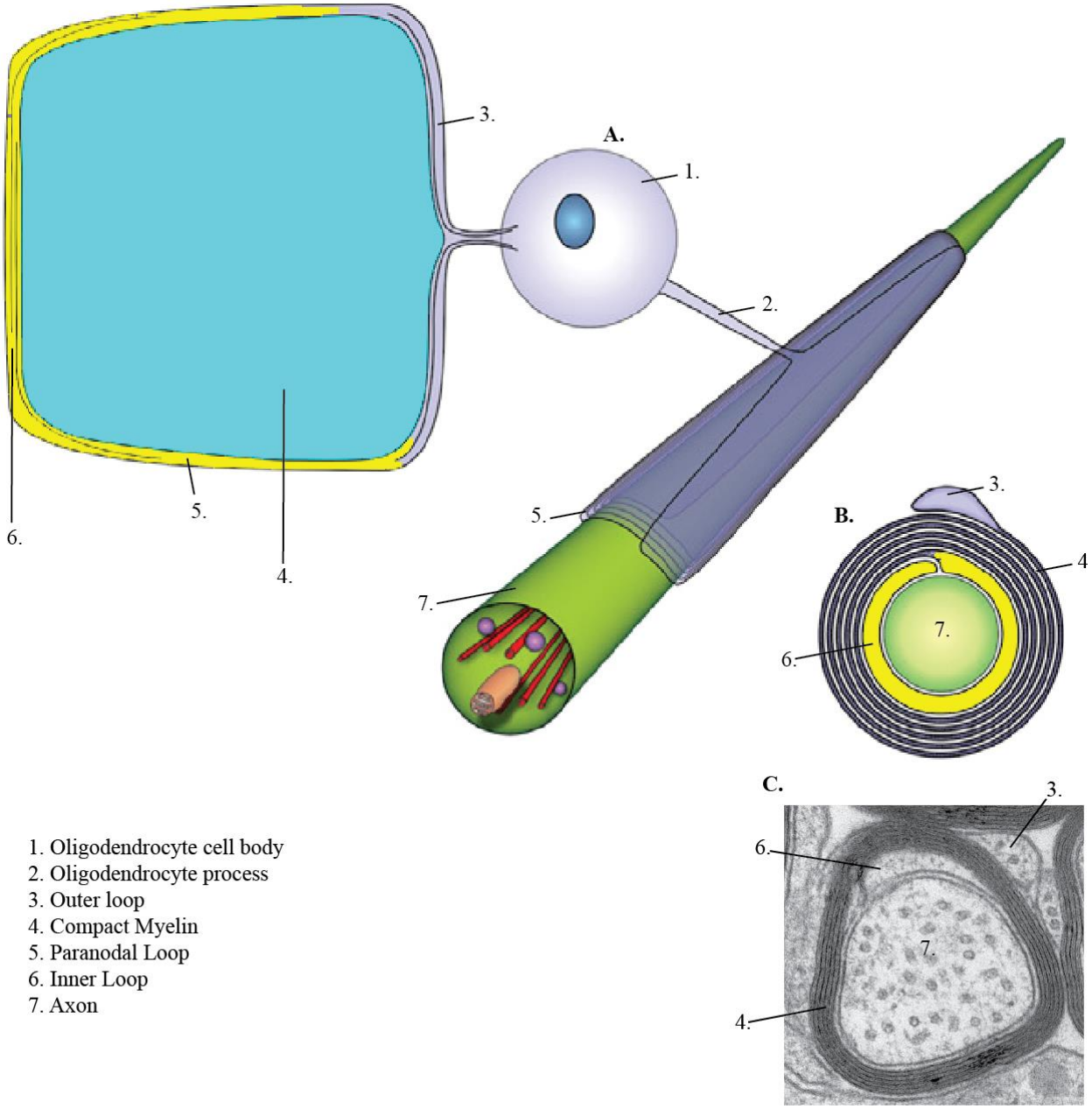

Figure 1.1 Morphology of the Myelin Sheath. Adapted from (Snaidero and Simons, 2014).
A. Schematic of an oligodendrocyte with one myelin sheath wrapped around an axon and another unrolled myelin sheath.
B. Schematic of a cross section of an axon.
C. Electron micrograph of a cross section of an axon.

velocity of an unmyelinated axon is directly proportional to its diameter, myelin permits the maintenance of conduction velocity in larger animals without an untenable increase in axon diameter and energy expenditure, ultimately enabling rapid thought and action (Morell and Quarles, 1999). For example, an unmyelinated giant squid axon requires a diameter of about 500 μm to conduct at a speed of 25 m/s, whereas a myelinated mammalian axon can achieve the same speed with a diameter of about 5 μm while using 5000 times less energy (Hursh, 1939; Morell and Quarles, 1999). To further enhance conduction velocity, OLs and neurons have co-evolved to form structures known as nodes of Ranvier , in which ion channels cluster between myelin sheaths (also known as internodes).

In addition to facilitating rapid and reliable conduction of action potentials, OLs are also necessary to maintain axonal integrity. Not only does the loss of myelin cause severe axonal pathology, but myelin lacking core proteins such as myelin proteolipid protein (PLP) or 2',3'-cyclic-nucleotide 3'-phosphodiesterase (CNP), as well as insults to the myelin sheath, can lead to axonal degeneration as well (DeBoy et al., 2007; Edgar et al., 2009; Griffiths et al., 1998; Hoflich et al., 2016; Lappe-Siefke et al., 2003; Rasband et al., 2005). It is well established that OLs provide trophic support that is essential to axonal survival (Fruhbeis et al., 2013; Lappe-Siefke et al., 2003; Rasband et al., 2005; Wilkins et al., 2003), but recent studies indicate that OLs also actively provide axons with metabolic support (Funfschilling et al., 2012; Lee et al., 2012). Mature OLs use aerobic glycolysis, which generates lactate and pyruvate, as their primary energy source (Funfschilling et al., 2012). The lactate generated in OLs is then shuttled via the monocarboxylate transporter MCT1 on the myelin sheath to the underlying axon as an essential source of metabolic support (Lee et al., 2012). Channels of cytoplasm that run throughout the myelin sheath known as

intramyelinic cytoplasmic nanochannels have been suggested to be essential for this process (Lappe-Siefke et al., 2003; Snaidero et al., 2017).

1.2 Oligodendrocyte Development

1.2.1 Introduction

Myelination of the CNS is a complex yet elegant process. It begins with the specification of OPCs, which proliferate, migrate and ultimately differentiate into oligodendrocytes. During differentiation and maturation, the cell extends many processes that sample the environment and interact with axons and—upon stabilization of the nascent myelin sheath—synthesize and traffic membrane to facilitate wrapping and compaction of the myelin sheath along with the establishment of axo-glial junctions. Perturbations in myelin development during fetal and early postnatal life cause a variety of leukodystrophies including Canavan, Krabbe, and Pelizaues-Merzbacher diseases, which can manifest in infancy with gradual loss of movement and delayed mental and motor development. In adults, damage to myelin disrupts proper neural function, as evidenced by traumatic CNS injuries and autoimmune diseases like multiple sclerosis. Moreover, white matter deficits are also found throughout a wide array of neurodevelopmental and neurodegenerative disorders (reviewed in (Fields, 2008)).

1.2.2 Extrinsic cues driving OL differentiation

In mice, generation of OLs begins with the specification of OPCs during late embryonic gestation, beginning at E12.5 in the ventral ventricular zone of the spinal cord (pMN domain), followed by a second wave from the dorsal Dbx1-expressing ventricular zone shortly thereafter

(Cai et al., 2005; Fogarty et al., 2005; Lu et al., 2002; Tekki-Kessaris et al., 2001; Vallstedt et al., 2005; Warf et al., 1991) (Figure 1.2). In humans, OPCs first appear at about 45 days post-conception (Hajihosseini et al., 1996). Within a few days of their appearance, OPCs proliferate and distribute themselves evenly throughout the gray and white matter of the developing spinal cord (Pringle and Richardson, 1993). About 80% of OPCs in the postnatal spinal cord of mice are ventrally derived, whereas the remaining 20% originate from the dorsal cord (Tripathi et al., 2011). OPCs are identified by their expression of platelet-derived growth factor alpha (PDGFα) and chondroitin sulfate proteoglycan 4, also known as neuron-glial antigen 2 (NG2) (Figure 1.3). These OPC markers are down-regulated during OPC differentiation, making these markers specific to this stage of the oligodendroglial lineage.

OPC specification in the brain is quite similar to that in the developing spinal cord. In forebrain, OPCs are first produced from the ventral medial ganglionic eminence, but as development progresses they originate from the lateral and caudal ganglionic eminences as well as from the cortex (Kessaris et al., 2006). These highly proliferative OPCs—with a cell cycle time of just six hours in the embryo—migrate along the vasculature to populate the entire brain before

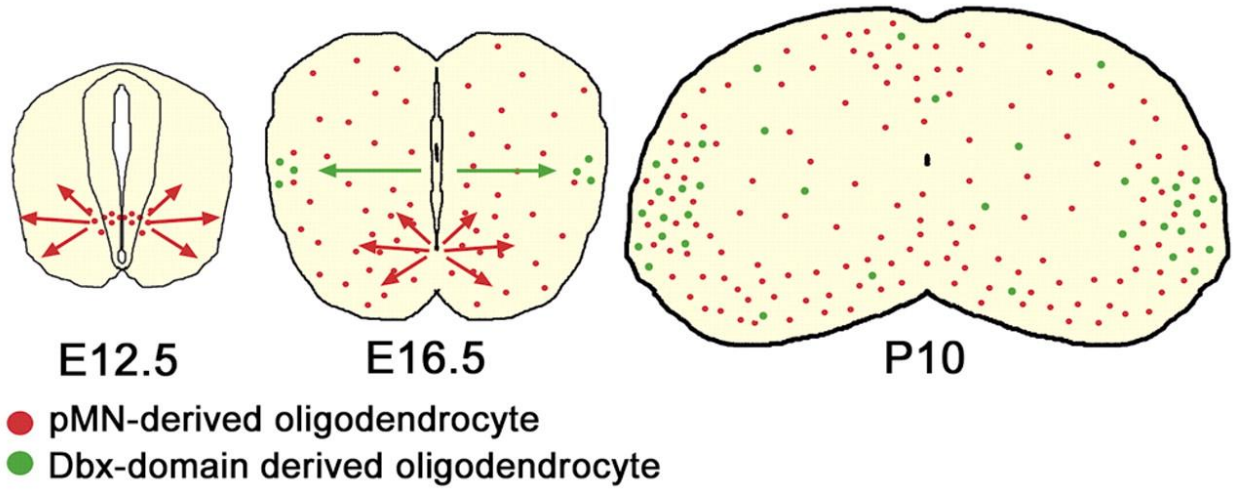

Figure 1.2 The origins of oligodendrocytes in spinal cord. Adapted from (Fogarty et al., 2005).
Starting at E12.5 in the mouse spinal cord, OPCs are generated from the pMN domain in the ventral ventricular zone. A few days later, another population emerges from radial glia in a dorsal Dbx1-expressing domain.

birth (Calver et al., 1998; Pringle et al., 1992; Tsai et al., 2016). Interestingly, unlike in spinal cord, only about 20% of OPCs in the corpus callosum are ventrally derived, whereas the remaining 80% originate dorsally (Tripathi et al., 2011).

PDGF is an important mitogen for OPCs that is produced by astrocytes and neurons to regulate OPC proliferation and survival (Noble et al., 1988; Raff et al., 1988; Richardson et al., 1988). Another factor known to induce the proliferation of OPCs is neuronal activity, but whether this is mediated by PDGF or other mitogens remains unknown (Barres and Raff, 1993; Gibson et al., 2014). Alternatively, as OPCs receive synaptic input from neurons, it is possible that neuronal activity may regulate OPC proliferation and differentiation in this way (Bergles et al., 2000; De Biase et al., 2010; Kukley et al., 2007; Mangin et al., 2012; Ziskin et al., 2007). Interestingly, although OPC proliferation and survival are dependent upon axonal signaling, OPC specification and migration are not (Almeida and Lyons, 2016).

Progression from an OPC through a premyelinating stage to a mature myelinating OL is controlled by a broad array of extrinsic and intrinsic cues, including growth factors, extracellular

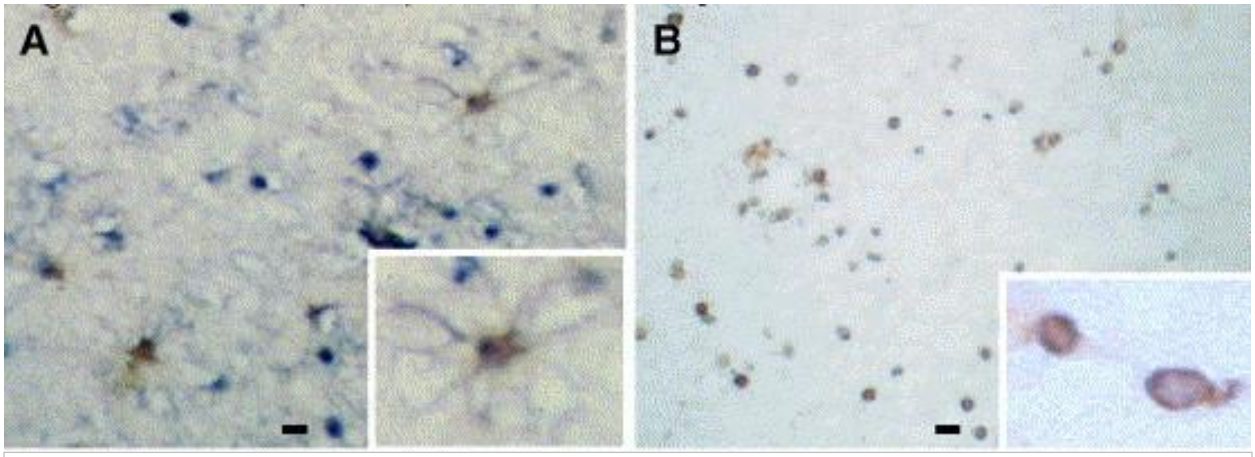

Figure 1.3 PDGFαR+ cells co-express NG2 protein and mRNA. Adapted from (Wilson et al., 2006).
A. Immunostaining of frozen human tissue for PDGFαR (brown) and NG2 (blue) reveals a population of cells expressing both PDGFαR and NG2.
B. In situ hybridization for NG2 mRNA (blue) and co-stained for PDGFαR (brown) identify cells that express NG2 mRNA and PDGFαR protein.

matrix composition, transcription factors, and histone modifications. These cues tightly regulate both the temporal and spatial properties of myelination during development throughout the CNS. Oligodendroglial specification is in part determined by the relative levels of Bone Morphogenic Protein (BMP), Sonic Hedgehog (Shh), and Wnt/β-catenin. In the developing spinal cord, the oligodendrocyte transcription factor 2 (Olig2)-expressing pMN domain first produces motor neurons and then switchs to generating OPCs (Cai et al., 2005). Olig2 eventually specifies the OL lineage as it is downregulated during neuronal differentiation.. This transition from motor neuron to OPC production is dependent on Shh levels, which are regulated by heparan sulfate distribution and the Notch signaling pathway (Dessaud et al., 2010; Kim et al., 2008; Park and Appel, 2003; Touahri et al., 2012): The inhibition of Notch signaling prevents OPC specification, and constitutive Notch signaling drives excess OPC formation (Kim et al., 2008; Park and Appel, 2003; Zaucker et al., 2013). This may be particularly relevant to cerebral autosomal dominant arteriopathy with subcortical infarcts and leukoencephalopathy (CADASIL syndrome), which is caused by mutations in the human *NOTCH3* gene (Ducros et al., 1996; Herve and Chabriat, 2010; Zaucker et al., 2013). In addition to OPC production, Notch signaling may contribute to OL differentiation as well (Hu et al., 2003; Wang et al., 1998). The transition to OL formation is also affected by Wnt and BMP, which inhibit OPC specification in the dorsal spinal cord (See and Grinspan, 2009).

Similar to the spinal cord, Shh stimulates the generation of OPCs in the ventral forebrain through the induction of Olig1 and Olig2 expression (Nery et al., 2001; Tekki-Kessaris et al., 2001). While Wnt signaling may inhibit OPC specification in the spinal cord, Wnt3 actually promotes oligodendroglial specification in the subependymal zone of the brain (Ortega et al., 2013). In addition, epidermal growth factor (EGF) signaling also increases OPC generation

(Cantarella et al., 2008; Gonzalez-Perez and Alvarez-Buylla, 2011), along with fibroblast growth factor (FGF) signaling through FGF receptor (FGFR)-1 and -2, in possible cooperation with Shh signaling (Furusho et al., 2011). Although FGF signaling does not contribute to OPC proliferation, FGF signaling *in vivo* is also important for myelination and may regulate myelin sheath thickness (Furusho et al., 2012)..

OL development is also affected by a variety of signals associated with the extracellular matrix (ECM) as well as cues secreted by blood vessels. For example, laminin is one of the most important ECM proteins that regulates the generation of OLs: Deletion of the α2-subunit of laminin in mice causes a significant reduction in OPC production in the subventricular zone, leading to reduced numbers of OPCs in the corpus callosum (Relucio et al., 2012). It has also been shown that the endothelial cells of blood vessels in the CNS can promote OPC specification; in culture, this was found to be mediated by the release of the chemokine CCL2/MCP1 (Chintawar et al., 2009; Plane et al., 2010).

1.2.3 Transcriptional regulation of OL differentiation.

Although much is known about how environmental cues determine the regions of the CNS that will produce OLs, the regulation of OL specification is best understood in the context of transcription and epigenetic factors (Figure 1.4). Olig2 is a basic helix-loop-helix transcription factor expressed throughout the OL lineage, from OPCs to mature myelinating OLs. Olig2 is stimulated by ventrally-derived Shh in the spinal cord and is the most thoroughly characterized transcription factor involved in OL development (Lu et al., 2000; Takebayashi et al., 2000; Zhou et al., 2000). Loss of Olig2 during development suppresses OPC generation, whereas induction of Olig2 expression leads to increased OPC production in the CNS (Ligon et al., 2006; Lu et al.,

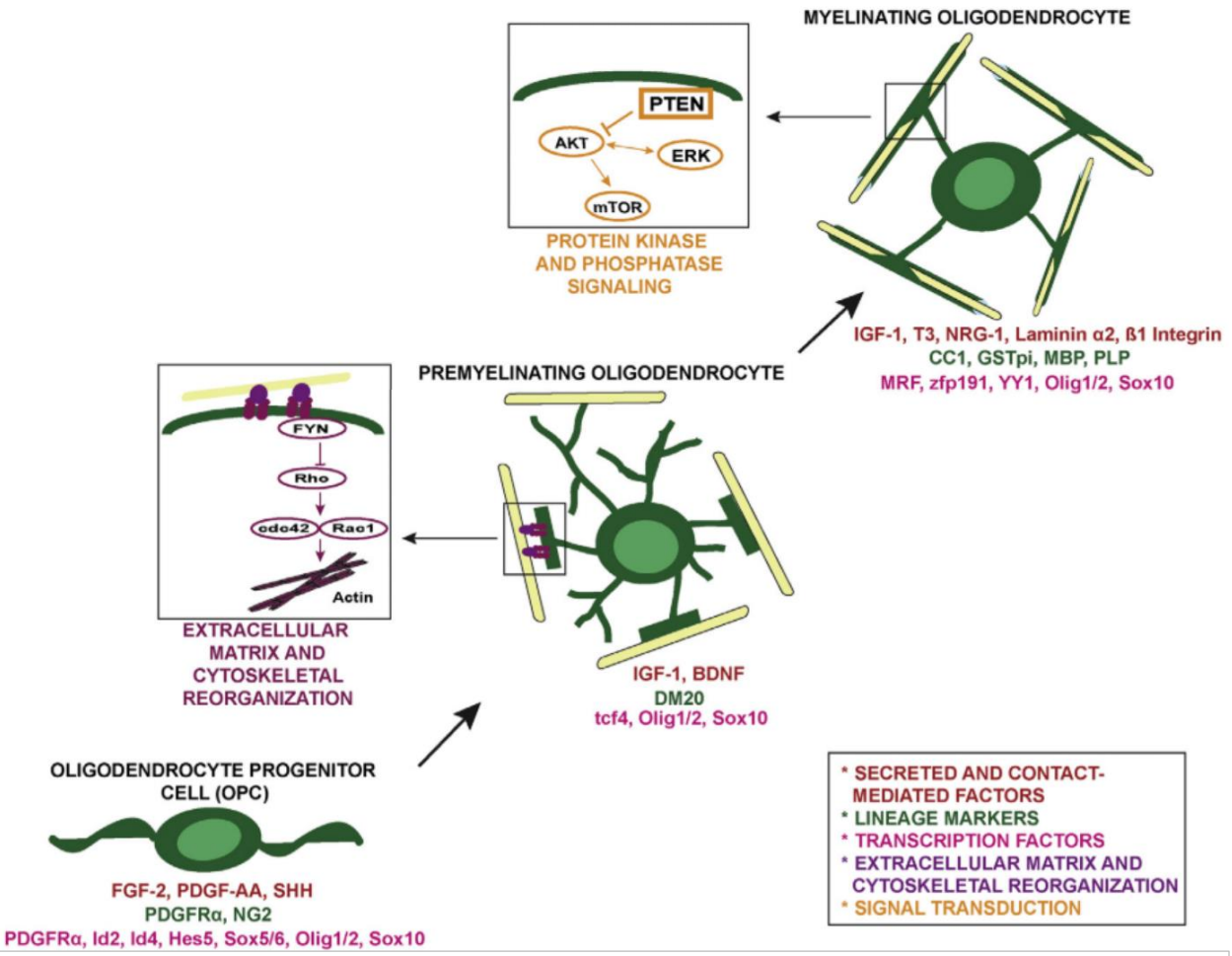

Figure 1.4 Factors regulating oligodendrocyte development. Adapted from (Bercury and Macklin, 2015). Oligodendrocyte differentiation is mediated by numerous extrinsic and intrinsic cues. For example, signaling from the extracellular matrix (subfigure) is critical in modulating the cytoskeletal reorganization during the transition from premyelinating to myelinating oligodendrocyte. Additionally, signal transduction through the Akt/mTOR pathway, which can be modified by PTEN, has been suggested to be involved in myelin formation.

2002; Maire et al., 2010). OPC production is not completely eliminated in Olig2 knockout (KO) mice, presumably through compensation by Olig1, another basic helix-loop-helix transcription factor involved in OL development and maturation (Lu et al., 2002; Zhou and Anderson, 2002). Interestingly, Olig1 is not essential for OL specification or maturation during development, but is required for remyelination in the CNS (Arnett et al., 2004; Paes de Faria et al., 2014).

In the subventricular zone, Olig2 opposes the neurogenic role of Pax6 to promote generation of OLs (Hack et al., 2005). It has also been shown that the inhibitory effects of BMP4 on OL development are mediated by the interaction of Olig2 with the inhibitor of differentiation

(ID) family of helix-loop-helix transcriptional inhibitors (Samanta and Kessler, 2004). Due to its importance in OL lineage specification, it is unsurprising that Olig2 is required for direct reprogramming of mouse fibroblasts into OLs (Najm et al., 2013; Yang et al., 2013).

Achaete-scute homolog 1 (Ascl1, also known as Mash1) is another basic helix-loop-helix transcription factor that regulates OL development. Loss of Ascl1 in mice decreases the production of OPCs in the brain and spinal cord early in development, but the OPC number recovers later possibly due to the expression of the similar Ascl3 and Ascl5 in the OL lineage during development (Parras et al., 2007; Sugimori et al., 2008). In the postnatal brain, Ascl1 expression is limited to OPCs and neural progenitors in the subventricular zone (Nakatani et al., 2013). The inducible deletion of Ascl1 in the postnatal brain inhibits the generation of OLs and instead promotes the production of astrocytes, suggesting that Ascl1 may function as a genetic switch (Nakatani et al., 2013). This function of Ascl1 is maintained throughout life, as the inhibition of oligodendrogenesis upon the loss of Ascl1 occurs during both developmental myelination as well as remyelination after injury (Nakatani et al., 2013).

Many members of the Nkx and Sox families are also involved in OL development. For instance, the simultaneous elimination of both Nkx6.1 and Nkx6.2 prevents the production of OLs from the pMN domain, a restricted domain of the ventral ventricular zone of the spinal cord responsible for the generation of motor neurons and oligodendrocytes (Cai et al., 2005; Vallstedt et al., 2005). Although the loss of Sox9 in mice reduces OL and astrocyte production, double KO of Sox8 and Sox9 almost completely eliminates the generation of OLs, indicating a possible redundancy between Sox8 and Sox9 (Stolt et al., 2003; Stolt et al., 2005). Sox10, a marker commonly used to identify cells of the OL lineage, does not affect OL specification, but is required for terminal differentiation of the OL (Stolt et al., 2004). In OPCs, Sox5 and Sox6 counters the

actions of Sox 9 and Sox10 to prevent the expression of genes that would induce OL differentiation (Stolt et al., 2006). Similarly, Hes5-mediated inhibition of myelin gene transcription is mediated by its inhibitory effects on Sox10 and the aforementioned Ascl1 (Liu et al., 2006). In fact, Hes5 likely acts downstream of the Notch signaling pathway (Rabadan et al., 2012). Interestingly, Olig1 associates with Sox10 to drive transcription of myelin genes (Li et al., 2007). Similarly, after interacting with a transcriptional corepressor to block β-catenin signaling at the onset of OL differentiation, Tcf4 (also known as Tcf712) recruits Sox10 to drive myelin formation (Zhao et al., 2016). It has been suggested that myelin regulatory factor (MRF)—another transcription factor important for the transcription of myelin genes and myelin formation—may cooperate with Sox10 to facilitate CNS myelination (Bujalka et al., 2013; Emery et al., 2009). As expected, given the central role of Sox10 in oligodendrocyte differentiation, Sox10 is also necessary for direct lineage conversion of fibroblasts to the oligodendroglial lineage (Najm et al., 2013; Yang et al., 2013). Another transcription factor necessary for oligodendrocyte maturation and myelination is zinc finger protein 191 (Aaker et al., 2016; Howng et al., 2010). The transcription factor Yin-Yang 1 (YY1) has been shown to promote oligodendrocyte differentiation by repressing transcriptional inhibitors of oligodendrocyte maturation (He et al., 2007a; He et al., 2007b).

1.2.4 Other factors affecting OL differentiation.

In recent years, it has been demonstrated that micro-RNAs (miRNAs) are important for both neural development and regulation of neural cell function. Unsurprisingly, miRNAs have been found to be involved in OL and myelin development, and there are sets of miRNAs that are expressed specifically by OLs (Jovicic et al., 2013; Lau et al., 2008). Studies showing that prevention of miRNA processing by OL-specific deletion of Dicer1 disturbs myelin development

emphasize the importance of miRNAs to OL development and maturation (Dugas et al., 2010; Zhao et al., 2010). For example, miR219 and miR338 downregulate repressive transcription factors, like Sox6 and Hes5, to promote OL differentiation and myelination (Dugas et al., 2010; Zhao et al., 2010). miR-7a has also been shown to be important for both OPC specification and proliferation (Zhao et al., 2012). Moreover, miR-23a has been shown to promote both OL differentiation and myelin synthesis, at least in part through its effects on the mTor/Akt/PTEN/PI3K pathway (Lin et al., 2013). Several papers have shown that mTor activation, constitutively active Akt, and conditional loss of PTEN all increase myelination in the CNS without altering the number of OLs, although unsurprisingly mTor activity is necessary for OL differentiation (Flores et al., 2008; Goebbels et al., 2010; Narayanan et al., 2009; Tyler et al., 2009; Wahl et al., 2014). In addition to miRNAs, long, non-coding RNAs (lncRNAs) are also involved in OPC specification, oligodendrocyte differentiation, and myelin development as well (Dong et al., 2015; He et al., 2017a).

Given the importance of transcriptional and translational regulation in OL specification, it is perhaps unsurprising that OL specification in the neonatal subventricular zone is also affected by the activity of histone deacetylases. For example, inhibition of histone deacetylases suppresses generation of oligodendrocytes and their progenitors *in vitro* (Foti et al., 2013; Siebzehnrubl et al., 2007). This is likely in part caused by HDAC-mediated suppression of factors that normally inhibit OL differentiation, like Wnt/β-catenin signaling, Id4, and Tcf4 (He et al., 2007b; Ye et al., 2009). Along with histone deacetylation, histone methylation has also been implicated in OPC and oligodendrocyte specification: Overexpression of enhancer of zeste homolog 2—a protein involved in gene silencing through histone methylation and deacetylation—causes an increase in

oligodendrocyte number, while silencing of enhancer of zeste homolog 2 has the opposite effect (Sher et al., 2008).

Far more OLs are produced during development than are necessary for proper myelination, and their survival is likely dependent upon levels of axon-derived trophic factors (Barres et al., 1992; Barres et al., 1993). Even when excessive stimulation of OPCs by PDGF leads to increased numbers of oligodendrocytes during development, the excess oligodendrocytes die, leaving the appropriate number of myelinating oligodendrocytes (Calver et al., 1998). This correction in number of oligodendrocytes may be mediated by apoptosis secondary to myelination failure, as oligodendrocytes that do not myelinate axons will degenerate (Trapp et al., 1997).

1.3 Myelin Formation

1.3.1 The basics

The differentiation of an OPC into an oligodendrocyte leads to an impressive change in morphology, beginning with the extension of many new cellular processes. Timelapse imaging using the zebrafish model system has demonstrated that these oligodendroglial processes scan the environment until they contact an axon (Baraban et al., 2018; Czopka et al., 2013; Hines et al., 2015; Koudelka et al., 2016; Mensch et al., 2015). Interestingly, whereas some processes stabilize and form myelin sheaths, many processes retract shortly after contact with the axon. This retraction is often preceded by a high-amplitude, long-duration Ca^{2+} transient (Baraban et al., 2018). Although the exact determinants and mechanism of this retraction remains unknown, several molecules have been identified as repulsive guidance cues for myelination, including polysialic acid neural cell adhesion molecule (PSA-NCAM), class 3 semaphorins, limbic system-associated

membrane protein (Lsamp), and junctional adhesion molecule (JAM2) (Charles et al., 2000; Piaton et al., 2011; Redmond et al., 2016; Sharma et al., 2015; Syed et al., 2011).

After the nascent myelin sheath stabilizes on the axonal membrane, it rapidly grows around the axon to form the mature myelin sheath (Figure 1.5). The growth of the myelin sheath is mediated by growth of the leading edge (the distal end of the oligodendroglial process) around the axon along with lateral growth of the myelin membrane towards the future nodes of Ranvier (Snaidero et al., 2014). As the leading edge grows around the axon, it travels underneath the

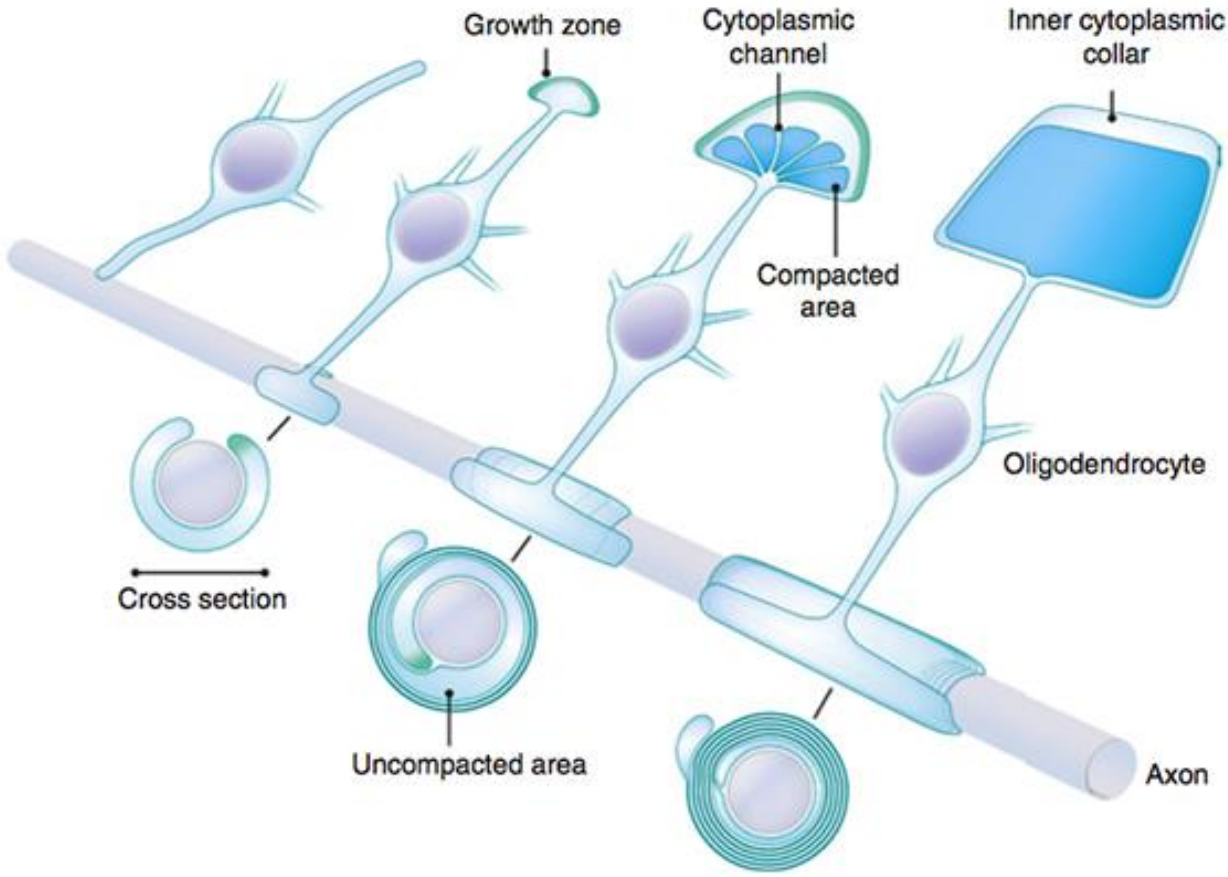

Figure 1.5 Schematic of Myelin Formation. Adapted from (Chang et al., 2016)
An illustration of a myelin sheath at several stages of development. While the lower process of each oligodendrocyte shows a myelin sheath wrapping around an axon, the upper process of each oligodendrocyte is an unrolled version of the lower myelin sheath. The corresponding cross sections are found beside the axon. From left to right: A maturing oligodendrocyte extends a process to an unmyelinated portion of an axon. After making contact with the axon, the process begins wrapping around the axon and spreading its membrane. The growth zone/leading edge, in green, grows beneath the previously deposited layers of myelin. Simultaneously, the myelin membrane elongates longitudinally as well. Myelin compaction initiates in the outermost layer of the sheath and spreads toward the inner layers, maintaining uncompacted intramyelinic cytoplasmic nanochannels to facilitate transport between the cell body and the leading edge.

previously deposited membrane (Snaidero et al., 2014). Meanwhile, during the lateral growth of the myelin sheath (which occurs in a coiling helical pattern), membrane at the lateral loops is likely attached to the axon, perhaps by contactin associated protein 1 (Caspr, also known as paranodin), Contactin, and Neurofascin155 (Pedraza et al., 2009; Snaidero et al., 2014; Zonta et al., 2008). Once the lateral loops have reached their final position at the future paranode, oligodendroglial expression of ankyrin-G facilitates the stabilization of the paranodal junctions (Chang et al., 2014).

As the leading edge of the growing myelin sheath extends beneath previously deposited membrane, force is required to disrupt the previously formed contact between myelin and axonal membrane. The driving force of myelin growth is likely largely driven by Arp2/3-dependent polymerization of the actin skeleton pushing the leading edge forward between the axonal and myelin membranes (Zuchero et al., 2015). The subsequent ADF/cofilin1-dependent disassembly of the actin cytoskeleton may facilitate the spreading of the myelin membrane across the axon and its subsequent stable adhesion (Nawaz et al., 2015). It has also been demonstrated that MBP is required for actin disassembly and may thereby induce myelin wrapping (Zuchero et al., 2015). Other proteins that may be involved in actin cytoskeleton-dependent myelin formation include neural Wiskott-Aldrich syndrome protein (N-WASP), Wiskott-Aldrich syndrome protein family verprolin homologous protein 1 (WAVE1, also known as Wiskott-Aldrich syndrome protein family member 1), cell division control protein 42 (cdc42), and Ras-related C3 botulinum toxin substrate 1 (Rac1) (Jin et al., 2011; Kim et al., 2006; Novak et al., 2011; Thurnherr et al., 2006).

Most of the lipids that will be added to the growing myelin sheath are synthesized in the endoplasmic reticulum, where some myelin lipids are packaged with proteolipid protein (PLP) early in the secretory pathway and then trafficked to the myelin membrane through transcytotic transport (Baron et al., 2015; Simons et al., 2000). It has been suggested that vesicles of newly

synthesized myelin membrane and protein transport through intramyelinic cytoplasmic nanochannels and are delivered to the growing leading edge (Snaidero et al., 2014). These intramyelinic cytoplasmic nanochannels are found between layers of compacted myelin and connect the growing innermost layer of myelin with the major source of myelin membrane and protein biosynthesis, the oligodendroglial cell body. Interestingly, it was recently shown that 2',3'-cyclic nucleotide 3'-phosphodiesterase (CNP) directly associates with the actin cytoskeleton to maintain intramyelinic cytoplasmic channels, and loss of this function of CNP has been suggested to cause axonopathy and neurodegeneration (Lappe-Siefke et al., 2003; Snaidero et al., 2017).

In addition to vesicular trafficking of myelin membrane and proteins to the leading edge, myelin components may be added at the outer layers of the sheath and freely diffuse throughout the developing myelin sheath (Gould, 1977; Gould and Dawson, 1976; Steshenko et al., 2016; Yurlova et al., 2011). Interestingly, myelin basic protein (MBP)—a major cytoplasmic component of myelin essential for myelin compaction—is transported by kinesins as mRNA in RNA granules from the cell body into the growing myelin sheath, where it is locally translated (Laursen et al., 2011; Lyons et al., 2009; Readhead et al., 1987; Torvund-Jensen et al., 2014; Wake et al., 2011; White et al., 2008). As myelin compaction progresses from the proximal (outermost) layers of myelin distally (inwards), it is likely that MBP mRNA granules are translated at the outermost non-compact layer of myelin to prevent premature compaction at the growing leading edge (Snaidero et al., 2014). After local translation of the unstructured and positively charged MBP, MBP binds to the cytoplasmic leaflets of the lipid bilayer and polymerizes to drive clearance of cytoplasm and compaction of the myelin sheath (Aggarwal et al., 2013; Aggarwal et al., 2011; Boggs, 2006). Interestingly, the extracellular leaflets are held together by weaker interactions

(mediated by PLP) than those that hold the cytoplasmic leaflets together, perhaps to allow the membrane bilayers to slide along one another during myelin growth (Bakhti et al., 2013).

Towards the end of myelin formation, anilin/septin filaments form a scaffold in the adaxonal inner loop of myelin that extends longitudinally along the axon (Patzig et al., 2016). Interestingly, the loss of myelin septins causes compact myelin to focally detach and form myelin outfoldings (also known as redundant myelin) (Patzig et al., 2016). These myelin outfoldings may serve a biological function during myelin development, but in the adult these outfoldings are generally considered pathological (Snaidero et al., 2014).

The myelination process described above occurs in each myelin sheath of an oligodendrocyte, but most oligodendrocytes extend about thirty myelin sheaths, and some may even extend eighty or more (Chong et al., 2012; Young et al., 2013). Because of this, it has been estimated that an oligodendrocyte may synthesize $20x10^5$ μm^2 of myelin membrane, meaning that the oligodendrocyte is the most prolific membrane producer in the human body (Pfeiffer et al., 1993). Amazingly, according to time-lapse imaging in zebrafish, this enormous amount of myelin in synthesized during a period of just five hours (Czopka et al., 2013). Interestingly, this rapid growth may be facilitated by Ca^{2+} activity: high-frequency Ca^{2+} transient activity in growing myelin sheaths predicts faster growth of the sheath (Baraban et al., 2018).

1.3.2 The role of membrane trafficking in myelination

Phosphatidylinositol (PtdIns) is a common membrane lipid that can be phosphorylated by lipid kinases and regulate diverse cellular functions and that has a profound role in vesicle trafficking. Dysregulation of PtdIns phosphorylation and resulting disruption of vesicle trafficking disrupts myelin formation. Mutations within human factor-induced gene 4 (*FIG4*), which is

required for the interconversion of phosphatidyl inositol 3-monophosphate (PI(3)P) and phosphatidyl inositol 3,5-bisphosphate ($PI(3,5)P_2$), can cause a variety of neurological disorders including Charcot-Marie-Tooth type 4J, a severe demyelinating peripheral neuropathy (Chow et al., 2007; Nicholson et al., 2011). Loss of Fig4 in mice causes juvenile lethality secondary to hypomyelination and spongiform degeneration (Chow et al., 2007; Ferguson et al., 2009; Winters et al., 2011). A subsequent paper clarified that alterations in any element of the Fig4-PIKfyve-VAC14 enzyme complex causes impairments in OL differentiation, intracellular trafficking of myelin proteins, and myelin formation in the CNS (Mironova et al., 2016). Similarly, conditional loss of the PtdIns kinase, vacuolar protein sorting 34 (Vps34), in Schwann cells causes severe hypomyelination in peripheral nerves by disturbing endosomal trafficking (Logan et al., 2017). Phosphatidyl inositol 3,4,5-triphosphate ($PI(3,4,5)P_3$) signaling is also important for myelin formation: inactivation of phosphatase and tensin homolog (PTEN) during development increases the thickness of myelin sheaths (Goebbels et al., 2010). Moreover, inducible inactivation of PTEN in mature OLs of adult mice reinitiaties myelin growth leading to thicker myelin sheaths (Goebbels et al., 2010; Snaidero et al., 2014)

In addition to PtdIns regulation, mutations within vacuolar protein sorting 11 (Vps11), members of the homotypic fusion and vacuole protein sorting (HOPS) tethering complex, essential for vesicle fusion to the lysosome, suffer from hypomyelination, developmental delay, and leukoencephalopathy (Edvardson et al., 2015; Zhang et al., 2016). Although the HOPS complex is involved in all forms of lysosome fusion, one study suggested that these defects were associated with dysfunction of autophagosome trafficking (Zhang et al., 2016).

In order to form all of their myelin sheaths in a matter of hours (Czopka et al., 2013), OLs likely require a high rate of exocytic membrane addition. Soluble N-ethylmaleimide-sensitive

factor attachment protein receptor proteins (SNAREs) are required for vesicle fusion to the appropriate target membranes (Rothman, 1994). Docking and fusion of a vesicle with the appropriate target membrane is mediated by the specific recognition of v(esicle)-SNAREs with their corresponding t(arget)-SNAREs. Distinct SNAREs have been identified for certain trafficking routes: For example, the v-SNARE vesicle associated membrane protein 7 (VAMP7) binds to the t-SNARE syntaxin 3 to mediate trafficking to the apical membrane of polarized cells epithelial cells (Lafont et al., 1999). VAMP3 and VAMP7, along with their binding partners syntaxin 4 and syntaxin 3 respectively, have been identified in OLs (Feldmann et al., 2011; Feldmann et al., 2009; Madison et al., 1999). Loss of VAMP3 or VAMP7 function diminishes transport of the myelin protein PLP to the OL cell surface in culture (Feldmann et al., 2011). Although KO of VAMP3 in mice does not affect myelin formation, mutations in VAMP7 can reduce the levels of certain myelin proteins, including PLP (Feldmann et al., 2011).

GTPases, known to be essential for membrane trafficking, may also be important for myelin formation (Pfeffer, 1994). Silencing of Rab3a, a GTPase involved in exocytosis, delayed myelin biogenesis in maturing OLs (Anitei et al., 2009). Moreover, Rab3A has been suggested to regulate SNAP-29-mediated membrane fusion during myelin formation (Schardt et al., 2009). Cdc42 and rac1, two GTPases of the Rho subfamily have also been shown to be important for proper myelination, although whether this is mediated by their roles in organizing the actin cytoskeleton, membrane trafficking, or one of their many other functions is unknown (Etienne-Manneville and Hall, 2002; Hall, 1998; Jaffe and Hall, 2005; Nawaz et al., 2015; Thurnherr et al., 2006; Zuchero et al., 2015). Interestingly, proteomic analysis of purified myelin identified regulators of intracellular vesicle transport including many Rab-GTPases, like Rab3A, along with cdc42 and Rac1 (Jahn et al., 2009).

1.3.3 Myelin Plasticity

For decades following their discovery, myelin and OLs were considered static elements of the CNS (Kondiles and Horner, 2017), but recent evidence indicates that this is not the case. One compelling study shows that training individuals with no prior experience to juggle induces changes in their white matter suggestive of myelin growth (Scholz et al., 2009). Similarly, learning a new language can also induce changes in white matter architecture (Schlegel et al., 2012). Studies have shown that new myelin is continually generated, even in the nearly completely myelinated optic nerve (Dangata et al., 1996; Yeung et al., 2014; Young et al., 2013). Given these studies, it has been postulated that the discontinuous myelination along the length of many axons indicates areas available for additional myelination, perhaps as a mechanism for neural plasticity (Tomassy et al., 2014). Should active myelin remodeling and formation occur, there are three primary mechanisms available to the adult CNS: the generation of new OLs, the extension of new myelin sheaths from preexisting OLs, and the remodeling of preexisting myelin sheaths.

1.3.3.1 The generation of new OLs and myelin plasticity

Many studies that have shown that OPCs continue to differentiate into new myelinating OLs in the adult CNS. For example, it has been shown in several studies through genetic fate mapping in mice that OPCs continuously differentiate into mature myelinating OLs especially in CNS white matter (Dimou et al., 2008; Kang et al., 2010; Psachoulia et al., 2009; Rivers et al., 2008). However, it should be noted that these adult-born OLs have been shown to have different properties than those born during development; adult-born OLs extend more myelin sheaths, but these myelin sheaths are shorter in length (Young et al., 2013). There have also been several studies

showing that neuronal activity can drive oligodendrogenesis in adult mice. For example, OPC-specific elimination of the transcription factor MRF, which is essential for OL maturation during development, in adult mice prevented mice from learning a complex motor skill (Emery et al., 2009; McKenzie et al., 2014). Given that this loss did not affect myelination in the adult mice, these results suggest that skilled motor learning in mice requires the generation of new OLs and myelin (McKenzie et al., 2014). A subsequent study indicated that the production of new oligodendrocytes within several hours facilitates this skilled motor learning (Xiao et al., 2016). Blocking formation of new OLs in the adult mouse causes motor deficits and slowing of conduction in the corpus callosum (Schneider et al., 2016). It should be noted that although these studies demonstrate that the formation of new OLs contributes to rapid and long-lasting myelin plasticity in adult mice, they have not ruled out the possibilities of preexisting oligodendrocytes producing new myelin sheaths or that preexisting myelin sheaths are remodeled.

Another study examined the effects of short-term optogenetic stimulation of the premotor cortex in awake, behaving mice (Gibson et al., 2014). This stimulation induced OPC proliferation, followed by oligodendrogenesis and thicker myelin sheaths. It was unclear to the authors however, whether the thicker myelin sheaths were derived from new or preexisting OLs. A critical observation derived from these studies is that the formation of new oligodendrocytes and thicker myelin sheaths led to an altered gait, suggesting that alterations in myelination can have behavioral consequences. Interestingly, voluntary running has been shown to induce OPC proliferation, oligodendrogenesis, and increased myelin formation in the cerebellum of a mouse model of ataxia, further highlighting the importance of activity on oligodendrogenesis in adult animals (Alvarez-Saavedra et al., 2016). How oligodendrogenesis was evoked remains uncertain however, given

that it is unclear in the literature whether exercise alone is sufficient to increase oligodendrocyte formation (Simon et al., 2011; Xiao et al., 2016).

1.3.3.2 The extension of new myelin sheaths and myelin plasticity

To ask whether mature myelinating oligodendrocytes can form new myelin sheaths, several studies have examined post-mitotic oligodendrocytes that survived a demyelinating insult and found that they do not lay down new myelin sheaths (Crawford et al., 2016; Keirstead and Blakemore, 1997). Another study transplanted irradiated cells (to ablate all mitotic cells) into a demyelinated lesion and found that almost none of the transplanted oligodendrocytes were able to form myelin sheaths (Crang et al., 1998). Subsequent studies in zebrafish *in vivo* and in a murine coculture system showed that mature oligodendrocytes have very little capacity to form new myelin sheaths after a brief developmental window (Czopka et al., 2013; Watkins et al., 2008). However, it should be noted that one study demonstrated the capability of mature OLs in culture to retract and regenerate a damaged process after insult, and another suggested that constitutive activation of ERK1/2 in preexisting mature OLs allows them to form new myelin sheaths after a demyelinating insult (Jeffries et al., 2016; Makinodan et al., 2013). Thus, it appears that if mature oligodendrocytes can form new myelin sheaths, this capacity is extremely limited.

1.3.3.3 Remodeling of preexisting myelin sheaths and myelin plasticity

There is limited data regarding whether the thickness of preexisting myelin sheaths can be modulated. As mentioned above, optogenetic stimulation of premotor cortex *in vivo* increases myelin thickness of associated axons (although a contribution of newly formed oligodendrocytes to this phenotype cannot be excluded) (Gibson et al., 2014). In fact, there is some evidence that

mature OLs may be able to modulate the thickness of their myelin sheaths: As mentioned above, inducible inactivation of PTEN in mature OLs of adult mice leads to reinitiation of myelin growth and thicker myelin sheaths (Goebbels et al., 2010; Snaidero et al., 2014). Similarly, inducible activation of ERK1/2 in mature OLs of adult mice stimulates myelin growth and results in thicker myelin sheaths (Jeffries et al., 2016). Conversely, social isolation of adult mice leads to thinner myelin sheaths, along with behavioral and transcriptional changes in OLs (Liu et al., 2012), and sensory deprivation of the auditory system in adult mice causes a decrease in the thickness of myelin sheaths as well (Sinclair et al., 2017). Although a mechanism by which the thickness of a preexisting myelin sheath can be remodeled is unknown, evidence suggests that the thickness of preexisting myelin sheaths may be modulated in response to experience and activity.

1.3.4 Myelin Turnover

It was suggested more than half a century ago that myelin turnover is slower than that of most other components of the brain or other tissues (Davison and Dobbing, 1960; Waelsch et al., 1940a; Waelsch et al., 1940b, 1941). It was subsequently determined that certain components of myelin membranes in the mouse and rat have half-lives that range from weeks to perhaps greater than one year (Fischer and Morell, 1974; Smith, 1968). More recent unbiased screens have confirmed that the half-life of myelin proteins is on average a few months (Savas et al., 2012; Toyama et al., 2013). How myelin is turned over, however, remains unknown.

Theoretically, myelin could be turned over by replacement of entire oligodendrocytes, substitution of myelin sheaths, or remodeling of existing myelin sheaths. Replacement of OLs or myelin sheaths would theoretically be enormously inefficient: not only would it cause focal demyelination and possibly temporarily disrupt neurotransmission, it would also require an

incredible amount of energy expenditure anytime a component of the myelin sheath needed to be replaced. Moreover, neither of these two hypotheses can explain how different components of the myelin sheath are turned over at different rates (Fischer and Morell, 1974; Savas et al., 2012; Smith, 1968; Toyama et al., 2013). On the other hand, remodeling of the preexisting myelin sheath could certainly allow for differential turnover of myelin components. In addition, as mentioned above, there is limited evidence that mature OLs are capable of retracting myelin sheath or forming new ones (Crang et al., 1998; Crawford et al., 2016; Czopka et al., 2013; Jeffries et al., 2016; Keirstead and Blakemore, 1997; Makinodan et al., 2013; Watkins et al., 2008).

Little is known about whether myelin within a sheath can be remodeled. A recent paper discovered that, in the aging brain, spheres of compact myelin can pinch off of myelin sheaths and be cleared by microglia (Safaiyan et al., 2016). Another possible mechanism for myelin turnover is suggested by data from the peripheral nervous system: During Wallerian degeneration, dedifferentiating Schwann cells employ a combination of macroautophagy and phagocytosis to degrade their myelin sheath (Brosius Lutz et al., 2017; Gomez-Sanchez et al., 2015; Jang et al., 2016). Whether any of these mechanisms are employed by OLs under non-pathological conditions for homeostasis or in response to network inactivity remains unknown.

A significant recent study has provided insight into the similarities and differences between humans and experimental model systems regarding oligodendrogenesis and myelin remodeling in adult white matter (Yeung et al., 2014). Taking advantage of the changes in atmospheric ^{14}C levels over the past century due to the proliferation of nuclear bomb testing, the study was able to determine the age of myelin *versus* oligodendroglial nuclei in post-mortem human tissue. Carbon-dating human oligodendroglial nuclei indicated that the cells were born almost exclusively in the first five years of life, with a turnover rate of about 0.3% annually thereafter. Of note, this is less

than 1/100th of the rate of oligodendrocyte turnover predicted by fate mapping in adolescent and adult transgenic mice (Rivers et al., 2008; Young et al., 2013; Zhu et al., 2011). In sharp contrast, however, carbon dating the myelin from the same brain samples indicated that the myelin was formed close to the time of death, indicating that the myelin sheath is continuously exchanged within months throughout life in humans. This is consistent with the aforementioned rodent data (Fischer and Morell, 1974; Savas et al., 2012; Smith, 1968; Toyama et al., 2013). Not only do these results suggest that oligodendrocyte turnover cannot be responsible for myelin turnover in humans, the study also demonstrates that oligodendrocyte turnover cannot account for the levels of white matter plasticity observed in response to activity and experience in humans (Bengtsson et al., 2005; Scholz et al., 2009; Yeung et al., 2014). Instead, the study proposes that myelin remodeling must be performed by mature OLs, and that mature OLs are responsible for myelin plasticity in the adult.

1.3.5 Dynamic Myelination and Circuit Tuning

As many CNS axons are myelinated for sub-maximal conduction velocity (and in fact, irregularly along their lengths), it is safe to assume that conduction velocity is not optimized to maximize speed, but rather to ensure that action potentials arrive at the appropriate time (Tomassy et al., 2014; Waxman, 1980). The importance of signal timing has been explored thoroughly in the auditory system (reviewed in (Seidl, 2014)): The auditory system processes microsecond differences in the arrival time of sounds between the two ears; consequently, it requires finely tuned signal timing. Interestingly, the temporal precision of the auditory system may be mediated in part by dynamic adjustment of myelin structure (Seidl et al., 2014; Stange-Marten et al., 2017). Moreover, recent evidence suggests that the thickness of myelin sheaths in the auditory system can

be modulated by experience even in the adult, just as myelination of the prefrontal cortex is modulated by social experience (Liu et al., 2012; Sinclair et al., 2017). Together, these studies emphasize the importance of precise signal timing and suggest that OLs may be able to modify myelin sheath morphology to optimize conduction velocities. These studies suggest that myelin remodeling may not be simply required to maintain the health of the myelin sheath, but may in fact be activity dependent and essential for neural circuit function. In fact, several studies have shown behavioral consequences that accompany activity-dependent changes in myelin structure (Gibson et al., 2014; Liu et al., 2012). Moreover, even small changes in g-ratio can significantly alter conduction velocity. It has been proposed that changes in conduction velocity—mediated by activity-dependent alterations in myelin structure—could have profound effects on neuronal network function (Pajevic et al., 2014). Disruption of activity-dependent myelination and adaptive timing of action potentials likely contribute to many disorders involving asynchronous neuronal firing causes dysfunction, like epilepsy, schizophrenia, and dyslexia.

1.3.6 Conclusion

In summary, much is known about OPC specification, oligodendrocyte differentiation, and myelin formation by oligodendrocytes in the CNS. How myelin is turned over, however, remains unclear. In humans, myelin remodeling is likely mediated by mature oligodendrocytes. As mature oligodendrocytes have limited capacity to generate new myelin sheaths, we must ask whether mature oligodendrocytes can remodel the myelin at preexisting myelin sheaths. The significance of this question is underscored by the importance of myelin remodeling for neural function and activity-dependent myelin plasticity.

Chapter 2.

Glial Macroautophagy

2.1 Introduction

Cells employ two systems to degrade cytosolic substrates: the proteasome and the lysosome. Whereas the proteasome rapidly turns over ubiquitinated proteins, the lysosome degrades a much wider array of cytosolic cargo, including proteins, lipids, and organelles (Ciechanover et al., 2000; Muller et al., 2012; Weissman et al., 2011). The import of cytosolic substrates into the lysosome is called autophagy. There are three primary mechanisms by which intracellular cargo can be delivered to the lysosome: microautophagy, chaperone-mediated autophagy, and macroautophagy (Yamamoto and Yue, 2014). In microautophagy, a pinocytosis-like process that is primarily described in yeast, cargo is directly taken up by the lysosomal membrane (Yamamoto and Yue, 2014). Chaperone-mediated autophagy, largely described in mammals, involves the recognition of substrates carrying a peptide motif similar to KFERQ by

hsc70, which traffics and directs cargo into the lysosome via LAMP2A (Yamamoto and Yue, 2014). The most conserved autophagic pathway, however, is macroautophagy. Macroautophagy (MA) is responsible for the lysosome-mediated elimination of cytosolic proteins, lipids, and organelles, through packaging into a de novo synthesized, transient, multilamellar organelle known as an autophagosome (AP) (Figure 2.1). MA can act either as a non-selective response to cellular stress such as starvation to degrade bulk cytosol and its contents, or as a highly selective quality-control mechanism to degrade aggregated proteins or damaged organelles (Filimonenko et al., 2010). Non-selective and selective MA processes are regulated differently. For example, non-selective MA occurs in a mammalian target of rapamycin (mTOR)-dependent manner, and

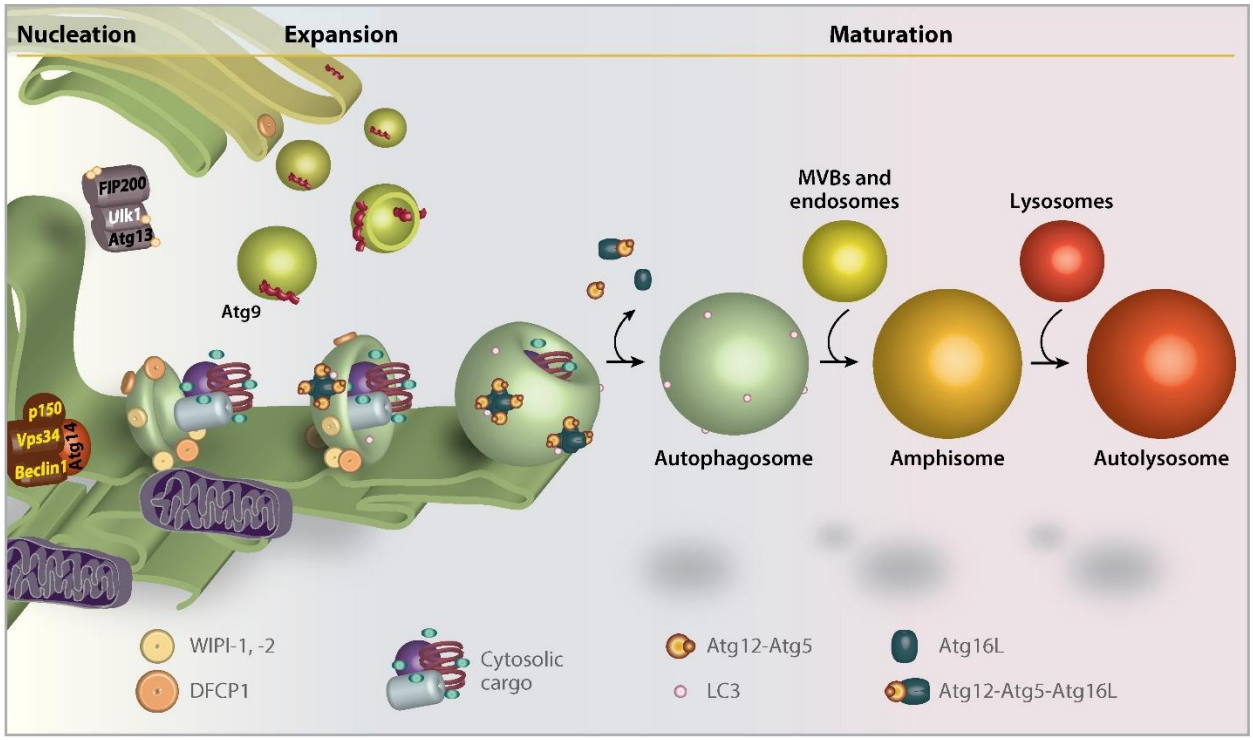

Figure 2.1 Degradation of cargo by macroautophagy. Adapted from (Yamamoto and Yue, 2014).
An illustration depicting the three steps of autophagosome (AP) formation: nucleation, expansion and maturation. MA proteins are attracted to the forming isolation membrane (IM) depending on the phosphorylation status of the Ulk1 complex. The Beclin1-Atg14L-Vps34 complex drives PI3P formation at the IM as well as surrounding membranse which draws effector proteins like WIPI-1 and -2. DFCP1 also shuttles from the Golgi to the PI3P-rich IM. As the IM elongates around its cargo, the tetrameric Atg12-Atg5-Atg16L complex promotes the conjugation of LC3 onto PE of the growing AP membrane. Only LC3 remains on the complete AP. During maturation, the AP fuses with endosomes, multivesicular bodies (MVBs), and lysosomes to form amphisomes and autolysosomes, leading to degradation of the contents of the AP along with inner AP membrane.

requires only the core autophagic machinery, whereas selective MA can act in an mTOR-independent manner, and also relies on the coordinated activity of adaptor proteins such as protein 62/sequestesome-1 (p62/SQSTM1).

2.2 MA, the basics

Central to MA is the formation of the AP, and thus our current understanding of this process centers upon this. AP formation and completion occurs through a hierarchical assembly process driven by autophagy-related (Atg) proteins (reviewed in (Johnson et al., 2012)). Briefly, the isolation membrane and surrounding membranes are enriched with PI3P by a Class III PI3K complex comprised of Beclin1, Atg14L, and Vps34. This enrichment of PI3P attracts effector proteins such as DFCP1, WIPI-1, and WIPI-2, which defines the pre-autophagosomal structure. The elongation of the autophagosome membrane around its cargo is highly dependent on a ubiquitin-like conjugation process that relies upon the E1-like enzyme Atg7, E2-like enzyme Atg3, and the E3-like tetrameric Atg12-Atg5-Atg16L complex to promote the conjugation of the ubiquitin-like Atg8 and its orthologs (such as MAP1 light chain 3 (LC3)) to the phospholipid phosphatidylethanolamine (PE) within the growing autophagosome membrane. LC3 conjugation occurs on both sides of the growing AP membrane, leading to its presence on both the outer and inner AP membrane. After closure of the growing AP, via a yet unknown mechanism, the outer membrane of the autophagosome fuses with endosomes to form amphisomes then to lysosomes to form autolysosomes. Although mechanistically MA is highly conserved from yeast, the consolidation of cytosol-derived lysosomal cargoes with membrane-derived ones through amphisome formation, is unique to mammals (Klionsky et al., 2007).

Multiple studies have shown that MA is required for neural function and health (Hara et al., 2006; Komatsu et al., 2006; Liang et al., 2010). Elimination of MA via excision of the essential MA gene Atg7 in all neural cells (using the Cre-loxP system under the Nestin promoter) causes neural dysfunction, neurodegeneration, and early death, highlighting the importance of MA in maintaining proper neural function (Betz et al., 1996; Komatsu et al., 2006). Another paper published at the same time found comparable results upon the loss of Atg5 throughout the CNS as well (Hara et al., 2006). Subsequent genetic elimination of other core autophagy protein encoding genes yielded similar results, including deletion of Family Kinase-Interacting Protein Of 200 KDa/ Autophagy related protein 17 (FIP200/Atg17) (Liang et al., 2010). Whereas the significance of neural MA is often attributed to its role in neurons, it is often disregarded that the approaches used impair MA in another critical class of neural cells, namely glia. Unfortunately, however, our current understanding of MA in glia is fairly limited.

2.3 MA in Astrocytes

Astrocytes have many important roles in the CNS including regulating K^+ buffering, neurotransmitter levels, energy levels, growth factor production, and the blood brain barrier. MA has been suggested to be important for astrocyte development (Wang et al., 2014). Studies of lysosomal storage disorders indicate that neuronal health may depend on MA in astrocytes (Di Malta et al., 2012). MA in astrocytes has also been suggested to be important for clearing a variety of aggregated proteins, including aggregated proteins in models of Alexander disease, amyotrophic lateral sclerosis, and Parkinson's disease (Barmada et al., 2014; Gan et al., 2012; Janen et al., 2010; Tang et al., 2008; Zschocke et al., 2011). As astrocytes are essential energy regulators in the brain,

one intriguing yet heretofore unexplored possibility is the importance of MA in astrocytes for energy regulation in the brain. Several studies have shown that neurons depend upon astrocyte-derived lactate to maintain activity for extended periods of time (Hu and Wilson, 1997; Pellerin and Magistretti, 1994; Rouach et al., 2008). It would be interesting to know whether MA is mobilized in astrocytes during periods of high neuronal activity or during starvation to maintain proper CNS function.

2.4 MA in Microglia

Microglia are the resident phagocytic immune cell of the CNS. MA may play a role in modulating microglial inflammation (He et al., 2017b; Su et al., 2016). Interestingly, microglia may be subject to autophagy-induced cell death following hypoxia or Toll-like receptor 2 activation (Arroyo et al., 2013; Yang et al., 2014). It has also been suggested that MA in microglia plays a role in amyloid-β clearance in models of Alzheimer's disease, and that this may occur in a beclin-1 dependent manner (Lucin et al., 2013; Shibuya et al., 2014). In addition, recent work has indicated that MA is important for microglia-mediated synaptic pruning during development (Kim et al., 2017). It should be noted that all of these studies claim that MA is involved in clearing extracellular cargo. As MA is an intracellular process, it is more likely that these observations are mediated by LC3-associated phagocytosis (LAP), a process that has been thoroughly characterized in macrophages, which are close relatives of microglia (Martinez et al., 2011; Martinez et al., 2016; Martinez et al., 2015). LAP is a process wherein a subset of the MA machinery is recruited to pathogen-containing phagosomes to improve degradation of phagocytosed cargo (Figure 2.2) (Martinez et al., 2011; Martinez et al., 2015). For example, LAP is dependent upon Atg5, Atg7,

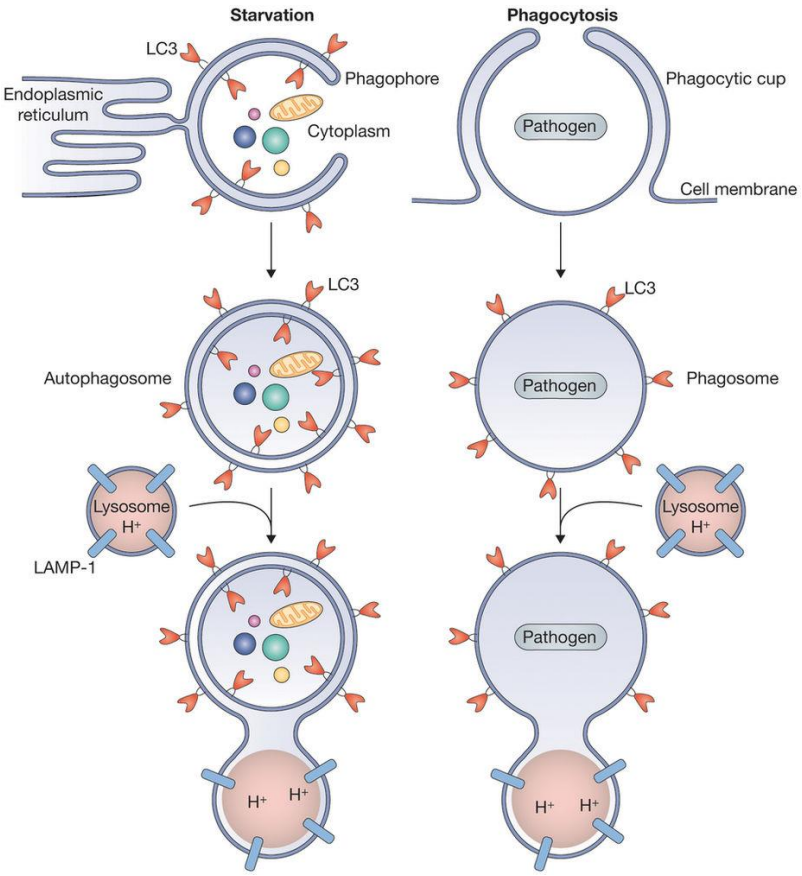

Figure 2.2 Comparison of macroautophagy and LC3-associated phagocytosis. Adapted from (Boyle and Randow, 2015). During nutrient starvation (as well as other cues), cells encapsulate portions of their cytoplasm into double-membrane APs (left). On the other hand, during infection (as well as other cues), phagocytic cells ingest extracellular microbes into single-membrane phagosomes (right). LC3 can be conjugated to phosphatidylethanolamine in either structure, which aids trafficking of the vesicles and fusion to the lysosome.

and Beclin1, whereas other autophagic proteins like ULK1, Atg14, and Ambra1 are dispensable for LAP (Martinez et al., 2011; Martinez et al., 2015). The association of LC3 directly to the phagosomal membrane has been shown to facilitate more efficient lysosome-mediated clearance of these phagosomes (Martinez et al., 2011; Martinez et al., 2016; Martinez et al., 2015). Interestingly, defects in LAP can cause a systemic lupus erythematosus (SLE)-like syndrome in mice and may contribute to SLE pathogenesis in humans (Martinez et al., 2016).

2.5 MA in Schwann cells and Oligodendrocytes

As little is known about MA in OLs, we will examine the literature regarding MA in OLs and Schwann cells together. We will infer from what has been learned about MA in Schwann cells

to OLs, while keeping in mind the caveats of extrapolating data between these cell types. Like many other cell types, MA has been implicated in the clearance of aggregated proteins by both Schwann cells and oligodendrocytes, in models of Charcot-Marie-Tooth disease and multiple systems atrophy respectively (Fortun et al., 2003; Nicks et al., 2014; Odagiri et al., 2012; Pukaβ et al., 2015; Rangaraju et al., 2010; Schwarz et al., 2012; Tanji et al., 2013). Interestingly, one study suggested that MA in Schwann cells may be involved in developmental pruning of axons (Song et al., 2008). Moreover, MA in Schwann cells has been suggested to be associated with axon regeneration in the peripheral nervous system (Mohseni, 2011).

Several studies have proposed that MA may also play a role in myelin formation and degradation. One paper examined the role of MA in the Long-Evans shaker (*les*) rat, a dysmyelination mutant with a mutation in the gene that encodes myelin basic protein (Smith et al., 2013). The authors discovered that there was an accumulation of autophagosomes in *les* oligodendrocytes by electron microscopy. They found in culture that induction of MA by glucose and serum starvation increased the survival of *les* oligodendrocytes and promoted an increase in membrane extensions. Moreover, *in vivo*, induction of MA through intermittent fasting increased myelin sheath thickness and the percentage of axons that were myelinated in *les* spinal cord. Although the authors proposed that MA may facilitate oligodendroglial survival and function, it is important to note that the effects of MA in *les* oligodendrocytes may have been mediated by reduced aggregate burden. Although the study notes an increase in myelination in control animals as well, starvation and intermittent fasting are non-specific inducers of MA with many off-target effects. Nonetheless, this study suggests that MA may facilitate myelin formation. In support of this, a recent study using whole exome sequencing of human patients indicated that a mutation in

Vps11 that causes leukoencephalopathy is associated with defects in MA (Zhang et al., 2016). This may also indicate that MA is important for myelin formation.

Like the study of *les* rats, several papers have suggested that induction of MA may increase myelin formation by Schwann cells in mouse models of Charcot-Marie-Tooth (Madorsky et al., 2009; Nicks et al., 2014; Rangaraju et al., 2010). For example, one study of Trembler J mice (a model of Charcot-Marie-Tooth 1A) found that induction of MA by intermittent fasting reduced PMP22 aggregate burden in mutant mice and increased myelination by Schwann cells (Madorsky et al., 2009). Interestingly, just as in the CNS in the aforementioned study of *les* rats, intermittent fasting increased myelin thickness in control sciatic nerves as well (Madorsky et al., 2009). Although a follow up study found that induction of MA through rapamycin treatment (mTor inhibition) increased myelin formation by Trembler J Schwann cells in culture, it did not significantly alter myelin formation by Schwann cells from control mice (Rangaraju et al., 2010). Induction of MA through mTor inhibition by treatment with rapamycin *in vivo* once again caused an increase in myelin thickness and percentage of fibers that were myelinated in Trembler J mice (Nicks et al., 2014). The data, however, was inconclusive regarding whether mTor inhibition alone increased myelination in control sciatic nerves (Nicks et al., 2014). Just like intermittent fasting, mTor inhibition has pleiotropic effects on cellular function and it is unclear what if any effects of mTor inhibition are truly mediated by induction of MA.

As MA is known to degrade organelles and bulk cytosol, one study asked whether MA was necessary for the reduction of cytoplasm during Schwann cell development (Jang et al., 2015). Indeed, the authors found that abaxonal cytoplasm—which is normally lost during the development of myelinating Schwann cells—persisted into adulthood after conditional loss of Atg7 in Schwann cells.

Another study examined the role of MA in myelinating Schwann cells during Wallerian degeneration in the peripheral nervous system (when the part of the axon distal to an injury degenerates) (Gomez-Sanchez et al., 2015). During Wallerian degeneration, there was an increase in autophagosomes (by LC3 immunofluorescence) in dedifferentiating Schwann cells, and some of these autophagosomes appeared to contain myelin (by immunofluorescence and electron microscopy). Moreover, the authors demonstrated that pharmacological inhibition of MA (through disruption of membrane trafficking with 3-methyladenine and inhibition of lysosomal function with bafilomycin and ammonium chloride) and genetic inhibition of MA (through the conditional loss of Atg7) impaired myelin clearance by the dedifferentiating Schwann cells during Wallerian degeneration. These findings were confirmed by another laboratory shortly thereafter (Jang et al., 2016). A recent study expanded on this work, first by confirming that the loss of MA in Schwann cells impairs myelin clearance during Wallerian degeneration (Brosius Lutz et al., 2017). The authors went on to show, however, that Schwann cells also employ TAM receptor-mediated phagocytosis to clear myelin debris during Wallerian degeneration (Brosius Lutz et al., 2017). Importantly, it remains unknown whether MA is necessary for myelin remodeling at baseline conditions in either Schwann cells or oligodendrocytes.

Chapter 3.

Myelin Remodeling is Mediated by Oligodendroglial Macroautophagy

3.1 Introduction

Myelination of axons in the central nervous system (CNS) is critical for the rapid and reliable conduction of action potentials, as evidenced by the severe disabilities associated with myelin loss in multiple sclerosis and other demyelinating diseases. Much is known about OPC specification, oligodendrocyte (OL) differentiation, and myelin formation by OLs, but how myelin is turned over remains unclear.

Decades following their discovery, myelin and OLs were considered static elements in the adult nervous system (Kondiles and Horner, 2017). However, recent evidence shows that myelin in the CNS is actually plastic (Baraban et al., 2016; Scholz et al., 2009; Zatorre et al., 2012), and

that, at least in humans, myelin remodeling is likely mediated by mature OLs (Yeung et al., 2014). As mature OLs have limited capacity to generate new myelin sheaths, we must ask whether mature OLs can remodel the myelin at preexisting myelin sheaths. One intriguing but unproven possibility is that myelin at individual internodes may be remodeled cell-autonomously by mature OLs to modulate neural circuit function.

Macroautophagy (MA) is responsible for the lysosome-mediated elimination of cytosolic proteins, lipids, and organelles, by capturing cargo in a transient, multilamellar organelle known as an autophagosome (AP). MA can act either as a non-selective response to cellular stress such as starvation to degrade bulk cytosol, or as a highly selective quality-control mechanism to degrade aggregated proteins and damaged organelles (Yamamoto and Yue, 2014). Given that MA is the most versatile degradative pathway available to any cell, it has the potential to be able to degrade myelin, which is a mixture of the aggregation-prone, unstructured protein myelin basic protein (MBP), several transmembrane proteins and importantly, membrane. Data from Schwann cells—the myelinating cells of the peripheral nervous system—suggests that during Wallerian differentiation, MA may contribute to myelin turnover (Brosius Lutz et al., 2017; Gomez-Sanchez et al., 2015; Jang et al., 2016). Taken together, we hypothesize that MA in OLs may be important for myelin remodeling in the adult CNS.

3.2 Oligodendrocytes Express the Molecular Machinery of Macroautophagy

To test whether OLs require MA to remodel individual myelin sheaths (also known as internodes), we first asked whether OLs express the molecular machinery necessary for MA. Although previously published RNA sequencing datasets indicate that OLs have the potential to

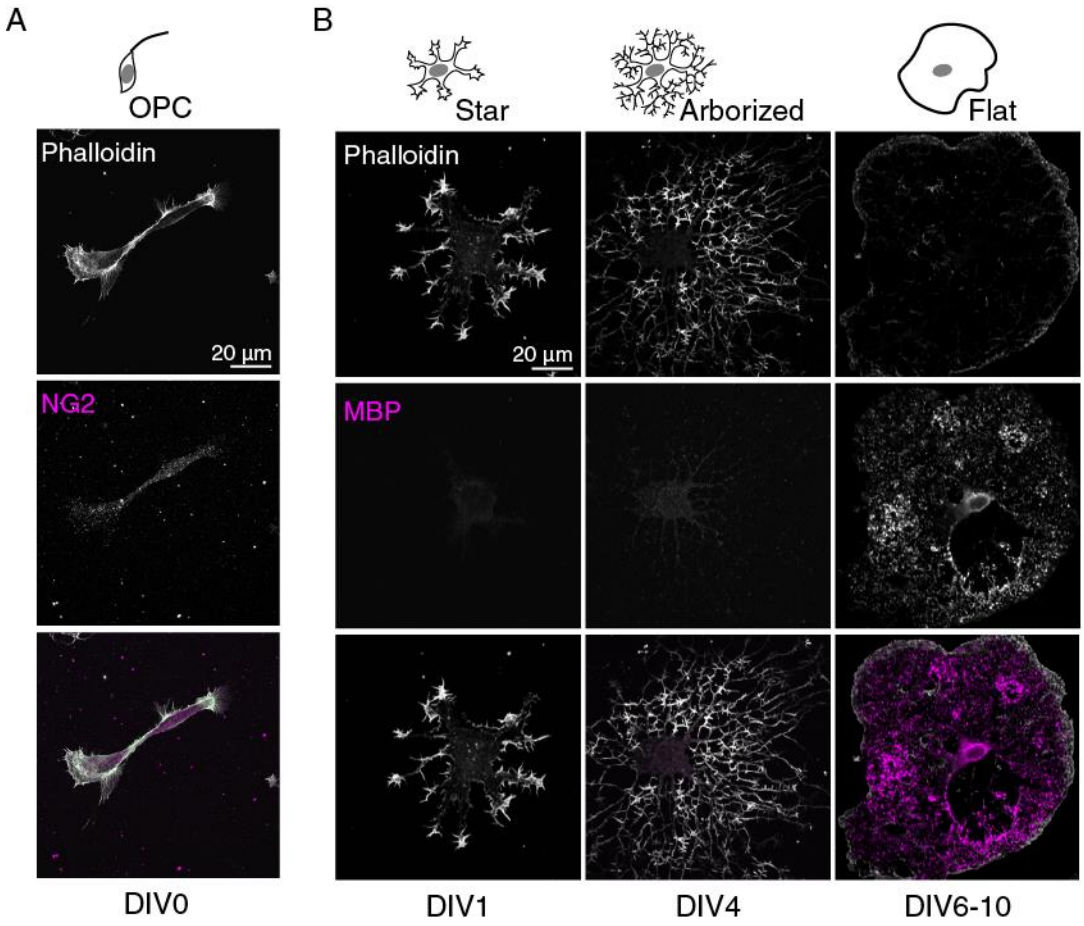

Figure 3.1. **Maturation of OLs *in vitro*.** OPCs are isolated from P6-8 mice then differentiated *in vitro* as described (Emery and Dugas, 2013). A. $NG2^{+}$ (magenta) OPCs. B. OPCs mature through discrete stages over time as described phenotypically using immunofluorescence against phalloidin (white) and MBP (magenta). The number of days *in vitro* (DIV) during the differentiation protocol is indicated at the bottom of the image.

express MA proteins (Zhang et al., 2014), we examined when during OL maturation and where within the cell OLs express key MA-associated proteins. To do this, we used a cell-based approach by isolating oligodendrocyte precursor cells (OPCs) from postnatal day 6-8 mice and induced their differentiation into OLs using the method established by Barres and colleagues (Barres et al., 1992; Emery and Dugas, 2013) (Figure 3.1). Phalloidin staining reveals that over the 6-10 days of differentiation *in vitro*, OPCs undergo a stereotyped series of morphological changes as they differentiate, extending numerous cellular processes to form a branched morphology that subsequently flattens out into a large sheet of myelin akin to several unrolled myelin sheaths fused

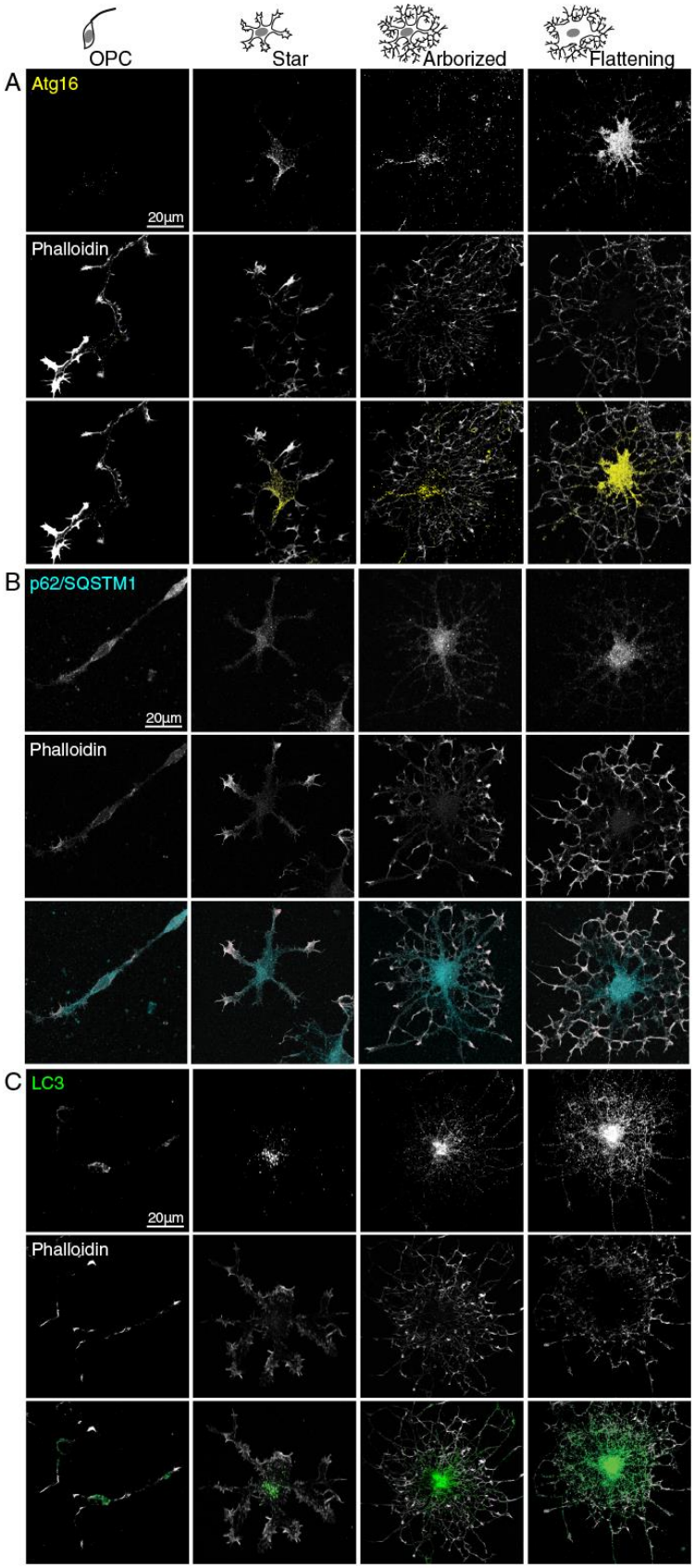

Figure 3.2. Maturation of OLs *in vitro* reveals that the expression of different macroautophagy markers can be found throughout the different stages of OL differentiation. Staining in OPCs and immature stages of OL development against A. Atg16 (yellow), an indicator of early stages of autophagosome biogenesis, B. p62/SQSTM1 (cyan), an adaptor for cargoes destined for degradation by macroautophagy, and C. LC3 (green), a marker for autophagosome-membranes. Staining appears to intensify as the cells mature. Phalloidin is in white. Representative images from n = 100 cells / 3 litters.

together (Figures 3.1A and B) (Zuchero et al., 2015). The presence of the marker neuron-glial antigen 2 (NG2, also known as chondroitin sulfate proteoglycan 4) and MBP confirms the identity of OPCs and mature OLs, respectively (Figures 3.1A and B).

Next, to determine when and where MA is active in the cells, we probed for three different markers commonly used to monitor MA. These cultures were probed for markers of various aspects of MA: Autophagy protein 16 (Atg16), which is found at sites of AP

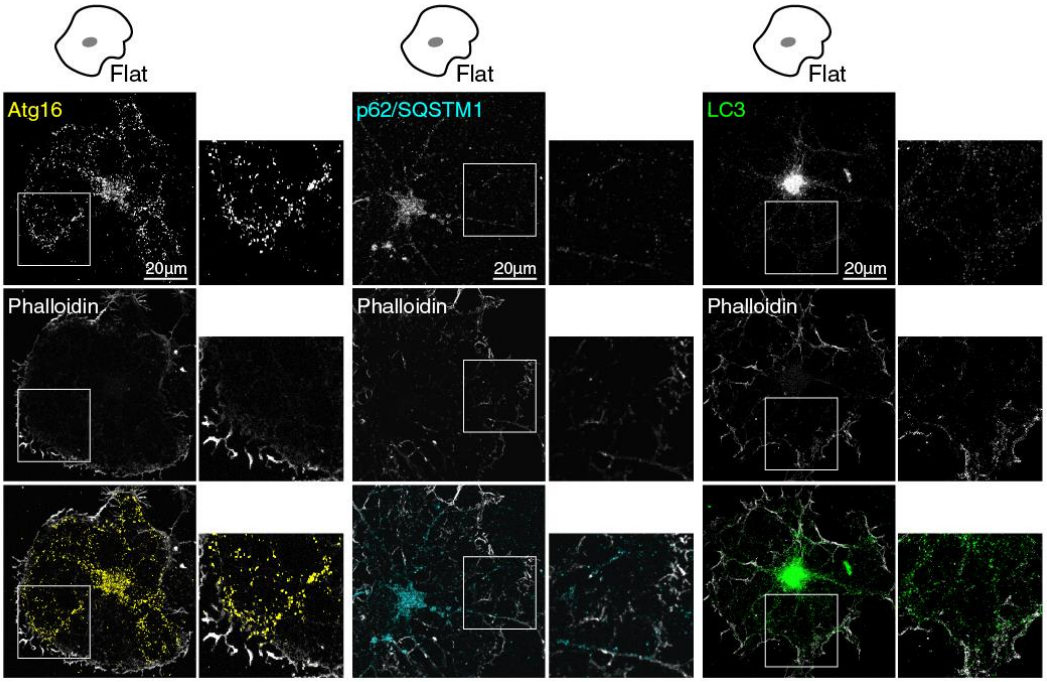

Figure 3.3. Immunofluorescence against different macroautophagy markers in mature OLs. Staining against Atg16 (yellow), p62/SQSTM1 (cyan), and LC3 (green) reveals a strong presence of these markers in the cell body of mature OLs, as well as a notable presence throughout the cell (inset). Phalloidin is in white. Representative images from n = 30 cells / 3 litters.

biogenesis; protein 62/Sequestesome-1 (p62/SQSTM1), a cargo adaptor protein; and microtubule-associated protein 1A/1B-light chain 3 (LC3), which is covalently bound to AP membranes throughout their maturation (Figures 3.2 and 3.3). Throughout the course of differentiation, we found $Atg16^{+}$, $p62^{+}$, or $LC3^{+}$ puncta expressed in the cell body as well as distal processes (Figure 3.2). In mature OLs, all three markers continued to be expressed throughout the entire OL, from the cell body to the cytoplasmic channels dispersed throughout the myelin sheath (Figure 3.3). These data suggest that degradation by MA is not limited to the cell body of the OL, but autophagosome biogenesis and cargo capture can occur even in the most distal regions of the cell, surrounded by the myelin membrane.

3.3 Vesicle Dynamics of Autophagosomes in OLs

To gain a better understanding of where MA was occurring in the mature OL, we used live-cell confocal microscopy of OLs immunoisolated from mice transgenically expressing GFP-tagged LC3 (GFP-LC3) (Mizushima et al., 2004) in the presence of the fluorescent acidotropic probe Lysotracker to better understand the sub-cellular localization of autophagosome biogenesis, trafficking, and acidification (Figure 3.4). As we observed some regional heterogeneity in MA activity throughout the cytoplasmic channels, we devised nomenclature to clarify which regions within the cytoplasmic channels are of interest, as depicted in Figure 3.4A: arteries are the largest cytoplasmic channels, branches are small cytoplasmic channels that are found within the myelin sheath, edges are found at the edge of the cell, and bulbs are enlargements within the cytoplasmic channels, often found at the distal ends of arteries. Due to their location with respect to the myelin sheath, we believe that arteries may correspond to the outer loop and paranodal loop of the myelin sheath, that edges are this culture system's equivalent of the inner loop, and that branches are related to intramyelinic cytoplasmic nanochannels (Snaidero et al., 2014; Snaidero et al., 2017).

A total of 143 cells from 2 independent cultures were imaged for both GFP-LC3 and Lysotracker for at least 60 minutes. The appearance of *de novo* formed GFP-LC3+ puncta, their acidification and their disappearance were analyzed across 6 representative movies with a total of 185 puncta and summarized in Figure 3.4B and C. As expected, most APs formed and acidified in the cell body of OLs; strikingly however, there were a considerable number of APs that both formed and acidified in the cytoplasmic channels within the myelin sheath, appearing at especially high frequency in bulbs and artery-branch intersections (Figure 3.4D). In addition, we found that the time until acidification of APs in OLs varied by subcellular region, and this correlated with distance from the cell body (Figures 3.4E and 3.4F). The movies revealed that most of the APs

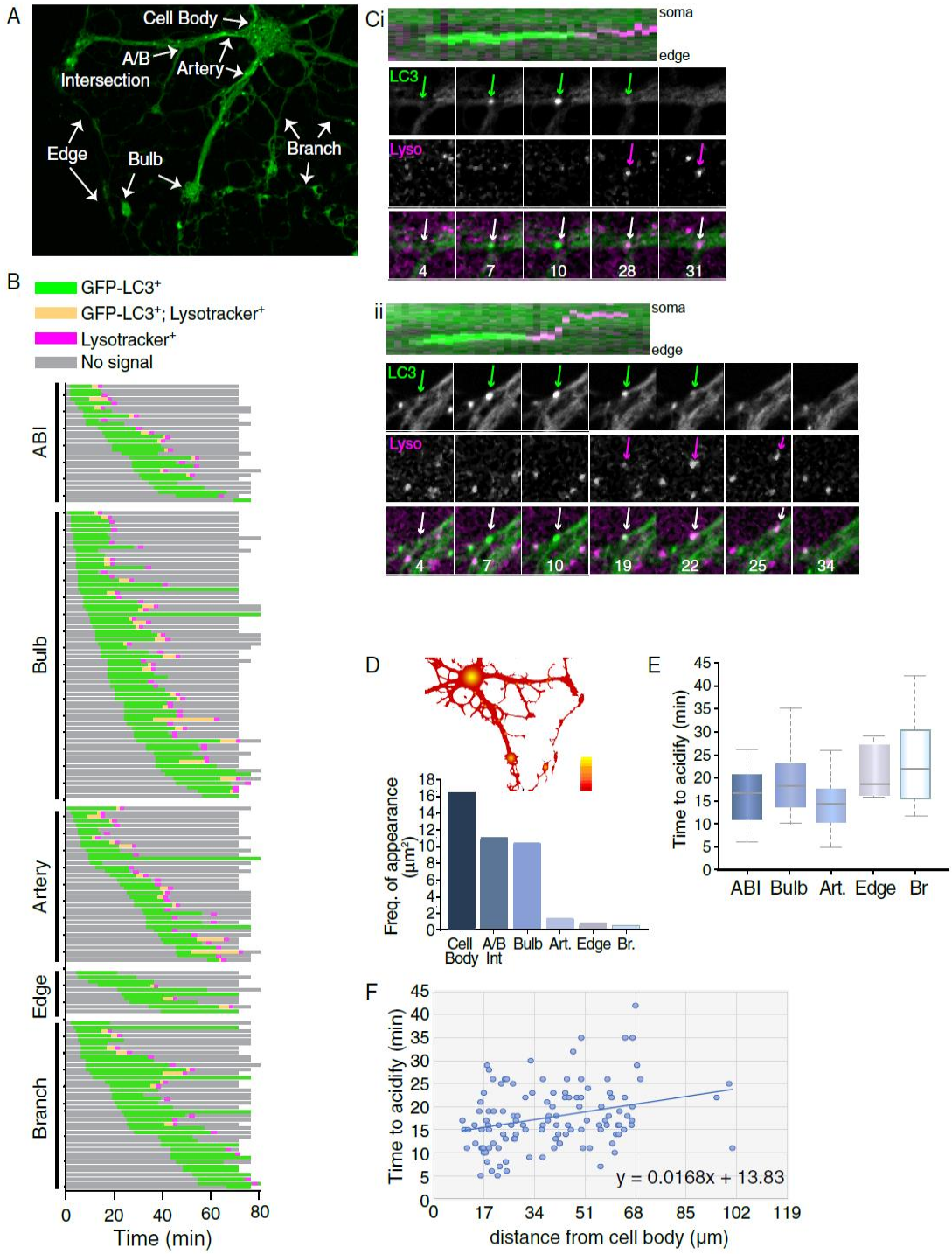

Figure 3.4. Live cell imaging of primary, mature OLs derived from OPCs isolated from GFP-LC3 mice indicate autophagosome formation and maturation can occur throughout the cell.
All live cell imaging was performed in collaboration with Tim Davies and Julie Canman.
A. Regions of the OL. The mature OL is visually divided into discrete regions as indicated: cell body, artery, branch, artery/branch (A/B) intersection, bulb and edge.
B. Summary of the movies analyzed. GFP-LC3 is monitored for autophagosome formation and Lysotracker Red for maturation and lysosome-fusion. Overlay in yellow. The formation of 185 GFP-LC3$^+$ puncta were monitored throughout the cell, then analyzed for time through maturation. Structures that were only Lysotracker$^+$ were not
Continued on next page.

Figure 3.4, Continued from previous page.
analyzed. Movies analyzed from n = 6 cells, N = 2 cultures were representative of the 143 cells from 2 independent cultures that were imaged.
C. Selected frames from videos of puncta in OLs. GFP-LC3 in green, Lysotracker Red in red. Arrows indicate particle of interest.
D. Summary of the location of autophagosome formation. Analyses of the movies indicate that LC3-positive structures can form and mature in all regions of the OL. The schematic representation (top) is quantified as frequency of autophagosome appearance corrected for area (bottom).
E, F. Plot of time required for GFP-LC3 positive vesicles to acidify after formation. Analyses of all imaged GFP-LC3 vesicles that acidify summarized in B. E. Time to acidification in minutes versus region of cell. ABI, Artery-Branch intersection; Art, Artery; Br, Branch. F. Time to acidify in minutes versus the relative distance from the cell body in μm.

acidified where they formed (Figure 3.4C), with only about 20% traveling either towards or away from the cell body before acidification, whereas about 10% traveled towards the cell body after acidification (data not shown).

Given the evidence of AP formation in the comparatively inert cytoplasmic channels of OLs, we asked whether potential membrane sources for the isolation membrane are present there. Although several membrane sources ranging from the plasma membrane (Ravikumar et al., 2010) to mitochondria (Hailey et al., 2010) have been proposed to donate membrane to the growing AP, membranes associated to the endoplasmic reticulum (ER) (Axe et al., 2008; Hamasaki et al., 2013; Hayashi-Nishino et al., 2009, 2010; Uemura et al., 2014) are the most likely source, especially in mammalian cells. We therefore performed immunofluorescence in mature OLs for the integral ER membrane protein calnexin. Immunofluorescence revealed calnexin staining throughout the OL even within small cytoplasmic channels (Figure 3.5). This corroborates previous findings also suggesting the presence of endoplasmic reticulum throughout the OL (Simpson et al., 1997). Taken together, our data indicates that autophagosome biogenesis and maturation can occur throughout the mature OL.

Although the activity of a highly conserved degradation pathway that is known to maintain cellular homeostasis might be expected to occur in the cell body, why APs form and acidify in the myelin sheath, a part of the cell generally believed to be relatively inert was unclear. Given the

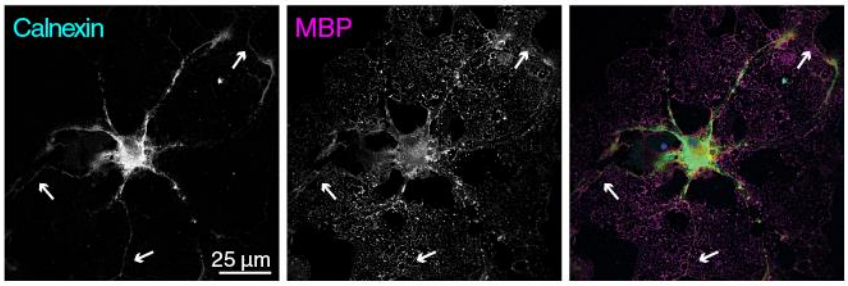

Figure 3.5. The ER-associated, integral membrane protein calnexin is present throughout mature OLs, suggesting that a membrane source for autophagosome biogenesis is available. White arrows indicate the breadth of calnexin expression. Calnexin (cyan), MBP (magenta), and Dapi (blue). Representative images from n = 20 cells/2 cultures.

degradative capacity of MA and that myelin is a tightly organized structure of membrane and proteins, we hypothesized that MA could degrade myelin associated proteins as cargo. One protein with strong potential is MBP, which is a natively highly unstructured protein that can homo-mulitmerize (Boggs, 2006). Given that proteins like MBP have a high propensity towards aggregation, they are prime cargo for degradation by selective-autophagy, a form of MA that degrades cargos upon recognition by adaptor proteins such as p62/SQSTM1. To address this, we used confocal microscopy to determine whether MBP can colocalize with APs, as identified by $LC3^{+}$ puncta. Under basal conditions, we detected colocalization of MBP with LC3 in discrete puncta in most cells, but within each cell it was a relatively infrequent event (Figure 3.6, left). Treatment with the mild lysosomal inhibitor leupeptin increased the prevalence of this event, which is typical of cargoes trafficked for degradation by MA (Figure 3.6, right). These data suggest that MA may be responsible for trafficking components of the myelin sheath to the lysosome for degradation.

3.4 Loss of Macroautophagy in OLs *In Vivo* Does Not Affect the Development of OLs or Myelin

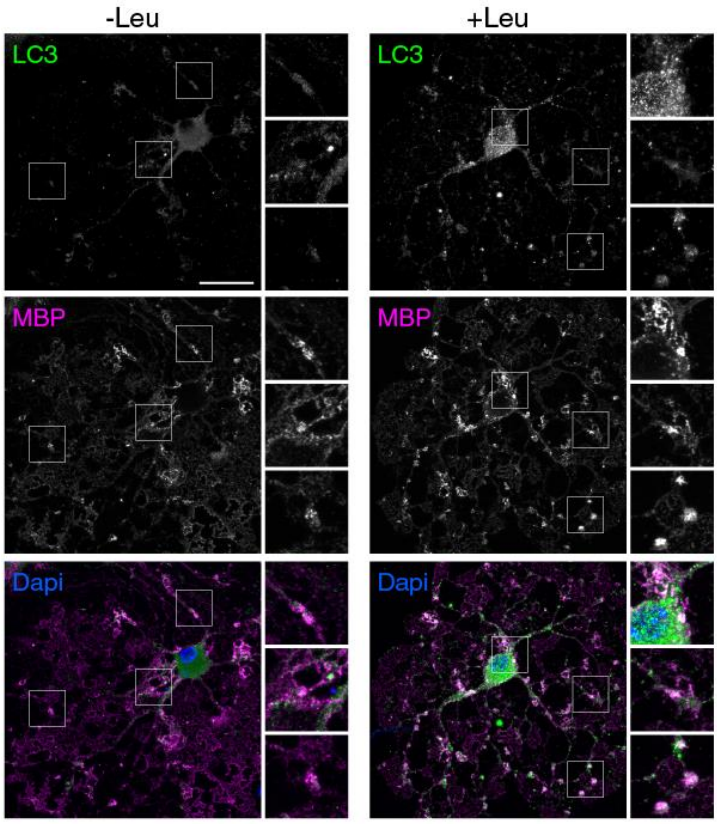

Figure 3.6. Co-localization of MBP in autophagosomes suggest that myelin associated proteins are degraded by macroautophagy. MBP (magenta) and endogenous LC3 (green) staining indicate that co-localization can occur throughout the cell. Leupeptin (Leu) treatment, which mildly impedes lysosome-function and leads to autophagosome accumulation, increases the autophagosome accumulation as shown by LC3 staining. Representative images from n = 90 cells/5 cultures. Scale bar is 25 µm.

Having established that APs carrying the myelin-associated protein MBP are forming and acidifying in the cytoplasmic channels of cultured OLs, we decided to ask whether MA had any functional significance in OLs *in vivo*, either in myelin development or in myelin remodeling. To test this, we conditionally deleted *Autophagy related-protein 7*, *Atg7*, an E1-like ligase essential for LC3 conjugation in MA, in early OLs. To do so, we bred mice carrying a conditional allele for *Atg7* ($Atg7^{fl/fl}$) (Komatsu et al., 2005) and Cre recombinase knocked into the *2',3'-cyclic-nucleotide 3'-phosphodiesterase* (*CNP1*) locus (CNP^{Cre}) (Lappe-Siefke et al., 2003) to create Atg7(CNP) conditional knockout (cKO) mice. CNP is expressed by early OLs at the start of myelination (Chandross et al., 1999), and CNP^{Cre} has been used across multiple studies to establish

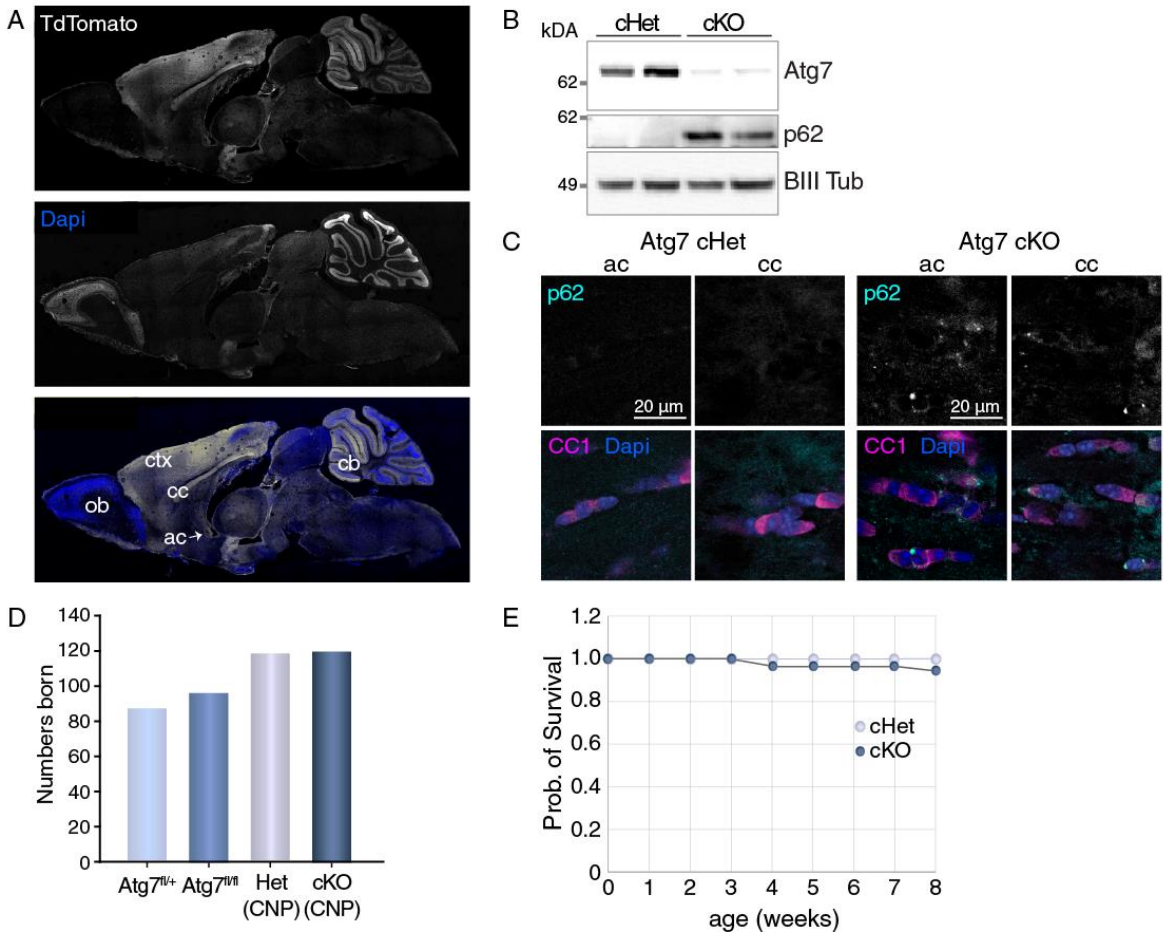

Figure 3.7. CNP^{Cre}-mediated inactivation of macroautophagy *in vivo:* Atg7(CNP) cKO mice.
A. TdTomato expression pattern resulting from CNP^{Cre} mice crossed to the Ai9 reporter line. TdTomato (white) demonstrates clear expression in corpus callosum (cc), anterior commissure (ac), cortex (ctx) and cerebellum (cb). Little to no expression was detected in olfactory bulb (ob).
B. Western blot of isolated white matter from spinal cord in Atg7(CNP) conditional heterozygous (cHet) mice and Atg7(CNP) conditional knockout (cKO) mice. Immunoblotting reveals a significant loss of Atg7. p62 levels are also higher in cKO white matter, consistent with an inactivation of macroautophagy.
C. Co-immunofluorescence of CC1^{+} cells in anterior commissure (ac) and corpus callosum (cc) reveal p62-positive puncta in Atg7(CNP) cKO tissue. P62 (cyan), CC1 (magenta), and dapi (blue).
D. Number of littermate genotypes born across 60 litters. Atg7(CNP) cHet (Het) and Atg7(CNP) cKO mice are born in numbers comparable to each other.
E. Survival plot of Atg7(CNP) cHet and cKO mice through 2 months of age reveals no difference in survival despite the loss of macroautophagy in OLs.

the role of protein in developing and mature OLs (Emery et al., 2009; Hussien et al., 2015; Zuchero et al., 2015). As the heterozygous loss of *CNP1* has been suggested to have a mild phenotype at 19 months and older, we compared Atg7(CNP) cKO mice to Atg7(CNP) conditional heterozygous (cHet) littermates in all experiments to control for any such effects (Hagemeyer et al., 2012).

We first confirmed that CNP^{Cre} drives recombination in white matter tracts, such as the corpus callosum and anterior commissure, by crossing CNP^{Cre} with the conditional fluorescent reporter *Gt(ROSA)26Sor*$^{tm9(CAG-tdTomato)Hze}$ (Ai9) (Madisen et al., 2010), such that any cell in which recombination had occurred would express the red fluorescent protein variant TdTomato (Figure 3.7A). Consistent with these results, immunoblotting of protein in microdissected CNS white matter from Atg7(CNP) cHet and cKO littermates confirmed the loss of Atg7 in cKO tissue. Consistent with the loss of MA in this tissue, immunoblotting against p62 revealed that it was accumulating (Figures 3.7B). Immunofluoresence against p62 in brains from Atg7(CNP) cHet and cKO revealed that this accumulation was specifically found in cells expressing CC1, a marker of mature OLs, in both the anterior commissure and corpus callosum (Figure 3.7C).

Given the importance of MA as a cellular process, and its prevalence through the stages of OL maturation revealed in vitro (Figures 3.2 and 3.3), it is possible that the loss of MA in CNP-positive cells would lead to a failure of myelination in the Atg7(CNP) cKO mice leading to death before the mice reached maturity. To account for the possibility of developmental failure in these mice, we compared the birth and survival rates of Atg7(CNP) cKO mice with that of Atg7(CNP) cHet mice and found that both were born and reached maturity at similar rates (Figures 3.7D and 3.7E), strongly suggesting that myelination may be proceeding normally. To explore further whether Atg7(CNP) cKO mice were indeed grossly normal at two months of age, we assessed spontaneous exploratory and locomotor behavior using the open field test, in which mice explore a novel environment for one hour. In both male and female mice, there was no difference across all genotypes in the total distance traveled or number of rearing events during that hour (Figure 3.8). Importantly, no difference was observed between CNP^{Cre}-carrying mice and $Atg7^{fl/fl}$ littermates, indicating that the presence of the CNP^{Cre} did not grossly impact the mice at this age.

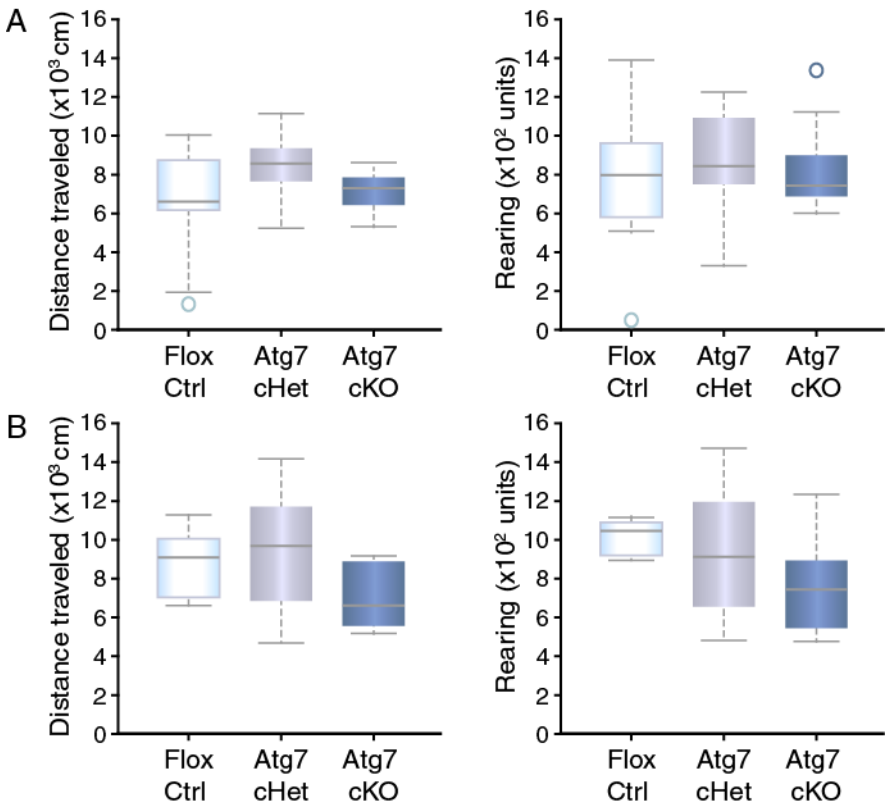

Figure 3.8. CNP^{Cre}-mediated inactivation of macroautophagy *in vivo* leads to no noticeable behavioral phenotype in the first two months of life.
Open Field analyses indicate that spontaneous locomotor behavior is normal in Atg7(CNP) cKO mice at 2 months of age (mo). Total distance traveled and rearing behavior of Atg7$^{fl/fl}$, Atg7(CNP) cHet and Atg7 cKO male (A) and female (B) mice over one hour. The inclusion of Atg7$^{fl/fl}$ mice reveal that the introduction of CNP^{Cre} has no impact on the behaviors performed.
A. Male mice. ANOVA reveals no significant difference between 'genotype' and 'total distance traveled ($F_{(2,24)}$ = 1.018; p = 0.377) or between 'genotype' and 'rearing' ($F_{(2,24)}$ = 0.332; p = 0.721).) n=9 mice per genotype.
B. Female mice. ANOVA reveals no significant difference between 'genotype' and 'total distance travelled ($F_{(2,24)}$ = 2.684, p = 0.089) or between 'genotype' and 'rearing' ($F_{(2,24)}$ = 3.076, p = 0.065).) n=9 mice per genotype.

These results corroborated our impression that home cage behavior of 2 mo Atg7(CNP) cKO mice is no different than that of Atg7(CNP) cHet mice (not shown).

To assess more directly how the loss of MA might affect myelination, we first examined two fundamental parameters in OL development: OPC number and OL number. The number of OPCs and OLs were quantified in corpus callosum of Atg7(CNP) cHet and cKO mice at two months of age. OPCs were identified by the presence of NG2, and OLs by the presence of oligodendroctye transcription factor 2 (Olig2) and positivity for staining with the antibody CC1,

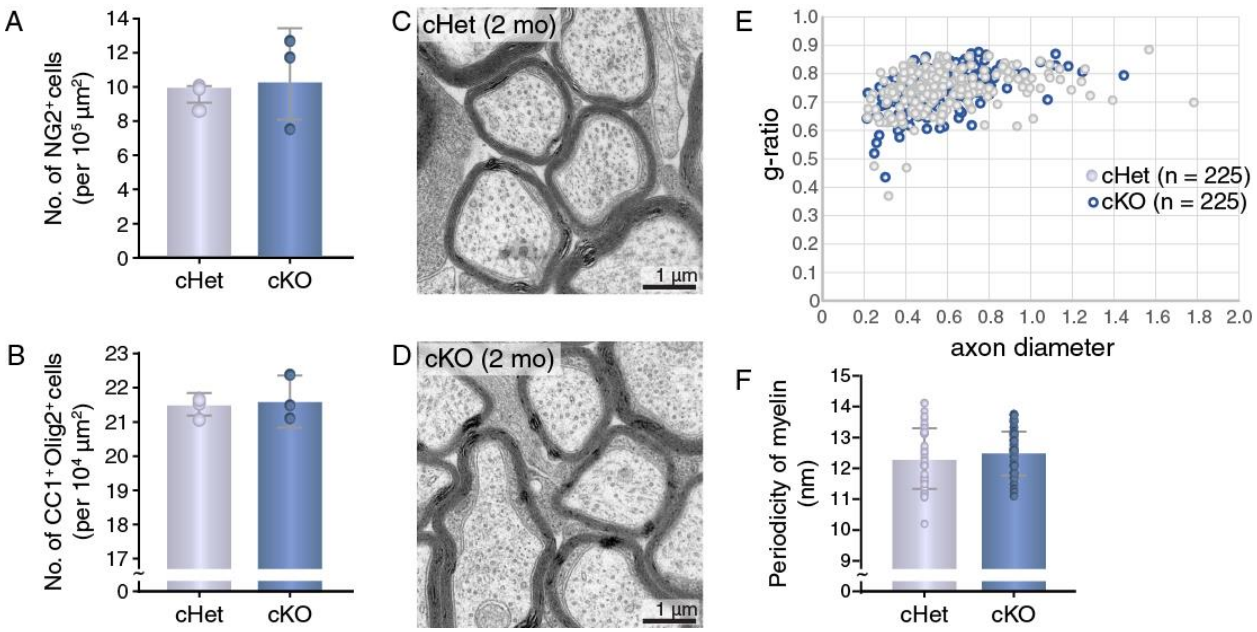

Figure 3.9. CNP^{Cre}-mediated inactivation of autophagy *in vivo* leads to no noticeable changes in myelin during the first two months of life.
A, B. Quantification of NG2$^+$ cells (A) and CC1$^+$/Olig2$^+$ cells (B) reveal no significant difference across genotype. Statistics: Student 2-tailed, unpaired t-test reveals no significant difference in NG2$^+$ cell number ($p = 0.603$) or CC1$^+$/Olig2$^+$ cell number ($p = 0.874$) between cHet and cKO mice. n = 3 brains/genotype. Bar chart plots mean ± St. Dev. Individual data points are plotted.
C-E. G-ratio analysis of EM images of optic nerve from 2-month-old (2 mo) Atg7 cHet (I) and cKO (J) mice reveal no significant difference in myelination. The myelin g-ratio of 225 axons/3 brains/genotype are plotted as a scatterplot (E).
F. Periodicity of myelin is unaffected in Atg7 cKO optic nerve. Statistics: Student 2-tailed, unpaired t-test reveals no significant difference between genotype ($p = 0.291$). n = 45 axons/3 brains/genotype. Bar chart plots mean ± St. Dev. Individual data points are plotted.

which has recently been found to identify the RNA binding protein Quaking 7 (Bin et al., 2016). We found no significant difference in either cell number across genotype (Figures 3.9A and 3.9B), indicating that the capacity for and ability to differentiate into mature OLs were unaffected by the loss of MA.

Next, to determine whether myelin formation occurred normally in these mice, we directly examined their myelin sheaths using transmission electron microscopy (EM). Given the heterogeneity of myelination in the corpus callosum, we examined the optic nerve, which is more uniformly myelinated. We found no measureable differences in either myelin sheath thickness, as measured by g-ratio, or periodicity in Atg7(CNP) cHet and Atg7(CNP) cKO optic nerve,

indicating that myelin formation was unimpeded despite the loss of MA (Figures 3.9C-F). This is consistent with previous studies that conditionally inactivated MA throughout the CNS using Nestin^{Cre}, all of which survived to adulthood without any reported deficits in myelination (Komatsu et al. 2006, Hara et al. 2006, Liang et al. 2010).

3.5 Loss of Macroautophagy in OLs *In Vivo* Leads to an Age-Dependent Increase in Myelin Thickness and Aberrant Myelin Outfoldings

Despite the normal development of OLs and CNS myelin in these animals, there was a variable penetrance of premature lethality that onset in adult Atg7(CNP) cKO mice (Figure 3.10A). Further in-cage observations of the mice revealed the late onset of tremor and motor disturbances (not shown). This unusual phenomenon of adult-onset deficits in a mouse with an OL-specific mutation further motivated us to test the hypothesis that MA was important for either myelin maintenance or remodeling in adult mice. To examine the myelin sheath, we performed EM-based studies of myelination of optic nerve. Although at two months of age, myelin structure was normal in Atg7(CNP) cKO mice, at 9 and 16 months of age it appeared as if myelin thickness of the optic nerve of Atg7(CNP) cKO mice was increasing over time (Figures 3.10B-D). Given the changes observed in optic nerve, we next examined corpus callosum from 16 mo Atg7(CNP) cKO mice, which revealed abnormally thick myelin secondary to a failure of myelin remodeling as well (Figure 3.10E). This suggests that OLs continuously remodel their myelin sheaths; OLs are regularly adding new myelin to their sheaths while continuously removing an equivalent amount of myelin. Without the degradative capacity of MA in OLs however, this delicate balance is disrupted, leading to the observed increase in myelin at the internode. These changes may have a

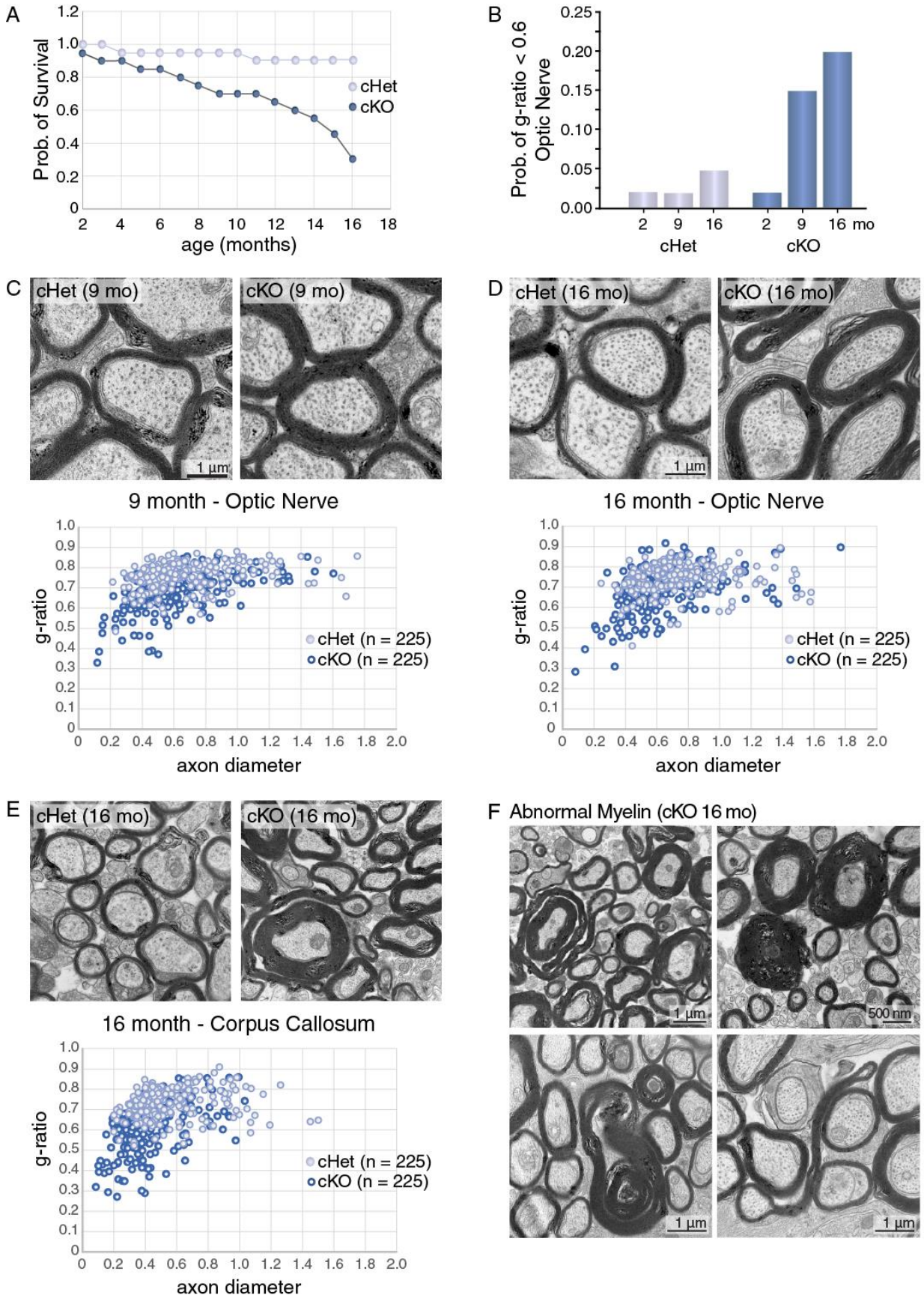
A
Prob. of Survival
age (months)
cHet
cKO
B
Prob. of g-ratio < 0.6
Optic Nerve
cHet
cKO
C
cHet (9 mo)
cKO (9 mo)
1 µm
9 month - Optic Nerve
g-ratio
axon diameter
cHet (n = 225)
cKO (n = 225)
D
cHet (16 mo)
cKO (16 mo)
1 µm
16 month - Optic Nerve
g-ratio
axon diameter
cHet (n = 225)
cKO (n = 225)
E
cHet (16 mo)
cKO (16 mo)
16 month - Corpus Callosum
g-ratio
axon diameter
cHet (n = 225)
cKO (n = 225)
F Abnormal Myelin (cKO 16 mo)
1 µm
500 nm
1 µm
1 µm

Figure 3.10. Adult Atg7(CNP) cKO mice reveal a requirement for macroautophagy to maintain myelin size and structure in the adult.
A. Survival plot of Atg7(CNP) cHet and cKO mice starting from 2 mo. Atg7(CNP) cKO mice demonstrate premature lethality in adulthood starting from around 6 mo.
B-D. Analysis of myelin g-ratio of optic nerve across several ages suggests increasing myelin thickness over time. B. Probability of finding myelin g-ratio greater than 0.6 of 225 axons examined at 2, 9, and 16 mo of Atg7 cHet and cKO optic nerves. C, D. Ultrastructural images of cHet and cKO optic nerves, and respective myelin g-ratio analyses from 9 mo (C) and 16 mo (D) mice. n = 3 brains/genotype.
E. Ultrastructural analysis of 16 mo corpus callosum reveals a dramatic difference between cHet and cKO myelin g-ratio. N = 3 brains/genotype.
F. Redundant myelin and abnormal myelin structures in 16 mo cKO corpus callosum (top) and optic nerve (bottom).

profound effect on CNS function, as conduction velocity is quite sensitive to even small changes in the thickness of the myelin sheath relative to axon caliber (Smith and Koles, 1970). It should be noted that although myelin remodeling was disrupted secondary to the loss of MA in OLs, the periodicity of the myelin was no different between Atg7(CNP) cHet and cKO mice (Figure 3.11A).

In addition to increased myelin thickness, we also discovered many abnormal myelin structures in the optic nerve and corpus callosum of Atg7(CNP) cKO mice at older ages, most notably redundant myelin (also known as myelin outfoldings) and myelin whorls (Figures 3.10F and 11B). These aberrant myelin structures reinforce the hypothesis that the loss of MA in OLs precludes the proper remodeling of myelin *in vivo*, as its absence causes the OL to fail to properly regulate myelin size and structure at the internode.

Beyond OLs, CNP^{Cre} also expresses in the myelinating cells of the peripheral nervous system, the Schwann cell (SC) (Chandross et al., 1999). A recent series of studies indicated that the loss of MA in SCs has no impact on their ability to form myelin (Gomez-Sanchez et al., 2015; Jang et al., 2016; Jang et al., 2015). Given the importance of MA for myelin remodeling in adult OLs of the central nervous system, we examined SCs in 16 mo sciatic nerves from Atg7(CNP) cHet and cKO mice. Consistent with previous findings, we observed no alteration in myelin thickness or structure in the peripheral nervous system of the Atg7(CNP) cKO mice (Figure

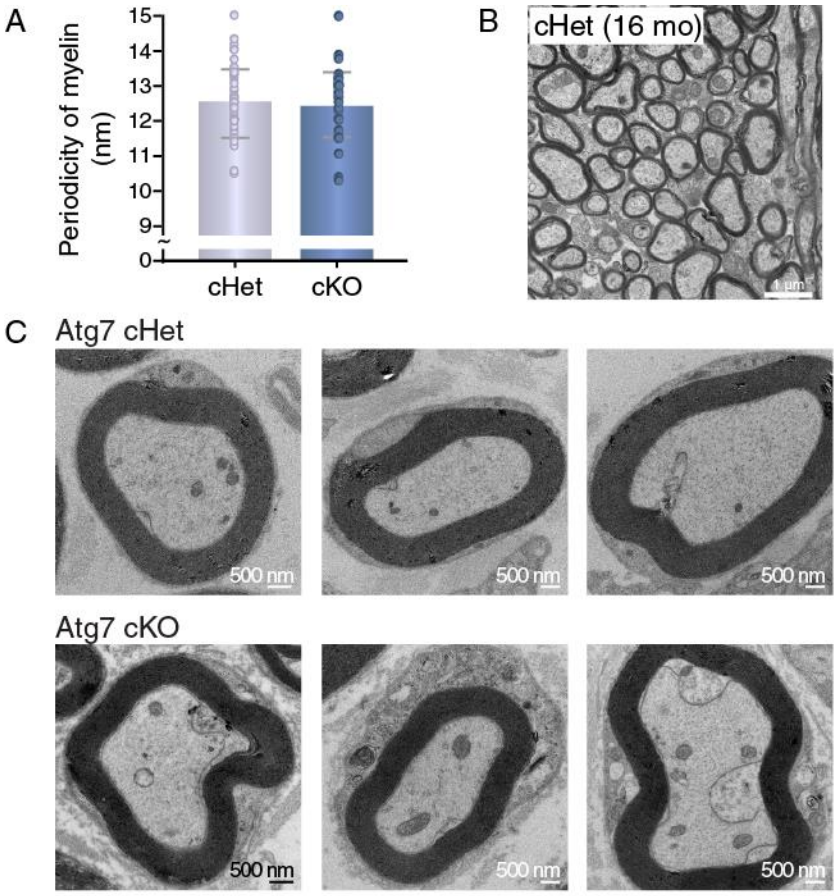

Figure 3.11. Atg7(CNP) cKO mice demonstrate an accumulation of myelin, suggestive of diminished myelin remodeling, at 9 and 16 mo.
A. Myelin periodicity was measured for myelin in the corpus callosum at 16 mo, as described for Figure 3L. Bars represent mean±St. Dev. Individual data points are also plotted. Unpaired, two-tailed Student t-test reveal no significant difference between Atg7(CNP) cHet (cHet) or cKO mice ($p = 0.714$; n=45 myelinated axons / genotype; n=3 brains / genotype.
B. Ultrastructural image from corpus callosum of 16 mo cHet mice.
C. Myelination by Schwann cells is unaffected in Atg7 cKO mice. Sciatic nerve from 16 mo Atg7 cHet and Atg7 cKO mice.

3.11C). These data indicate a fundamental difference in how OLs and SCs rely on MA, suggesting several possibilities, including that myelin remodeling in SC occurs in a MA-independent manner, that SC myelin is not remodeled, or the loss of MA has been compensated for in SCs.

3.6 Cytoplasmic and membranous components of myelin accumulate upon the loss of MA

To gain further insight into the mechanism through which MA impacts myelin turnover, we turned to MA-incompetent OLs in culture. To ensure that Cre-mediated recombination had occurred in the cells we studied, we took advantage of the Ai9 reporter line and monitored for the expression of TdTomato. Given that the *Rosa26* locus and *Atg7* are both on chromosome 6, we crossed CNP-Cre::Ai9 mice with mice expressing the conditional allele for *Atg5* ($Atg5^{fl/fl}$). Atg5

is an essential component of the E3-like ligase required for autophagosome biogenesis, and loss of *Atg7* and *Atg5* in the CNS cause comparable phenotypes (Geng and Klionsky, 2008; Hara et al., 2006; Komatsu et al., 2006).

Isolation of OPCs and their subsequent differentiation to OLs revealed that CNP^{Cre} expression can be active as early as the OPC stage (Figure 3.12A), and the loss of *Atg5* has no noticeable impact on OL differentiation, consistent with the *in vivo* findings in Atg7(CNP) cKO mice (Figures 3.12B and C). Immunoblotting of detergent soluble lysates generated from these cultures confirmed the loss of Atg5 expression and of the corresponding Atg12-5 conjugate, leading to the loss of the faster running LC3 form II, indicative of a loss of conjugation of LC3 to AP membranes (Figure 3.12D). Moreover, immunoblotting of the detergent insoluble pool revealed an accumulation of MBP in Atg5(CNP) cKO cultures, suggestive that the protein was accumulating and aggregating. Higher exposures of the blot of MBP shows that it smears to higher molecular weights, also suggesting aggregation. Co-immunofluorescence for p62 and MBP in OLs confirmed these findings: Not only did it reveal the typical accumulation of punctate p62 structures that have been reported upon the loss of Atg5 or 7 (Komatsu et al., 2007), but many of the $p62^{+}$ puncta in the cytoplasmic channels of Atg5(CNP) cKO OLs were also positive for MBP, which was also accumulating throughout the cell (Figure 3.12E). These data strongly suggest that MBP can be degraded by MA in a p62-dependent manner.

We next examined the status of integral membrane protein components of myelin, specifically MOG and PLP, upon the loss of MA (Figures 3.13A and B). Unexpectedly, but consistent with the myelin phenotype we observed in aging Atg7(CNP) cKO mice, immunofluorescence revealed an increased accumulation of structures that were positive for MOG and PLP in the Atg5(CNP) cKO OLs. Accumulation of these proteins was found throughout the

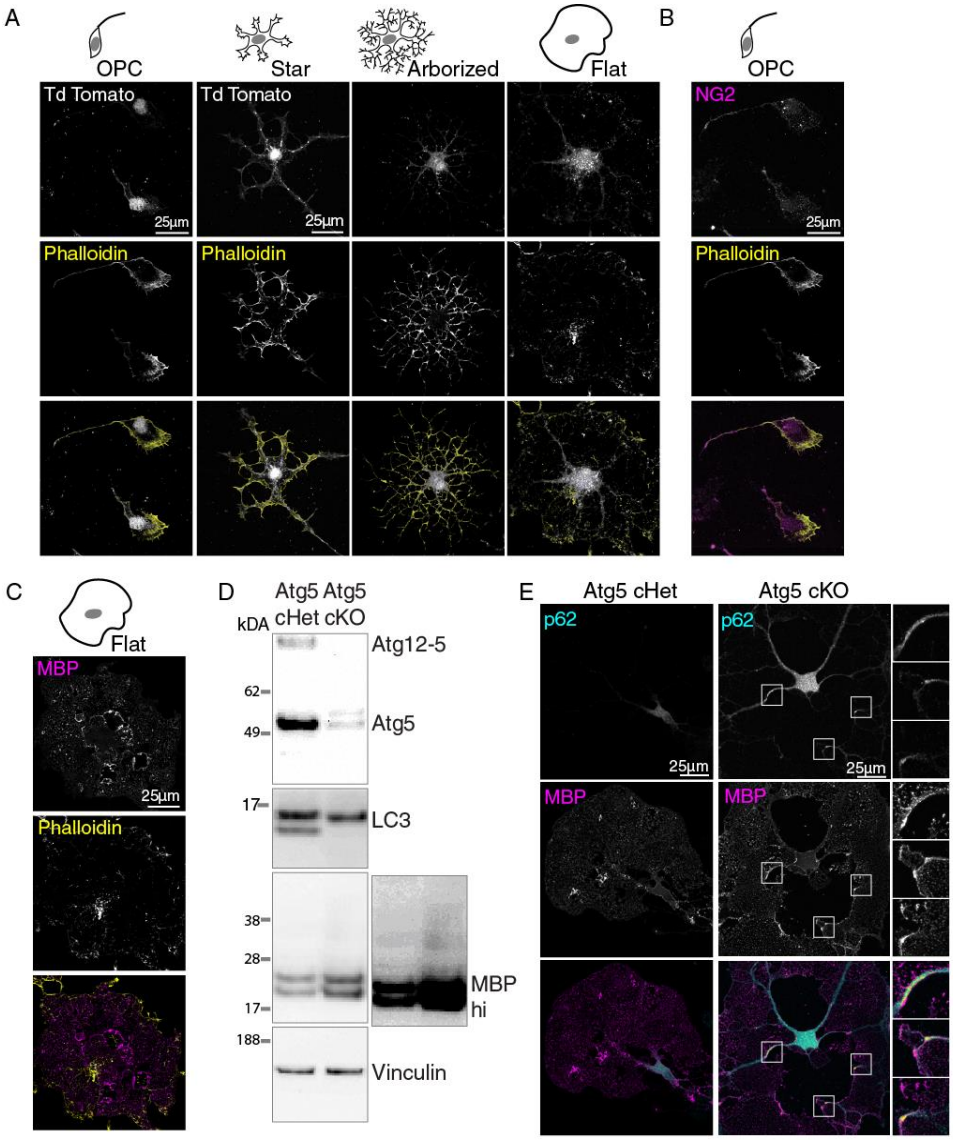

Figure 3.12. OL cultures from Atg5(CNP) cKO mice.
A-C. Primary OL cultures derived from P6-8 Atg5(CNP) cKO mice express Td-Tomato. To monitor CNP-Cre activity, Atg5fl/fl mice were crossed to the Ai9 TdTomato expressing reporter line. Given that the Rosa26 locus and Atg7 locus are on the same chromosone, Atg5fl/fl mice had to be used. A. TdTomato expression is present across the stages of OL maturation in culture. TdTomato (white), Phalloidin (yellow). B. To confirm OPC stage, cells were also stained for the presence of NG2, and checked for the presence of TdTomato. More than half, but not all OPCs expressed TdTomato. C. Similarly, mature OL stage was confirmed by staining with MBP.
D. Western Blot analysis of 1% Tx-100-soluble and -insoluble lysates from cultured Atg5(CNP) cHet and cKO cells. Immunoblotting for Atg5 reveals loss of Atg5 and Atg12-5 conjugate, as well as diminished conversion of cytosolic LC3 (LC3 I) to membrane bound LC3 (LC3 II). Probing the detergent insoluble pellet indicates greater accumulation of MBP suggesting that it is aggregating. High exposure of MBP shows that MBP is not only accumulating, but laddering, further suggestive of aggregation. Representative blot from n = 3 independent cultures/genotype.
E. Co-immunofluorescence of p62 and MBP in Atg5 cKO OLs. Accumulation of p62 (cyan) can be detected throughout the OL. Co-staining for MBP (magenta) reveals that regions of p62 accumulation also have high MBP, suggesting that aggregates of MBP are recognized by p62 (shown in inset). Images shown are maximum projections from a confocal z-stack. Representative images from n = 60 cells/3 independent cultures/genotype.

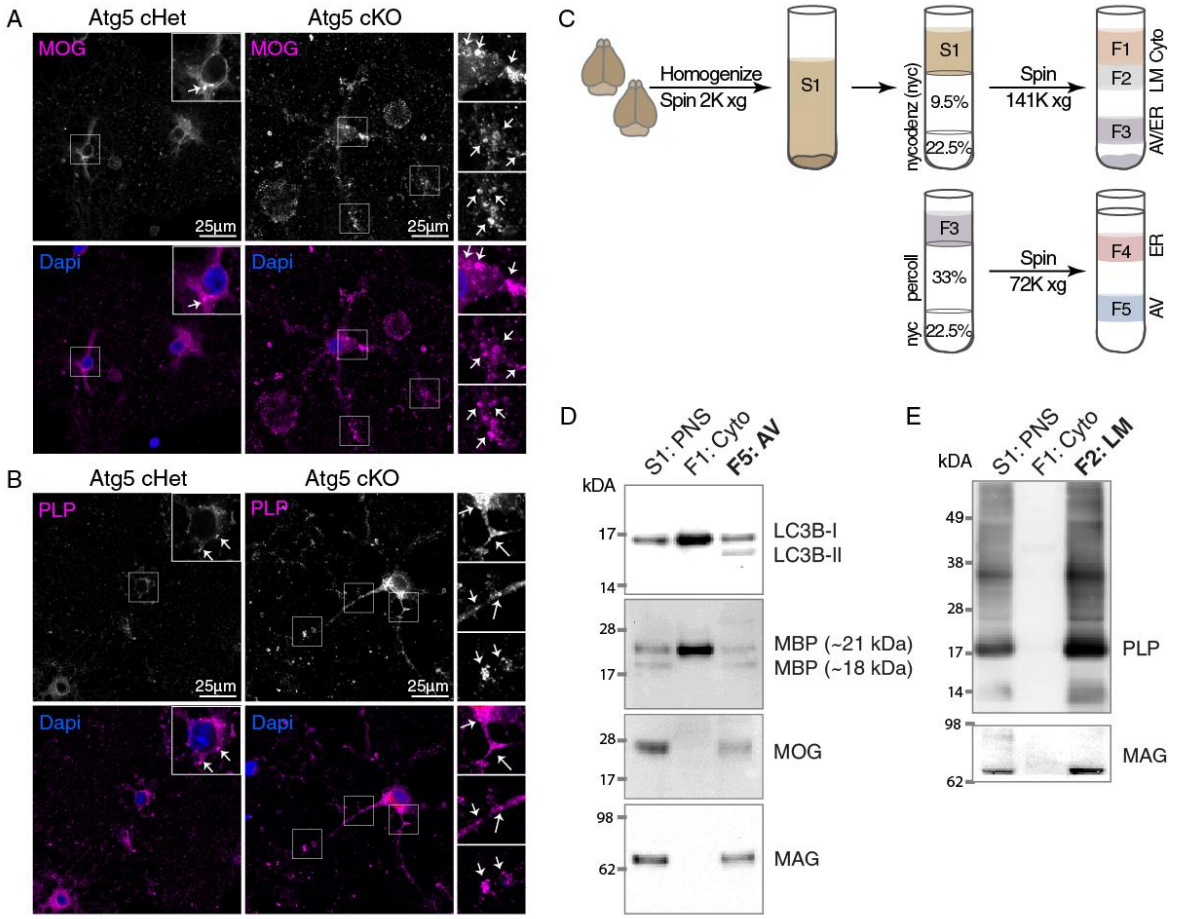

Figure 3.13. Myelin associated proteins are eliminated by autophagy.
A, B. Immunofluorescence of myelin associated integral membrane proteins in Atg5 cKO OLs. Staining for MOG (A) and PLP (B) reveal that both proteins accumulate in Atg5 cKO OLs. Areas of interest are shown in higher magnification. Images shown are maximum projections from a confocal z-stack. Representative images from n = 60 cells/3 independent cultures/genotype.
C-E. Fractionation of adult brain homogenates reveal that myelin associated proteins can be found in the autophagic vacuole (AV) fraction. C. Fractionation protocol as adapted from Stromhaug et al., 1998 for autophagic vacuoles, which collectively encompasses autophagosomes, as well as more mature structures that have fused into the endolysosomal system. Fractionation of the postnuclear supernatant (PNS, S1) across a step gradient of nycodenz (nyc) segregates S1 into 3 fractions (F1, F2, F3) and a mitochondrial pellet. F1 represents the cytosol (Cyto), F2 the light membrane (LM) fraction, and F3 a mixed fraction of autophagic vacuoles and ER (AV/ER). Further fractionation across a Percoll gradient segregates F3 into fractions F4 and F5. The dense-most fraction, F5 enriches for AVs. D. Immunoblotting of PNS, Cyto and AV fractions reveal that presence of MBP, MOG and MAG in the AV fraction. E. Fraction F2 generates the light membrane (LM) fraction, in which cholesterol and sphingolipid enriched membranes fractionate. Probing for myelin proteins PLP and MAG demonstrate that myelin proteins enrich in this light fraction. Fractions from n = 5 brains/preparation. N = 3 independent preparations.

cell, including within the cytoplasmic channels, similar to MBP (Figure 3.12E). These data indicate that disruption of MA leads to an accumulation of membrane components as well.

Like all integral membrane proteins, the integral membrane proteins of the myelin sheath would be expected to be degraded through the endolysosomal system, and previous studies have suggested this as well (Notterpek et al., 1997; Winterstein et al., 2008). Although MA directly encapsulates cytosolic cargoes upon AP formation, during the course of maturation, it can fuse into the endolysosomal system to form an intermediate structure known as the amphisome (Berg et al., 1998; Fengsrud et al., 2000; Gordon and Seglen, 1988; Stromhaug and Seglen, 1993). This stepwise maturation step has been suggested to enhance the efficiency of lysosomal-degradation (Filimonenko et al., 2007; Kochl et al., 2006; Razi et al., 2009). To first confirm if myelin proteins can be found in amphisomes *in vivo*, we used an established protocol involving differential and density gradient centrifugations to enrich for autophagosomes, amphisomes, and autolysosomes, which are collectively known as autophagic vacuoles (AVs) (Stromhaug et al., 1998). Wildtype adult brains were homogenized then fractionated, and the PNS, cytosol, AV and light membrane (LM) fractions were probed for the presence of myelin proteins (Figures 3.13C-E). As expected, the LM fraction, which enriches for sterol and sphingolipid membranes, enriched for myelin proteins (Figure 3.13E). Nonetheless, the far denser AV fraction, identified by the presence of LC3 form II, also contained the myelin proteins MBP, MOG, and MAG under basal conditions. This *in vivo* data suggests that integral membrane myelin proteins are found in AVs, leading to our hypothesis that the turnover of integral membrane myelin associated proteins traffic through an amphisome to be degraded by the lysosome.

3.7 Amphisome formation is required for the turnover of myelin associated proteins in mature OLs.

To test our hypothesis, we first confirmed that integral membrane proteins such as MOG are continuously internalized from the cell surface in Atg5(CNP) cKO OLs. To do so, we labeled the OL cell surface overnight with mCLING, a fluorescently-labeled fixable probe that efficiently labels the plasma membrane (Revelo et al., 2014), and then probed for MOG. MOG^+ structures in the cell body of both Atg5(CNP) cHet and cKO OLs were also $mCLING^+$, suggesting that membrane from the cell surface was incorporated into these MOG^+ structures (Figure 3.14A). These structures were found throughout the cell, indicating that this event is not limited to the cell body. Moreover, the loss of MA did not impede this event, therefore implying that the accumulation of MOG and PLP in the cKO cells is due to continuous internalization of these

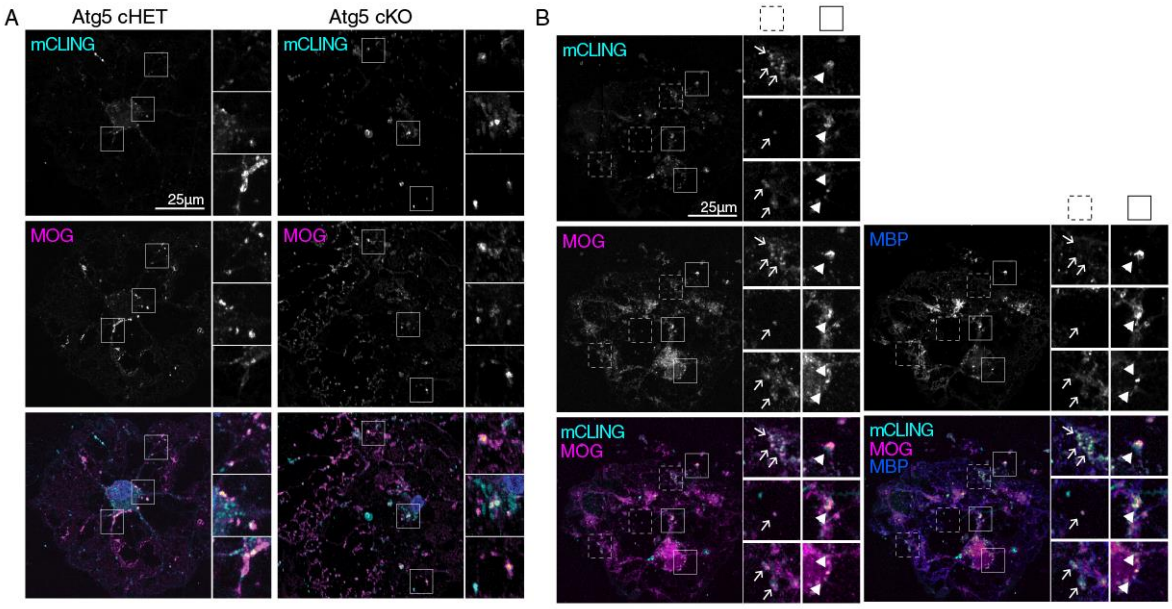

Figure 3.14. Myelin associated integral membrane proteins such as MOG are internalized by an endocytic process, as revealed by mCLING.
A. Endocytosis of MOG as revealed by overnight exposure to the surface membrane dye, mCLING. Examination of Atg5 cHet and cKO OL cultures revealed similar co-localization of MOG (magenta) and mCLING (cyan). Images shown are maximum projections from a confocal z-stack. Representative images from n = 60 cells/3 independent cultures/genotype.
B. Co-staining of mCLING, MOG and MBP reveal that cytosolic and integral-membrane myelin-associated proteins can be found together. Triple immunofluorescence revealed that although MOG (magenta) and MBP (blue) can both be found to simultaneously co-localize with mCLING (cyan), MOG-mCLING localization can also occur in the absence of MBP. Dashed-line boxes highlight MOG-mCLING localization events, whereas solid line boxes indicate sites of triple co-localization. Images shown are maximum projections from a confocal z-stack. Representative images from n = 40 cells/2 independent cultures/genotype.

proteins but slowed degradation. Co-immunofluorescence of MBP and MOG also revealed that some MOG^+ $mCLING^+$ structures also co-localize with MBP (Figure 3.14B). This partial co-localization is derived from two possibilities: at times, MBP remained associated to the membrane during MOG internalization, or that MBP-positive APs once internalized begin to fuse with the MOG-positive endosome. To explore the latter possibility, we determined if $mCLING^+$ structures co-localized with endogenous LC3 (Figure 3.15A). This staining revealed that a subset of $mCLING^+$ structures co-localized with LC3, strongly suggesting that these structures meet. Consistent with this observation, MOG was also found in LC3-positive vesicles (Figures 3.15B). Taken together, this evidence suggests that myelin associated proteins that are both cytosolic and transmembrane in origin enter the MA pathway for degradation.

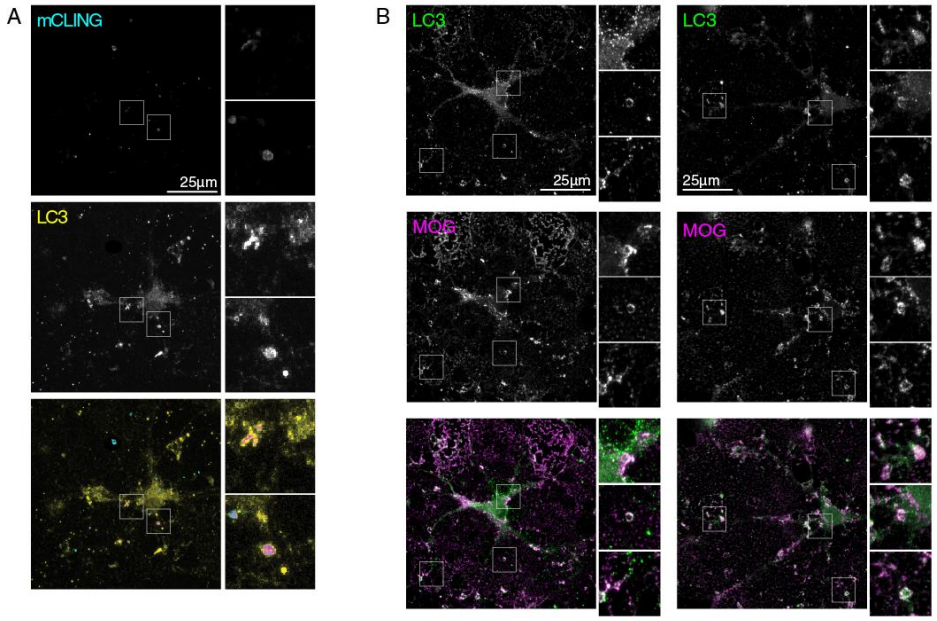

Figure 3.15. Myelin associated integral membrane proteins such as MOG ultimately traffic to an autophagosome compartment, as indicated by co-localization to endogenous LC3, consistent with amphisome formation.
A. mCLING-positive vesicles co-localize with endogenous LC3 (yellow). Overlay is in magenta. Images shown are maximum projections from a confocal z-stack. Representative images from n = 40 cells/2 independent cultures/genotype.
B. MOG can be found in LC3-positive vesicles, suggestive that integral membrane myelin-associated proteins can be found in autophagic vacuoles. Images shown are maximum projections from a confocal z-stack. Representative images from n = 40 cells/2 independent cultures/ genotype.

Taken together, the confocal microscopy data suggests that MBP becomes encapsulated in APs in a selective manner, and that endocytosis of membrane components meet these APs to form amphisomes. Although co-localization studies permit us to infer these events, we aimed to gain better resolution by turning to EM. EM permits us to use other determinants to establish parameters of MA, by determining if the structures are multilamellar, and of selective MA, by determining if the APs are packaged devoid of bulk cytosol and are electron dense. To slow lysosomal-degradation to accumulate these structures, all cells were treated with leupeptin. We identified double membrane structures filled with electron dense material but devoid of bulk cytosol, which are indicative of cargoes captured into APs by selective autophagy (Figure 3.16A). Within the electron dense material we could identify also membrane-like materials suggesting a mixed cargo, rather than a solid aggregate as previously described (Filimonenko et al., 2010). In addition, there were more complex structures that resembled double membrane structures that appeared to have fused with single membrane vesicles filled with myelin-like membranes (Figure 3.16B), suggestive of amphisomes (Figures 3.14 and 3.15). Finally, we also identified unilamellar structures filled with electron dense material and membranous structures, suggestive of the autolysosome (Figure 3.16C). Interestingly, some of the membranous structures identified in autophagosomes, amphisomes, and autolysosomes contained alternating thick and thin lines, which are suggestive of the major dense and intraperiod lines of the myelin sheath. In sum, these data indicate that components of myelin, including the membrane itself, can rely upon the MA pathway for degradation through consolidation of the MA and endocytic pathways during AP maturation. Put into the context of our findings *in vivo*, these data indicate that mature OLs in the adult brain rely upon this consolidation to efficiently degrade portions of the myelin sheath during remodeling events.

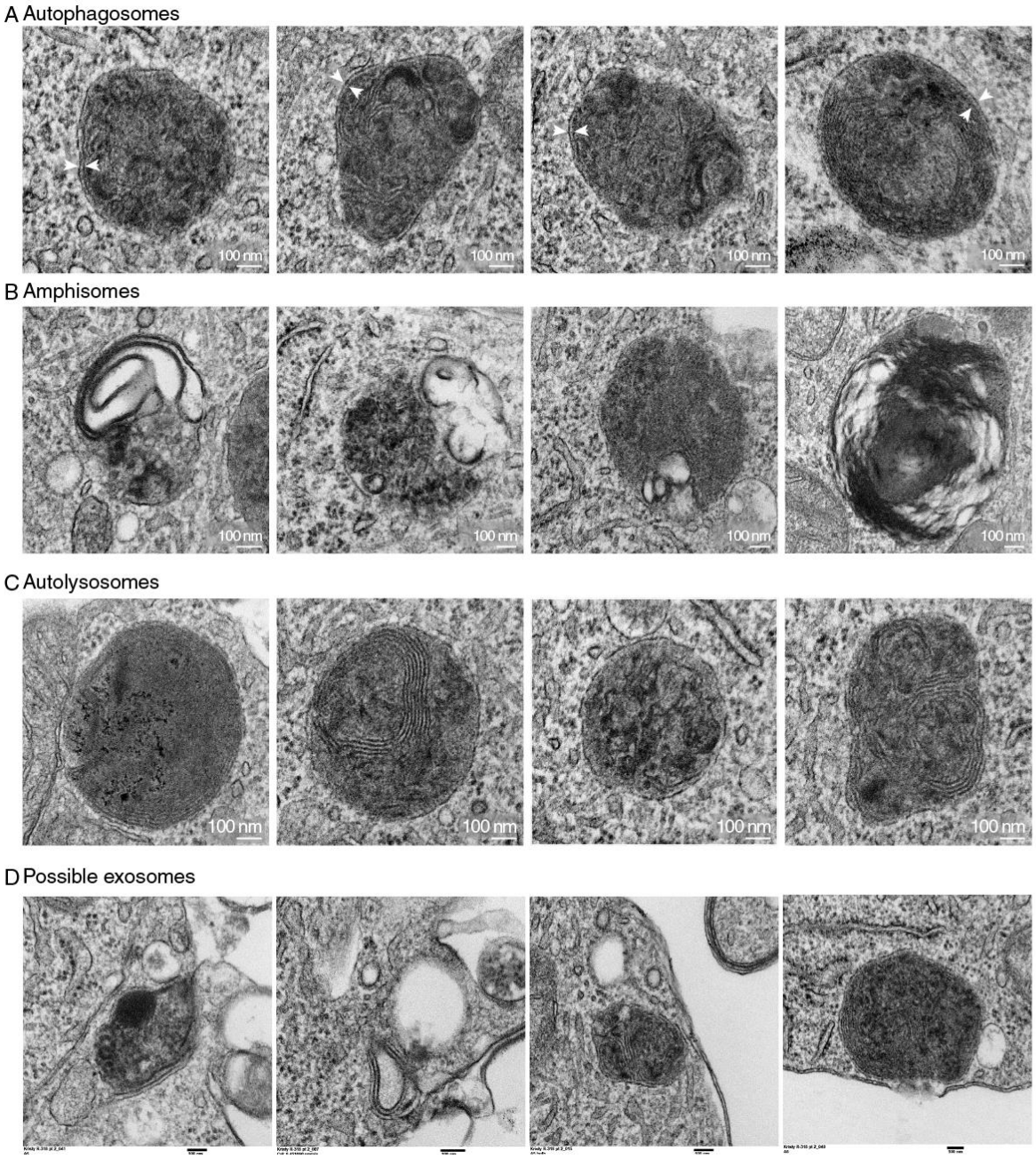

Figure 3.16. Myelin turnover in mature OLs occurs through a coordination of autophagy and endocytosis. A-C. Ultrastructural analyses of mature OLs in culture treated with leupeptin reveal different autophagic vacuoles. Cells were treated with Leu overnight to accumulate structures. A. Autophagosomes. Large (>1 micron) double membrane structures filled with electron dense material, but devoid of bulk cytosol are suggestive of autophagosomes captured via selective autophagy. B. Amphisomes. Double membrane structures appear to fuse with single membrane vesicles filled with myelin-like membranes. C. Autolysosomes. Unilamellar structures filled with electron dense material and membranes resembling myelin. D. Possible exosomes found near to or possibly fusing with the plasma membrane.

3.8 The potential presence of myelin containing exosome-like structures

In addition to observing APs, amphisomes, and autolysosomes, we also identified multivesicular body (MVB)-like structures close to the plasma membrane. Although preliminary, these structures are suggestive of exosomes, which have been suggested to be tightly linked to MA (Baixauli et al., 2014). Simons and colleagues have shown that in the aging brain, microglia can phagocytose extracellular myelin whorls, suggesting that microglia may play some role in eliminating myelin (Safaiyan et al., 2016). The mechanism through which this occurs is unclear. Based on these data, I would speculate that OLs may release exosomes containing myelin components, and these contents are engulfed by microglia. In fact, cultured OLs have been shown to secrete exosomes containing myelin proteins (Krämer-Albers et al., 2007). Studies examining lysosomal homeostasis suggests that lysosomes may also directly fuse with the plasma membrane for self-repair (Medina D et al., 2011; Settembre et al., 2013). Studies examining the content of the supernatant of cultured cells as well as microscopy based studies examining exosomes might shed further insight into this phenomenon.

3.9 Conclusion

In this study, we asked whether the myelin of individual internodes is remodeled. Using both cellular and *in vivo* techniques, we determined that $LC3^{+}$ structures forming within the cytoplasmic channels of the OL are responsible for the lysosome-mediated degradation of myelin. Moreover, we demonstrated that myelin remodeling occurs *in vivo* in a MA-dependent manner. Specifically, we found that the loss of Atg7 in OLs led to an age-dependent increase in myelin

thickness alongside abnormal myelin structures like myelin outfoldings. Subsequent studies of Atg5-deficient OLs indicated that amphisome formation is required for the efficient clearance of myelin-containing endocytic structures. Therefore, we propose that myelin is a dynamic structure that is regularly remodeled through cooperation between MA and endocytosis.

Chapter 4

General Discussion

4.1 Macroautophagy in Myelinating Glia

In this study, we used a combination of *in vivo* and cellular approaches to establish that the myelin of individual internodes is remodeled, and to elucidate the molecular mechanisms thereof. We found that LC3-positive structures form throughout the cytoplasmic channels of the OL and are responsible for lysosome-mediated elimination of myelin. Further, we show that the Atg conjugation system is necessary for myelin remodeling *in vivo*. Specifically, the loss of Atg7 in OLs led to a failure of myelin remodeling, as evidenced by an age-dependent increase of myelin at the internode and the formation of aberrant myelin structures, most notably redundant myelin. Moreover, our examination of the loss of MA in OLs in culture suggested that the formation of a mature AP structure, the amphisome, is necessary for the efficient degradation of myelin-containing endocytic structures. Together, we propose that myelin is a dynamic structure that is regularly remodeled through the cooperative effort of macroautophagy and endocytosis.

4.2 Macroautophagy in Myelinating Glia

Prior to this work, knowledge regarding MA in OLs was rather limited and based on indirect evidence. A leukoencephalopathy due to a mutation in *Vps11* was shown to associate with autophagic defects; however, given that Vps11 is part of the CORVET complex necessary for fusion to the lysosome, it is difficult to discern if the disorder is due to changes in MA exclusively, or lysosome function overall (Zhang et al., 2016). The loss of endo-lysosomal function during development *versus* adulthood could lead to profound differences. Rather than genetic observations, however, modifications in mTOR activity have been more often used to monitor the impact of MA in OLs. For example, the protective effects of intermittent fasting in the Long-Evans shaker rat, a dysmyelinating mutant, was suggested to be due to induction of MA upon mTOR inhibition in OLs (Smith et al., 2013). Although mTOR inhibition does induce a non-selective form of MA, given the importance of mTOR in cellular growth, nutritional status, and other essential cellular functions including transcription, translation, and cellular proliferation, other factors could be at play. The complexity of mTOR is highlighted by several papers that have found that rather than being protective, mTor inhibition in OLs leads to impaired OL and myelin development (Lebrun-Julien et al., 2014; Tyler et al., 2009; Wahl et al., 2014). These apparent differences could be due to cell autonomous as well as non-autonomous events: if mTOR inhibition disturbs the ability of OLs to interact with axons, OL and myelin development could be indirectly affected. Given our findings achieved by targeted disruption of MA in OLs, we can conclude that mTOR-dependent events other than MA are important for OL and myelin development.

Recently, a series of studies examining the relationship between myelination and MA has been published using Schwann cells (SCs): one found that MA is involved in the reduction of

cytoplasm during Schwann cell maturation and several others indicated that a combination of MA and phagocytosis is involved in myelin clearance during SC de-differentiation after nerve crush injury (Brosius Lutz et al., 2017; Gomez-Sanchez et al., 2015; Jang et al., 2016; Jang et al., 2015). Although our cell based data suggested an increase in the presence of autophagic proteins during OL maturation, we did not observe clear changes in cytoplasmic clearance upon the loss of MA, neither *in vivo* or in the Atg5(CNP) cKO-derived cultures, suggesting that if MA does play a role in cytoplasmic clearance during OL differentiation, its loss is efficiently replaced by other cellular pathways. Given that CNP^{Cre} also expresses in SCs, we were able to confirm that the loss of Atg7 in SCs has no gross impact on myelination in the PNS, even at 16 months of age at which time myelination in the CNS is grossly disrupted. Similar to SCs, we find that MA can be used by OLs to degrade myelin, but for OLs, there is no apparent need for a stressor to evoke this event. OLs are postmitotic and persist for the duration of the organism's lifespan whereas SCs divide and can be replaced, and thus it is unsurprising that OLs are much more dependent on cell-autonomous degradative processes like MA to remodel their myelin (Asbury, 1967; Pellegrino and Spencer, 1985; Yeung et al., 2014).

Besides the lifespan difference between these cells, differences between the structure of SCs and OLs may further explain the differential requirements for myelin remodeling in these cell types. SCs and OLs vastly differ in the amount of myelin per cell. For example, the number of myelin sheaths produced by each cell type, one per SC, up to eighty per OL, may explain the increased sensitivity of OLs to impairments in myelin degradation (Young et al., 2013). Additionally, the difference in distance between the myelin sheath and cell body could be another factor: Whereas the myelin sheath is connected directly to the cell body in SCs, each myelin sheath of an OLs is connected to the cell body through a long and slender process, making the myelin

sheath a distant and self-contained compartment. In light of our data implicating the importance of amphisome formation to drive myelin turnover, this might explain why endocytosis and MA must tightly collaborate to ensure efficient lysosomal degradation. As such, OLs may have adapted MA to enhance myelin formation either due to the enormous amount of myelin it must remodel or the distance between the cell body and the remodeling myelin sheath.

One question regarding this process is how might membrane from compact myelin be internalized. We postulate that local depolymerization of MBP would allow for "unzippering" of the myelin sheath and allow for endocytosis and MA to occur. In fact, it has recently been postulated that post-translational modifications of MBP may facilitate a loss of myelin compaction (Vassall et al., 2015). Further studies are required to determine, however, the signals that drive de-compaction of myelin and its subsequent degradation through endocytosis and MA.

4.3 Membrane Trafficking and Myelin Formation

Several studies have implicated disruptions in membrane trafficking to have a profound impact on myelination (Chow et al., 2007; Ferguson et al., 2009; Winters et al., 2011), from OL differentiation, intracellular trafficking of myelin proteins, and myelin formation in the CNS (Mironova et al., 2016) (Edvardson et al., 2015; Goebbels et al., 2010; Zhang et al., 2016). Studies examining the levels of one key phospholipid, phosphatidylinositol 3-monophosphate (PI3P) during oligodendroglial development have raised the question of whether disruption of MA may contribute to hypomyelination. Our examination of MA in cultured OLs indicates that MA is active throughout OL maturation, but together with our *in vivo* studies, indicate that MA is apparently dispensable during the first two months of life in mice when the vast majority of OL development

occurs. Our study indicates that although myelin formation may require endocytosis and other vesicle trafficking events, MA is not one of them. One possibility suggested by our culture studies however, is that the loss of macroautophagy in OLs may cause a mild delay in myelin formation during development that is corrected before adulthood. Alternatively, in contrast to the clear presence of CNP^{Cre} activity in many OPCs in our culture system, *in vivo*, this recombination might occur late enough in the oligodendroglial lineage that the necessity for MA is missed in the Atg7(CNP) cKO mice. Indeed, a recent study suggests that reporter lines using the *Rosa26* locus, such as the Ai9 reporter, might be more available for Cre-mediated deletion by CNP^{Cre}, thereby overestimating its activity (Tognatta et al., 2017). In fact, studies suggest that CNP1 activity may begin as early as OPC specification (Chandross et al., 1999). Although crosses with lines expressing Cre at the NG2 stage might help to clarify these issues, disruption of MA in early lineage cells using lines such as $NG2^{Cre}$ might give rise to phenotypes that are far more complex to decipher due to their impact on other cell types, such as astrocytes.

4.4 Amphisome Formation vs. LC3-associated Endocytosis

Our data suggests that both endocytosis and MA are important for myelin maintenance and remodeling in the adult, as endocytic structures containing myelin protein require the presence of Atg5 or Atg7 for efficient lysosome-mediated degradation. There are two possible events that could explain this fascinating phenomenon: amphisomes and LC3-associated endosomes. It is well established that endosomes and APs can fuse to form amphisomes before merging with a lysosome for degradation (Gordon and Seglen, 1988). In fact, it has been long known that APs and endosomes fuse in specialized subcellular compartments of the CNS before degradation

(Hollenbeck, 1993). Instead of being a passive intermediary structure, it is possible that amphisome formation is necessary to enhance lysosomal fusion for both endosomal and autophagic pathways, especially in highly compartmentalized cells such as the mature OL. In that case, the lack of amphisome formation would preclude efficient clearance of and therefore cause accumulation of non-degraded structures. This accurately predicts what we observed in the cells derived from Atg5(CNP) cKO mice. Given that studies indicate that local synthesis can occur in the distal tip of the myelin sheath, efficient local degradation occurring throughout each individual sheath makes sense (Laursen et al., 2011; Lyons et al., 2009; Torvund-Jensen et al., 2014; Wake et al., 2011; White et al., 2008).

Alternatively, there is growing evidence that the lipidation of LC3 is not exclusive to AP membranes, and can conjugate to other vesicles. Although the reason for this lipidation event is uncertain, it has been postulated that membrane-bound LC3 might enhance vesicle targeting to the lysosome (Martinez et al., 2015). Although the majority of and the strongest evidence for this has been established with phagosomes, through a pathway known as LC3-Associated Phagocytosis (LAP), this phenomenon has been suggested for other macroendocytic structures as well to lead to LC3-associated endocytosis (LAE) (Florey et al., 2011; Florey and Overholtzer, 2012; Martinez et al., 2011; Martinez et al., 2016; Martinez et al., 2015). Loss of Atg5 and 7 is effective at inhibiting MA because it prevents the conjugation of the Atg8 family of proteins, one of which is LC3. By virtue of this function, it is difficult to rule out if we've equally affected LAE. Unlike LAP, which has been rigorously established (Martinez et al., 2011; Martinez et al., 2016; Martinez et al., 2015), the paucity of evidence for LC3 conjugation to endosomal membrane outside of phagocytes makes it difficult to test directly. Nonetheless, our cell based work strongly suggests that both cytoplasmic and integral membrane protein components of myelin can be found in the

same structure, and given that it is well known that AP fusion to endosomes occurs in highly specialized subcellular compartments of the CNS, we believe that our data reflects the importance of amphisome formation in the myelin sheath of OLs. More mechanistic insight into LAE must be gained to determine if it is contributing to myelin turnover in any way.

A significant question raised by our observations is why endocytosed myelin-associated proteins and membranes need to traffic through the amphisome to be degraded efficiently. One possible explanation derives from the extraordinary amount of myelin that a given OL must maintain. As OLs can extend up to eighty myelin sheaths and must maintain $20x10^5$ μm^2 of myelin membrane, it may be very taxing on the endolysosomal system to be constantly remodeling this enormous volume of myelin (Pfeiffer et al., 1993; Young et al., 2013). As such, these highly specialized OLs may have become increasingly reliant on the cooperative actions of endocytosis with MA to enhance their capacity for myelin remodeling. Alternatively, the OL's highly polarized morphology may be responsible for this specialization. The myelin sheath is in fact quite distant from its parent cell body and is only connected to it through a rather narrow cellular process. Because of this, it would theoretically be more efficient to combine all cargo destined for degradation and fuse them to lysosomes within the myelin sheath. Interestingly, our data supports this latter hypothesis; we found that $LC3^+$ structures that formed within the cytoplasmic channels of OLs always acidified within them as well (e.g. APs that formed in cytoplasmic channels never trafficked into the cell body before acidifying).

Another significant question raised by this work is how might amphisome formation be increasing the efficiency of myelin turnover. One possible means by which amphisome formation could increase the rate of degradation would be by facilitating fusion to the lysosome. Although studies suggest that the role of membrane conjugation of the Atg8 family of proteins such as LC3

to the AP membrane is to promote membrane growth, a recent series of studies have shown that these same proteins might also facilitate the fusion of LC3-positive APs and amphisomes to the lysosome (McEwan et al., 2015; Nguyen et al., 2016; Wang et al., 2015). As proteins such as LC3 are found on the inner and outer autophagosomal membrane, they would also be available to facilitate lysosomal fusion on the amphisomal membrane. This would be consistent with the LC3-associated phagocytosis literature that indicates that the association of LC3 to the phagosomal membrane facilitates the fusion of phagosomes to lysosomes (Martinez et al., 2015). Moreover, induction of macroautophagy in ESCRT mutants, in which there is accumulation of endosomes secondary to failure of endosome maturation, facilitates the clearance of endosomes (Djeddi et al., 2012). This suggests that fusion of autophagosomes and endosomes to form amphisomes in these mutants enables lysosome-mediated degradation of endocytic cargo. The hypothesis that amphisomes fuse with lysosomes more efficiently than endosomes could be tested *in vitro* using purified endosomes, amphisomes, and lysosomes (Berg et al., 1998; de Araujo et al., 2015). Another reason amphisome formation could be necessary is if the vesicles containing endocytosed myelin are fundamentally different from canonical endosomes. Because myelin protein and lipid composition are strikingly different from those of typical plasma membrane, it is possible that certain proteins necessary for endosome maturation may be unable to associate with the membrane of endocytosed myelin (Alberts et al., 2002). If this is the case, then amphisome formation would be necessary to facilitate efficient maturation and fusion to the lysosome of endocytosed myelin. The rather unusual appearance of internalized myelin in our electron micrographs gives further credence to this theory.

4.5 Myelin Degradation and Remodeling

Not much is known about how myelin is degraded in the CNS, nor whether it is even remodeled. It is known that myelin is stable and has one of the longest half-lives of any structure in the CNS (Fischer and Morell, 1974; Savas et al., 2012; Toyama et al., 2013). Moreover, it is well established that activated microglia engulf myelin debris (Baumann and Pham-Dinh, 2001), and new work has shown that microglia can engulf myelin in the aging animal as well (Safaiyan et al., 2016). On the other hand, recent studies in mice have suggested that generation of new OLs is necessary for formation of new myelin (Gibson et al., 2014; Young et al., 2013), and the clear implication of this work—consistent with decades of data from models of demyelination—is that OL loss is necessary for myelin degradation. This however would pose an unnecessary burden on neurological function, as it would cause temporary focal demyelination of segments of axons, leading to inefficient signal propagation and reliability. A recent study, however, indicates that this is not the case: myelin turnover occurs at a much faster rate than OL turnover in human white matter, suggesting that myelin remodeling is independent of OL turnover (Yeung et al., 2014). In conjunction with our data emphasizing the importance of cell-autonomous MA for myelin remodeling, we can conclude that myelin turnover may be mainly carried out cell-autonomously by mature OLs in a macroautophagy-dependent manner.

Several interesting follow-up experiments come to mind. One question that these experiments raise is whether MA-dependent remodeling is necessary for all components of the myelin sheath or whether it is specific to certain components of the myelin sheath. To test this, one could revisit previous study designs by radioactively labeling myelin and comparing the half-lives of components of the myelin sheath in Atg7(CNP) cHet and cKO mice (Fischer and Morell, 1974; Savas et al., 2012; Smith, 1968; Toyama et al., 2013).

Our study established that myelin within individual myelin sheaths is regularly remodeled in a MA-dependent manner. It does not however, determine the relative contribution of OL replacement, myelin sheath replacement, and remodeling within a myelin sheath to total myelin remodeling in the CNS. To determine this, I propose crossing three mouse lines together to create mice that express PLP1-CreERT2 (an inducible Cre that causes recombination in mature OLs (Leone et al., 2003)), a GFP tagged myelin protein (fictional protein MyPr-GFP) that can be inducibly turned off (a floxed version of the MyPr-GFP allele), and an inducibly activated TdTomato tagged myelin protein (stop-flox MyPr-TdTomato). (Clearly the colors were selected arbitrarily and any fluorescent tags that have easily segregated excitation and emission spectra would work). Using this system, induction of Cre recombination with tamoxifen would stop the expression of MyPr-GFP and induce the expression MyPr-TdTomato. As such, myelin sheaths formed after tamoxifen treatment would be $TdTomato^{+}$ GFP^{-}, myelin sheaths formed before tamoxifen treatment in which myelin remodeling had not occurred would be $TdTomato^{-}$ GFP^{+}, and myelin sheaths formed before tamoxifen treatment in which myelin remodeling had occurred would be $TdTomato^{+}$ GFP^{+}. Moreover, the relative levels of GFP and TdTomato within $TdTomato^{+}$ GFP^{+} myelin sheaths would suggest the degree to which the myelin sheath had been remodeled.

Using *in vivo* time-lapse imaging in these mice will provide a lot of valuable information about myelin remodeling. For example, by observing the relative rate at which GFP fluorescence decreases and TdTomato fluorescence increases at different GFP^{+} myelin sheaths, we can determine whether there is heterogeneity in the rate at which myelin sheaths are remodeled or whether myelin remodeling occurs at a fixed rate across myelin sheaths. The latter would suggest that myelin remodeling may be a homeostatic function that is not activity dependent (as one would

expect variability in the level of activity in the underlying axons), at least in the region of the CNS that was examined under the experimental conditions (e.g. without an inciting incident). This system would also allow for the identification of newly formed sheaths and whether these new sheaths intercalate between previously existing sheaths, replace older myelin sheaths, or myelinate previously bare axons. Moreover, if newly formed myelin sheaths replace older myelin sheaths, it would be interesting to know whether sheaths that are replaced had been remodeling at the same rate as other sheaths, or if poorly remodeled sheaths are replaced more frequently. One could also examine the myelin sheaths of these mice in post-mortem tissue to study the regions of the CNS not easily accessible for time-lapse imaging, but this data lacking a temporal component would not be able to answer as many questions.

It would also be interesting to cross these mice with mice expressing the conditional allele for Atg7 and then ask which of the aforementioned processes are dependent upon macroautophagy. One intriguing possibility is that—in addition to being important for remodeling of existing myelin sheaths—macroautophagy may be necessary for retraction of myelin sheaths. It is known that mature myelin sheaths can be retracted, but how the cell is able to clear such an enormous amount of membrane and protein as that found in an entire myelin sheath remains a mystery (Czopka et al., 2013). Whether macroautophagy, a major intracellular bulk degradative process that is necessary for amphisome formation, is necessary for myelin sheath retraction could be easily answered in this model as well. Although this could also be answered with time lapse imaging of any fluorescently tagged protein expressed in Atg7(CNP) cHet and cKO) mice, performing these experiments with conditional expression of MyPr-GFP and MyPr-TdTomato would allow us to learn what the downstream effects of a failure to retract a myelin sheath would be on myelin remodeling.

A recently developed technique, spectral confocal reflectance microscopy (SCoRe), mitigates the need for these genetically complex mice (Schain et al., 2014). SCoRe micrsocopy allows for label-free *in vivo* imaging of myelinated axons. Using this technique, one can theoretically observe formation and retraction of myelin sheaths, along with changes in thickness and length of myelin sheaths. As such, this may be a particularly powerful tool for studying myelin remodeling both in control and Atg7(CNP) cKO mice. In fact, we have recently started a collaboration with the Grutzendler lab to pursue these experiments.

4.6 Activity-Dependent Myelin Remodeling

Over the past decade, a preponderance of evidence has shown that white matter is remodeled in response to experience, both in humans and in mice (reviewed in (Baraban et al., 2016; Zatorre et al., 2012)). Most of these studies have shown that learning, stimulation, or activity can drive an increase in myelination, which has been assumed to be from an increase in oligodendrogenesis. One recent study, however, challenged this assumption and showed that OL generation and turnover cannot account for the changes in myelin volume in response to experience in humans and concludes that myelin remodeling in white matter must be mediated by mature OLs (Yeung et al., 2014). In fact, there is some evidence that mature OLs may modulate the thickness of their myelin sheaths, as inducible activation of ERK1/2 or inactivation of PTEN in mature OLs of adult mice leads to reinitiation of myelin growth and thicker myelin sheaths (Goebbels et al., 2010; Jeffries et al., 2016; Snaidero et al., 2014). This induction of myelin growth in mature OLs can lead to increased myelin thickness along with redundant myelin, just as we observed in Atg7(CNP) cKO brains (Goebbels et al., 2010; Snaidero et al., 2014). This shared phenotype is

likely because in both cases the delicate balance between myelin growth and degradation is altered, leading to excessive growth of the myelin sheath and a disruption in myelin remodeling.

Increases in myelin thickness may be stimulated by neuronal activity; optogenetic stimulation of neurons *in vivo* leads to thicker myelin sheaths around associated axons (Gibson et al., 2014). It has not been determined, however, to what extent this is caused by newly synthesized myelin sheaths as opposed to remodeling of preexisting myelin sheaths. By crossing the $PLP^{CreERT2}$ MyPr-GFP^{ON} MyPr-$TdTomato^{OFF}$ mice with Thy1::ChR2 mice, one can directly visually examine myelin remodeling in response to neuronal activity. By doing this, one can determine to what extent neuronal activity induces formation of new myelin sheaths and to what extent preexisting myelin sheaths are remodeled in response to electrical activity of the underlying neurons.

Just as mature OLs can be induced to produce thicker myelin sheaths, so too can myelin thickness be decreased. Social isolation of adult mice leads to thinner myelin sheaths, along with transcriptional changes in OLs (Liu et al., 2012), and sensory deprivation of the auditory system in adult mice yields thinner myelin sheaths as well (Sinclair et al., 2017). The stability of the OL population throughout adulthood suggests that the thinner myelin sheaths in the aforementioned studies are likely due to a thinning of preexisting myelin sheaths of mature OLs (Yeung et al., 2014). Our study suggests a possible mechanism for this activity-dependent thinning of myelin sheaths in which low neuronal activity raises the rate of macroautophagy-dependent myelin turnover relative to myelin synthesis to remodel and thin the myelin sheath.

To test whether MA is necessary for activity-dependent thinning of myelin sheaths, one would need to decrease neuronal firing and test if any subsequent decrease in myelin thickness is macroautophagy-dependent. First to verify that decreased neuronal activity causes a decrease in myelin thickness, one can use an inhibitory DREADD (Designed Receptor Exclusively Activated

by Designer Drug) like hM4Di that is delivered to a subset of cortical neurons by electroporation or viral delivery along with a tag (like GFP) (Roth, 2016). By activating the DREADD with its corresponding drug, one can silence a subset of cortical neurons and then examine them to determine if myelination of their axons is decreased. Alternatively, this experiment could be performed with halorhodopsin as well (Zhang et al., 2007). Assuming that the previous experiment establishes that loss of neuronal activity causes a decrease in myelin thickness, one can then repeat the experiment in Atg7(CNP) cHet and cKO mice to determine whether this effect is macroautophagy-dependent. Alternatively, one could also simply socially isolate or earplug Atg7(CNP) cHet and cKO mice to determine whether the previously reported thinning of myelin sheaths in those cases requires macroautophagy (Liu et al., 2012; Sinclair et al., 2017). However, as social isolation and earplugging would be expected to have pleiotropic effects on their respective neuronal circuits, these experiments are not ideal.

4.7 Circuit Tuning

As many CNS axons are myelinated for sub-maximal conduction velocity (and in fact, irregularly along their lengths), it is safe to assume that conduction velocity is not optimized to maximize speed, but rather to ensure that action potentials arrive at the appropriate time (Tomassy et al., 2014; Waxman, 1980). The importance of signal timing has been explored thoroughly in the auditory system (reviewed in (Seidl, 2014)): The auditory system processes microsecond differences in the arrival time of sounds between the two ears; consequently, it requires finely tuned signal timing. Interestingly, the temporal precision of the auditory system is mediated in part by carefully calibrated myelination (Stange-Marten et al., 2017). Moreover, recent evidence

suggests that the thickness of myelin sheaths in the auditory system can be modulated by experience even in the adult, just as myelination of the prefrontal cortex is modulated by social experience (Liu et al., 2012; Sinclair et al., 2017). Together, these studies emphasize the importance of precise signal timing and suggest that OLs may be able to modify myelin sheath morphology to optimize conduction velocities. In conjunction with our data demonstrating that myelin is remodeled throughout life, these studies suggest that remodeling may not be simply required to maintain the health of the myelin sheath, but may in fact be activity-dependent and essential for neural circuit function. In fact, several studies have shown behavioral consequences that accompany activity-dependent changes in myelin structure (Gibson et al., 2014; Liu et al., 2012). Moreover, even small changes in g-ratio can significantly alter conduction velocity. It has been proposed that changes in conduction velocity—mediated by activity-dependent alterations in myelin structure—could have profound effects on neuronal network function (Pajevic et al., 2014). Disruption of activity-dependent myelination and adaptive timing of action potentials likely contribute to many disorders in which asynchronous neuronal firing causes dysfunction, like epilepsy, schizophrenia, and dyslexia.

Knowing all of this, the natural next question to ask is whether the loss of myelin remodeling in Atg7(CNP) cKO mice causes any measurable effects on neural circuitry or behavioral outcomes. For all the experiments listed below, it should be noted that a significant confound exists due to one difference between mice and humans: the rate of OL turnover in mice is exponentially larger than that in humans (Yeung et al., 2014). Because of this, it is possible that the effects of macroautophagy-dependent myelin remodeling will be masked by changes in OL number.

A simple way to test whether the loss of myelin remodeling in Atg7(CNP) cKO mice has behavioral significance would be to replicate studies that have indicated that myelin remodeling has effects on neural circuitry and behavior. For example, as social isolation of adult mice has been shown to cause alterations in the social interaction test, one can repeat this experiment in Atg7(CNP) cHet and cKO mice to determine whether these effects are mediated by macroautophagy-dependent myelin remodeling (Liu et al., 2012). Similarly, as earplugging can cause thinning of myelin sheaths as well as elevated auditory thresholds, reduced firing rates, and slower conduction speed, these same measures can be evaluated in Atg7(CNP) cHet and cKO mice after earplugging (Sinclair et al., 2017). It's also possible that macroautophagy-dependent myelin remodeling may be required for sound localization, as the temporal precision required for sound localization by the auditory system is mediated in part by carefully calibrated myelination (Stange-Marten et al., 2017). To test this, one could simply test whether Atg7(CNP) cKO show deficits in a task that requires fine discrimination in sound localization when compared to Atg7(CNP) cHet mice.

It is also possible that macroautophagy-dependent myelin remodeling is necessary for forgetting or reversal learning. It was previously shown that myelin formation occurs during and is required for motor skill learning (McKenzie et al., 2014; Scholz et al., 2009); is myelin remodeling also required for forgetting motor skills? One way to test this would be to train mice to run on a complex wheel with irregularly spaced rungs and then ask several months later if the loss of macroautophagy in OLs precludes the mice from forgetting how to run properly on this wheel (this is, of course, assuming that mice forget how to run on this complex wheel if they are not exposed to it for an extended period of time). Alternatively, macroautophagy-dependent myelin remodeling may be required for modification of or reversal of previous learning. For

example, conditional loss of macroautophagy in OLs may prevent learning how to run on a second wheel with a different pattern of irregularly spaced rungs. To test whether reversal learning requires macroautophagy-dependent myelin remodeling, one can compare the performance of Atg7(CNP) cHet and cKO mice in a reversal learning task in the T maze. For example, the mice are trained that a reward can be found in the left-hand arm of the maze, and then the reward is switched to the right-hand arm of the maze. If Atg7(CNP) cKO mice required significantly more trials to learn that the location of the reward had changed, then one could conclude that macroautophagy-dependent myelin remodeling may be necessary for reversal learning.

These findings may have considerable effects on our understanding of neural function. Clearly, we must revise how we think about the nervous system's ability to adapt to the environment: that preexisting myelin sheaths can be actively remodeled and affect neural circuitry adds a whole new layer of complexity to the system. Moreover, our models of the central nervous system *in silica* need to be updated to reflect the added complexities of activity-dependent myelin remodeling.

4.8 Modeling Mature OLs in Culture

One question that confounds all studies of cells in culture is how accurately do they model the biology of cells *in vivo*. This question holds extra significance in studies of OLs in culture, as OLs isolated from the rich extracellular milieu of the CNS cannot perform their classic function of wrapping axons with myelin sheaths. Nonetheless, these cultures do reflect many features of OL biology *in vivo*. For example, during OL differentiation and maturation, developing OLs extend many processes to sample the environment *in vivo* before formation of the flat myelin

sheath (Baraban et al., 2018; Czopka et al., 2013; Hines et al., 2015; Koudelka et al., 2016; Mensch et al., 2015). Similarly, in culture it has been shown that during differentiation OLs will extend processes that sample the environment and then form a flat (albeit unrolled) myelin sheath (Zuchero et al., 2015).

As mentioned before, we identified several subcellular structures in cultured OLs that we believe to correspond to the subcellular structures of the OL *in vivo*. We found structures in culture that were reminiscent of the inner loop (edge), outer loop and paranodal loop (artery), and intramyelinic cytoplasmic nanochannel (branch). The most striking element of our live imaging was the marked heterogeneity of AP biogenesis in these subcellular structures, which corresponds with our hypothesis that MA in the myelin sheath mediates myelin remodeling. It is not surprising that AP biogenesis is rare in the branches of these OLs; intramyelinic cytoplasmic nanochannels are believed to be transient structures involved in trafficking membrane to the growing leading edge, so there is little purpose for MA-mediated myelin remodeling within them (Snaidero et al., 2014). As newly deposited myelin is found beside the inner loop, this myelin would have the lowest need to be remodeled, and as such, it is logical for autophagosome biogenesis to be rare in the edge of our cultured OLs. On the other hand, AP biogenesis occurred frequently at artery-branch intersections. This makes perfect sense as it ensures that myelin synthesis and degradation are tightly linked. At artery-branch intersections, the site at which myelin compaction is disrupted to allow for autophagosome biogenesis and myelin turnover is also used to facilitate trafficking of membrane to the growing leading edge. It would be interesting to repeat some of the experiments reported here in a co-culture system of OLs with neurons to ensure that our results can be replicated in a three-dimensional culture system in which myelin sheaths are wrapped around axons. It should be noted, however, that many of these results would be much harder to capture when the OL is not

resting on a flat plane. Moreover, though our *in vivo* results complement our findings in culture, these experiments could also give better spatial understanding of how the degradation occurs.

4.9 Age-Dependent Decline of Atg7(CNP) cKO Mice

Another significant question raised by this work is why do these mice exhibit an age-dependent motor phenotype and premature lethality. Possible explanations include (1) that the loss of macroautophagy in OLs models the neurodegenerative disease multiple systems atrophy, (2) that there is off target Cre-mediated recombination in neurons, and (3) that increased myelin thickness or poor myelin quality secondary to a failure in myelin remodeling induces neurodegeneration.

4.9.1 Modeling multiple systems atrophy?

For a discussion of how the loss of macroautophagy may be a model for the neurodegenerative disease multiple systems atrophy, see Appendix I.

4.9.2 Cre-mediated recombination in neurons?

To test whether the motor phenotype and premature lethality could be caused by off-target Cre-mediated recombination in neurons of Atg7(CNP) cKO mice, one could perform dual fluorescent *in situ* hybridization for a neuronal marker and for Atg7 mRNA. It should be noted that examining whether the TdTomato reporter is expressed in neurons would be insufficient as CNP Cre-mediated recombination, like all Cre-mediated recombination, changes with the locus of the target gene (Tognatta et al., 2017). Because CNP is known to be expressed in the spleen and

to a lesser extent in liver, lung, and thymus, the motor phenotype and premature lethality may be mediated by the loss of macroautophagy in one these organs as well (Chandross et al., 1999).

A major limitation of the Cre-loxP system in general is that it is very difficult to design a Cre that is specific to a particular cell type. There are two major reasons for this: (1) that Cre-mediated recombination affects any cell in which Cre is even briefly expressed along with all of its progeny, and (2) our limited ability to identify promoters that are completely specific to the cell type of interest (for example, a recent study identified six different types of mature OL (Marques et al., 2016); however, it would be evolutionarily inefficient to have a separate promoter for each cell type generated, so this is very unlikely to actually exist). Drosophila geneticists use a more effective system for conditional expression and silencing of genes, known as the UAS-Gal4 system (Brand and Perrimon, 1993). The system has two parts: a yeast transcription activator protein called Gal4, and the Upstream Activation Sequence (UAS), an enhancer to which Gal4 specifically binds. By driving Gal4 expression under a specific promoter, a gene of interest that is inserted into the genome with a UAS will be expressed specifically in cells in which GAL4 is expressed. For example, if one crosses UAS-GFP flies with Yes1-Gal4 (Yes1 is a fictional promoter), GFP will only be expressed in $Yes1^{+}$ cells. Recent extensions to this system have made the UAS-Gal4 system even more powerful, by adding Gal80—a Gal4 inhibitor—and split Gal4, in which Gal4's DNA binding domain (DBD) and transcription activation (AD) are expressed under separate promoters (Fujimoto et al., 2011; Luan et al., 2006; Suster et al., 2004). In this case, flies with UAS-GFP, Yes1-DBD, Yes2-AD, and No1-Gal80 would only express GFP in $Yes1^{+}$ $Yes2^{+}$ $No1^{-}$ cells, thereby allowing for fine-tuned control of cell type expression.

So how can mouse genetics become more powerful like those of Drosophila? One way to dissect out more specific cell types using mouse genetics would be to simply combine some of the

currently available techniques such as Cre-loxP, FLP-FRT, and the tetracycline regulatable system (Gossen and Bujard, 1992; Schlake and Bode, 1994). For example, mice with Yes1-Cre, Yes2-flox stop FLP, and FRT Atg7 would conditionally delete Atg7 only in $Yes1^{+}$ $Yes2^{+}$ cells. To be used at scale, such combinatorial approaches would require an extraordinary number of mouse lines to be generated to satisfy all possible combinations (especially when you factor in negative regulation as well). Certainly, this is not the most efficient system possible. A more ideal system would involve only one recombinase that would be susceptible to modifiers that would facilitate or prevent transcription: in other words, a system with conditional activation or repression of the recombinase in which combinatorial targeting determines the cell type of interest. For example, if one could design a plasmid that drives tamoxifen expression under a promoter of interest, such a system would be feasible with the CreERT system, in which a modified Cre recombinase only translocates to the nucleus in the presence of tamoxifen (Brocard et al., 1997; Hayashi and McMahon, 2002). In this case, a mouse with Yes1-CreERT, Yes2-tamoxifen, and a floxed allele of Atg7 would have conditional loss of Atg7 specifically in $Yes1^{+}$ $Yes2^{+}$ cells.

4.9.3 Failure to remodel myelin causes neurodegeneration?

It is possible that increased myelin thickness or poor-quality myelin may cause the reported phenotype of Atg7(CNP) cKO mice. It is well known that alterations in myelin composition (e.g. the loss of certain myelin proteins like PLP and CNP) can cause axonopathy and neurodegeneration (Edgar et al., 2009; Griffiths et al., 1998; Lappe-Siefke et al., 2003; Rasband et al., 2005). As mentioned above conditional activation of PTEN in OLs, which leads to unregulated growth of the myelin sheath, increases myelin thickness and the formation of aberrant myelin structures like redundant myelin (Goebbels et al., 2010). Interestingly, the conditional activation

of PTEN also causes neuroinflammation in white matter, formation of axonal spheroids, and premature lethality. Considering that this paper and our data both cause an imbalance of myelin growth to myelin degradation, it is possible that there is a shared mechanism causing axonopathy and premature lethality. Two possible causes include: (1) poorly remodeled myelin may fail to provide the underlying axon with needed trophic or metabolic support, or (2) as myelin g-ratio is optimized for the spatial constraints of the CNS, it is possible that the axonopathy is secondary to excessive compression of axons (Chomiak and Hu, 2009).

4.10 Conclusion

Myelination of axons by OLs in the central nervous system is critical for the rapid and reliable conduction of action potentials, as evidenced by the severe disabilities associated with myelin loss in multiple sclerosis and other demyelinating diseases. Much is known about OL development and myelin formation by OLs. How myelin is turned over, however, remains unclear. In humans, myelin remodeling is likely mediated by mature OLs. As mature OLs have limited capacity to generate new myelin sheaths, we must ask whether mature OLs can remodel the myelin at preexisting myelin sheaths. The significance of this question is underscored by the importance of myelin remodeling for neural function and activity-dependent myelin plasticity.

Macroautophagy (MA) is responsible for the lysosome-mediated elimination of cytosolic proteins, lipids, and organelles, through packaging into a de novo synthesized, transient, multilamellar organelle known as an autophagosome (AP). MA can act either as a non-selective response to cellular stress such as starvation to degrade bulk cytosol and its contents, or as a highly selective quality-control mechanism to degrade aggregated proteins or damaged organelles. There is evidence that Schwann cells—the myelinating cells of the peripheral nervous system—utilize

macroautophagy to degrade myelin while dedifferentiating in response to systemic stress. It was unknown, however, whether MA is necessary for myelin remodeling at baseline conditions in either Schwann cells or OLs.

In this study we used a combination of *in vivo* and cellular approaches to establish that the myelin of individual internodes is remodeled and to elucidate the molecular mechanisms thereof. We found that LC3-positive structures form throughout the cytoplasmic channels of the OL and are responsible for lysosome-mediated elimination of myelin. Further, we show that the Atg conjugation system is necessary for myelin remodeling in vivo. Specifically, the loss of Atg7 in OLs led to a failure of myelin remodeling, as evidenced by an age-dependent accumulation of myelin at the internode and the formation of aberrant myelin structures, most notably redundant myelin. Moreover, our examination of the loss of macroautophagy in OLs in culture suggested that amphisome formation is necessary for the efficient degradation of myelin-containing endocytic structures. Together, we propose that myelin is a dynamic structure that is regularly remodeled through the combined efforts of macroautophagy and endocytosis.

Chapter 5.

Materials and Methods

5.1 Animals

Mice: All animals and procedures complied with the Guide for Care and Use of Laboratory Animals and were approved by the IACUC committee at Columbia University. Mice were maintained in a 12h/12h light/dark cycle in a temperature and humidity controlled environment, with ad libitum access to food and water. Previously created CNP-Cre (Lappe-Siefke et al., 2003), Atg7-floxed (Komatsu et al., 2005), Atg5-floxed (Hara et al., 2006), GFP-LC3 (Mizushima et al., 2004), and TdTomato-reporter (Madisen et al., 2010) mouse lines were maintained by breeding with C57BL/6 mice. All experiments with mice were performed blindly without knowledge of their genotype. We observed no sexual dimorphism of myelination in Atg7(CNP)cKO mice, so males and females were pooled for analysis.

5.2 Genotyping

DNA extraction: A tissue sample was obtained at weaning by ear punch and lysed overnight at 55˚C in buffer containing 10mM tris HCl pH 8.0, 5 mM EDTA, 0.1% SDS, and 200 mM NaCl with 0.5 mg/mL proteinase K. DNA was extracted in phenol/chloroform/isoamyl alcohol (Fisher Scientific) and centrifuged at 14,000 rpm for 5 minutes using an Eppendorf 5417R benchtop centrifuge. DNA was precipitated from the aqueous layer using 100% EtOH and spun at 14,000 rpm for 5 minutes to obtain a pellet. The ethanol was decanted, and the pellet was washed in 70% EtOH and spun at 14,000 rpm for 10 minutes. The ethanol was decanted, and the pellet was air-dried and resuspended in 10 mM tris HCl pH 8.0 at a concentration of 50-200 ng/µL.

Polymerase Chain Reaction: PCRs to detect genes of interest were performed with 50-200 ng of DNA using Illustra PureTaq Ready-To-Go PCR Beads (GE Healthcare) in an Eppendorf AG 22331 Hamburg Mastercycler. Primers are described in Table 5.1. Cycling conditions for all PCRs were 1 cycle at 94ºC for 2 minutes; 35 cycles at 94ºC for 30 seconds, 60ºC for 30 seconds, and 72ºC for 1 minute; and 1 cycle at 72ºC for 5 min.

Table 5.1: Primers for PCR.

Gene	Primers
Atg7 flox	1: CAT CTT GTA GCA CCT GCT GAC CTG G 2: CCA CTG GCC CAT CAG TGA GCA TG 3: GCG GAT CCT CGT ATA ATG TAT GCT AT
Atg5 flox	1: GAA TAT GAA GGC ACA CCC CTG AAA TG 2: GTA CTG CAT AAT GGT TTA ACT CTT GC 3: ACA ACG TCG AGC ACA GCT GCG CAA GG 4: CAG GGA ATG GTG TCT CCC AC
CNP-Cre	E3 sense: GCC TTC AAA CTG TCC ATC TC E3 antisense: CCC AGC CCT TTT ATT ACC AC Puro3: CAT AGC CTG AAG AAC GAG A
GFP-LC3	1: ATA ACT TGC TGG CCT TTC CAC T 2: CGG GCC ATT TAC CGT AAG TTA T 3: GCA GCT CAT TGC TGT TCC TCA A
B6.Cg-Gt(ROSA)26Sor$^{tm9(CAG-tdTomato)Hze}$/J:	WT Fwd: AAG GGA GCT GCA GTG GAG TA WT Rev: CCG AAA ATC TGT GGG AAG TC TG Fwd: CTG TTC CTG TAC GGC ATG G TG Rev: GGC ATT AAA GCA GCG TAT CC

5.3 Behavioral Testing

At least one week before starting behavioral testing, experimental mice were relocated to a reverse-cycle core facility with the lights off between 10 AM and 10 PM, so that experiments could be performed during the dark hours (i.e. the mice's active hours).

Open Field Testing: Atg7(CNP) cKO mice and littermate controls were placed inside an open field arena (43.2 cm x 43.2 cm x 30.5 cm) for one hour at two months of age. Measurements of distance traveled and number of rearings were recorded and measured using equipment and software from Med Associates. Number of droppings was quantified by hand.

Balance Beam: Mice were trained to cross a 12 mm wide, 80 cm long, 60 cm high metal beam. On training day, mice were exposed to the beam at least three times and gently encouraged across by the experimenter as necessary. On testing day, mice were videotaped across three trials, with resting periods between trials ranging from thirty seconds to three minutes. To determine the amount of time required for each mouse to cross the beam, videos were analyzed using custom MATLAB software, generously provided by Dr. Leora Fox. Any trial in which the mouse failed to cross the beam within twenty seconds (either due to falls or slow speed) was scored as twenty seconds. Only the two fastest trials for each mouse were included in the analysis.

Gait Analysis: Mice were made to walk a 40-cm runway after their forepaws were painted with red paint and their hindpaws were painted in blue. All paints used were non-toxic watercolor

paints. 3 tandem sets of footprints were selected and measured for stride length, forepaw base, hindpaw base, and stride overlap.

5.4 Post-mortem Analyses

Immunohistochemistry: Mice were deeply anesthetized with isoflurane and transcardially perfused with 0.9% saline followed by 4% paraformaldehyde (PFA). Brains and spinal cords were dissected, fixed in 4% PFA for 1 hour at room temperature and then 4^{O}C overnight, cryoprotected in 30% sucrose in phosphate buffer at 4^{O}C, snap-frozen in powdered dry ice, embedded in O.C.T. Compound (Fisher), and stored at -80^{o}C. Free-floating brain cryosections (30 or 50 μm) were cut on a cryostat and stored at 4^{o}C in phosphate buffer containing 0.02% sodium azide. 12 μm spinal cord cryosections were mounted directly onto slides. For antigen retrieval, sections were placed at 80^{o}C in 10mM sodium citrate (pH=9.0). Sections were permeabilized with 0.4% Triton and blocked with 10% BSA in PBS, and then incubated in primary antibody diluted in PBS 0.01% Triton-X 100 overnight at 4^{O}C (when staining for NG2, sections were left in primary antibody for three nights) (see Table 5.2 for a list of antibodies). Sections were subsequently incubated in Alexa Fluor conjugated secondary antibodies (Life Technologies) diluted in 0.01% Triton-X 100 PBS for 1 hr at room temperature, stained with Hoechst (Invitrogen) for ten minutes, mounted onto glass slides, and coverslipped using Prolong Gold antifade reagent (Life Technologies).

Cell Counting: Every eighth serially-cut coronal brain sections were used for all cell counting. Matching sections from 1.10 mm to -0.82 mm Bregma were used to count NG2^{+} and Olig2+, CC1^{+} cells in the corpus callosum. Unbiased counts were obtained using NIH ImageJ. For NG2^{+} cells, pericytes were excluded based on their morphology.

Electron Microscopy: Transmission electron microscopy was performed in conjunction with the Electron Microscope Facility at Columbia University Medical Center. Briefly, mice were deeply anesthetized with isoflurane and transcardially perfused with 0.9% saline followed by 2.5% glutaraldehyde, 2% PFA in 0.1 M sodium cacodylate buffer (pH = 7.2). Optic nerves, corpus callosi, and sciatic nerves were dissected, post-fixed in 2.5% glutaraldehyde, 2% PFA in 0.1 M sodium cacodylate buffer for 1 hour at room temperature and then $4^{O}C$ at least overnight. Tissue was then postfixed with 1% OsO4 also in Cacodylate buffer for one hour. After dehydration tissue was embedded in Lx-112 (Ladd Research Industries, Inc.).

A similar procedure was employed for cultured oligodendrocytes. Cells were fixed with 2.5% glutaraldehyde in 0.1M Sorenson's buffer (PH 7.2) for at least one hour. Cells were then postfixed with 1% OsO4 also in Sorenson's buffer for one hour. After dehydration cells were embedded in a mixture of Lx-112 (Ladd Research Industries, Inc.) and Embed-812 (EMS, Fortwashington, PA). For both tissue and cells, thin sections were cut on the PT-XL ultramicrotome at 60nm thick. The sections were stained with uranyl acetate and lead citrate and examined under a JEOL JEM-1200 EXII electron microscope. Images were captured with an ORCA-HR digital camera (Hamamatsu) and recorded with an AMT Image Capture Engine.

All imaging and analysis were conducted blinded to the experimental condition. For measuring g-ratios, 75 axons per animal were scored. For measuring percent axons myelinated in the corpus callosum, approximately 250 axons per animal were scored. Morphological features were identified manually, and NIH ImageJ was used to measure dimensions of interest.

Fresh-frozen tissue preparation for lysis: Mice were deeply anesthetized with isoflurane and decapitated. Brains were removed and placed into 1 mL Eppendorf tubes. Samples were flash-frozen on powdered dry ice and stored at -80˚C until processing.

Preparation of tissue lysates from frozen tissue: Brains were placed in a glass dounce homogenizer with an equal volume of 1x PBS containing Halt protease inhibitor cocktail (ThermoFisher) and disaggregated with 20 pumps of the pestle. The suspension was transferred to a tube and an equal volume of detergent (2% Triton-X-100 in PBS) was added. After 30 minutes on ice, samples were spun in an Eppendorf 5417R centrifuge at 2,000 g for 5 minutes at 4^{o}C. The supernatant (S1) was transferred to another tube for use in future experiments.

Isolation of Autophagic Vacuoles: Nycodenz cell fractionation methods were performed as previously described (Filimonenko et al., 2010). Briefly, mice were deeply anesthetized with isoflurane and decapitated. Brains were removed, mechanically disrupted, and fractionated using a discontinuos Nycodenz gradient (Stromhaug et al., 1998). Isolated fractions were then examined by immunoblotting

5.5 Cell Culture

Purification of Cells: OPCs were purified from enzymatically dissociated P6-8 C57BL/6 or transgenic mouse cortices by immunopanning and grown in serum-free defined medium, as described previously with minor modifications (Emery and Dugas, 2013). Briefly, tissue was diced and digested in papain (Worthington) at 37^{O}C for 90 min and then gently dissociated. Dissociated cortices were sequentially immunopanned on BSL1 (Vector Laboratories) and then O4 antibody-

coated plates to select for $O4^+$ OPCs. After rinsing nonadherent cells away, purified OPCs were removed from the final panning plate with trypsin and transferred to poly-D-lysine coated tissue culture dishes.

Primary Cultures: All cells were cultured at $37^{O}C$ under 5% CO_2 in serum-free defined media containing DMEM, transferrin (100 μg/ml), bovine serum albumin (100μg/ml), putrescine (16 μg/ml) , progesterone (60 ng/ml), sodium selenite (40 ng/ml), N-acetyl-L-cysteine (5 μg/ml), d-biotin (10 ng/ml), forskolin (4.2 μg/ml), insulin (5 μg/ml) (all from Sigma), glutamine (2 mM), sodium pyruvate (1 mM), B27 (2%), penicillin–streptomycin (100 U/ml) (all from Invitrogen), Trace Elements B (1x, Cellgro), and LIF (20 ng/ml, Chemicon). Proliferation medium also contained OPC mitogens PDGF-AA (20 ng/ml) and NT-3 (1 ng/ml) (both from PeproTech), while differentiation medium contained triiodothyronine (40 ng/ml, Sigma) without OPC mitogens. For experiments in which only mature OLs were examined (and not any intervening stages of differentiation), the differentiation medium was modified by using DMEM/F12 base media (Invitrogen) and a higher dose of insulin (25 μg/ml) to maximize OL survival.

Immunocytochemistry: After the appropriate number of days of differentiation, cells were fixed immediately or treated with either leupeptin (Sigma) for two hours or mCLING (Synaptic Systems) overnight through a half media change before fixation. Cells were fixed for 10 min with 4% paraformaldehyde, permeabilized in 0.01% Triton-X 100 in PBS, blocked in 10% BSA in PBS and stained with primary antibodies diluted in 0.01% Triton-X 100 in PBS overnight at 4°C or for 1 hour at room temperature (see Table 5.2 for a list of antibodies). Alexa Fluor conjugated secondary antibodies (Life Technologies) were diluted in 0.01% Triton-X 100 PBS, incubated with

coverslips for 1 hr at room temperature, and mounted with Prolong Gold antifade reagent with DAPI (Life Technologies) onto glass slides.

Live-cell Imaging of OLs: OPCs were plated on PDL-coated glass bottom imaging dishes (35mm, MatTek) and differentiated for 10-11 days as above. Prior to imaging, cells were incubated for 60 minutes at 37°C in DMEM with LysoTracker Red DND-99 (75 nM, Invitrogen), then washed once with and imaged in warm Hibernate A media (Invitrogen) to reduce phototoxicity. Cells were imaged using a spinning disc confocal unit (CSU-10; Yokogawa Electric Corporation) with Borealis (Spectral Applied Research) on an inverted microscope (Ti; Nikon) with a charge-coupled device camera (Orca-R2; Hamamatsu Photonics). Z-sectioning was done with a Piezo-driven motorized stage (Applied Scientific Instrumentation), and focus was maintained using Perfect Focus (Nikon) before each Z-series acquisition. An acousto-optic tunable filter was used to select the excitation light of two 100 mW lasers for excitation at 491 and 561 nm for eGFP and LysoTracker, respectively (Spectral Applied Research), and a filter wheel was used for emission wavelength selection (Sutter Instruments). The system was controlled by MetaMorph software (Molecular Devices). Temperature was maintained at 37 using an air stream stage incubator (Nevtek). 4 × 0.75 μm Z-sections were acquired every 60 sec for at least 60 minutes using a 60× 1.4 N.A. oil immersion PlanApochromat objective lens, with 2 × 2 binning.

ImageJ (Schneider et al., 2012) was used for all data analysis. Maximum intensity projections of GFP-LC3 and LysoTracker were generated for each frame. To remove static features, we subtracted a minimum projection of all the time points from each frame. Identification of puncta and area measurements was performed by hand using ImageJ. Image analyses were performed on still images by tracing and measuring puncta and cell contours using ImageJ.

5.6 Other

Fluorescence Microscopy: A Leica SP5 confocal microscope was used to image both fixed OL cultures and fixed brain sections. When necessary, confocal z-stacks were taken every 0.45 μm.

Immunoblotting: Whole cell lysates and tissue lysates from freshly frozen dissected brain were generated using 1% Triton-X 100 in PBS containing Halt protease inhibitor cocktail (ThermoFisher). All samples were cleared by centrifugation at 2,000 g for 5 min at 4°C. Cell lysates were subjected to an additional centrifugation step of 21,000 g for 10 minutes, the pellet of which was resuspended in 8 M Urea in PBS with 1% Triton-X 100 and protease inhibitor. Protein concentration was determined using the DC Protein Assay (Bio-rad Laboratories [Hercules, CA]) and equal amounts of protein (1-20 μg) were prepared and loaded onto 4–12% Bis-Tris and blotted to PVDF membranes as described by the manufacturer's recommendations (Life Technologies). PVDF membranes were blocked in 3% BSA in PBS containing 1% Tween-20. Antibodies were incubated overnight at 4°C (see Table 5.2 for a list of antibodies). The appropriate HRP-conjugated secondary antibodies (ThermoFisher Scientific) were diluted in 1% BSA PBS and a chemiluminescent reaction (West Dura SuperSignal, ThermoFisher Scientific) was detected by the Versadoc Imaging System (Bio-rad).

Quantification and Statistical Analysis: Statistical analyses were performed using Statview 5.0 (SAS Institute). Statistical significance was accepted at $p < 0.05$. Normally distributed data were subject to student t-test or, for multiple comparisons, analysis of variance (ANOVA). Complete F-statistics and calculated p-values are also available in the figure legends. Power analyses for

Table 5.2 Antibody information.

Antibody	Source	Identifier
Rat anti-MBP	Bio-Rad/Abd Serotec	MCA409S
Mouse anti-MBP	Covance	SM-199P
Mouse anti-APC [CC1]	abcam	ab16794
Rabbit anti-Olig2	Millipore	AB9610
Rabbit anti-NG2	Millipore	AB5320
Rabbit anti-PLP	abcam	Ab28486
Rabbit anti-MAG (D4G3)	Cell Signaling Technology	9043
Goat anti-MOG	abcam	Ab115597
Rabbit ant-B_{III}-tubulin	Covance	PRB-435P
Rabbit anti-Atg7 (D12B11)	Cell Signaling Technology	8558
Rabbit anti-Atg5	Cell Signaling Technology	12994
Rabbit anti-Vinculin	Invitrogen	700062
Rabbit anti-LC3A/B	abcam	Ab58610
Rabbit anti-LC3B	Abcam	Ab48394
Rabbit anti-Atg16	ProSci Inc.	4425
Guinea pig anti-p62	Progen	GP62C
Rabbit anti-Calnexin	Stressgen	SPA-860
Rabbit anti-α Synuclein	Millipore	04-1053
Rabbit anti-α+β Synuclein	abcam	ab51252
Rabbit anti-GFAP	Dako	Z0334
Rabbit anti-Iba1	Wako	019-19741
Rat anti-CD68	abcam	ab53444

behavioral studies were performed to achieve a power of 0.8 with a confidence of 0.95 using G*Power 3.1 (Faul et al., 2009). Effect sizes were based upon pilot studies, previously published, or unpublished materials. n-values are indicative of biological replicates and no data were excluded from analyses.

Image preparation: All images were prepared using NIH ImageJ, Adobe Photoshop CS5, and Adobe Illustrator CS5.

References

Aaker, J.D., Elbaz, B., Wu, Y., Looney, T.J., Zhang, L., Lahn, B.T., and Popko, B. (2016). Transcriptional Fingerprint of Hypomyelination in Zfp191null and Shiverer (Mbpshi) Mice. ASN neuro *8*.

Aggarwal, S., Snaidero, N., Pahler, G., Frey, S., Sanchez, P., Zweckstetter, M., Janshoff, A., Schneider, A., Weil, M.T., Schaap, I.A., *et al.* (2013). Myelin membrane assembly is driven by a phase transition of myelin basic proteins into a cohesive protein meshwork. PLoS biology *11*, e1001577.

Aggarwal, S., Yurlova, L., Snaidero, N., Reetz, C., Frey, S., Zimmermann, J., Pahler, G., Janshoff, A., Friedrichs, J., Muller, D.J., *et al.* (2011). A size barrier limits protein diffusion at the cell surface to generate lipid-rich myelin-membrane sheets. Developmental cell *21*, 445-456.

Alberts, B., Johnson, A., Lewis, J.M., D, Raff, M., Roberts, K., and Walter, P. (2002). The Lipid Bilayer. In Molecular biology of the cell (New York: Garland Science).

Almeida, R., and Lyons, D. (2016). Oligodendrocyte Development in the Absence of Their Target Axons In Vivo. PLoS One *11*, e0164432.

Alvarez-Saavedra, M., De Repentigny, Y., Yang, D., O'Meara, R.W., Yan, K., Hashem, L.E., Racacho, L., Ioshikhes, I., Bulman, D.E., Parks, R.J., *et al.* (2016). Voluntary Running Triggers

VGF-Mediated Oligodendrogenesis to Prolong the Lifespan of Snf2h-Null Ataxic Mice. Cell reports *17*, 862-875.

Anitei, M., Cowan, A.E., Pfeiffer, S.E., and Bansal, R. (2009). Role for Rab3a in oligodendrocyte morphological differentiation. Journal of neuroscience research *87*, 342-352.

Arnett, H.A., Fancy, S.P., Alberta, J.A., Zhao, C., Plant, S.R., Kaing, S., Raine, C.S., Rowitch, D.H., Franklin, R.J., and Stiles, C.D. (2004). bHLH transcription factor Olig1 is required to repair demyelinated lesions in the CNS. Science (New York, NY) *306*, 2111-2115.

Arroyo, D.S., Soria, J.A., Gaviglio, E.A., Garcia-Keller, C., Cancela, L.M., Rodriguez-Galan, M.C., Wang, J.M., and Iribarren, P. (2013). Toll-like receptor 2 ligands promote microglial cell death by inducing autophagy. FASEB journal : official publication of the Federation of American Societies for Experimental Biology *27*, 299-312.

Asbury, A.K. (1967). Schwann cell proliferation in developing mouse sciatic nerve. A radioautographic study. The Journal of cell biology *34*, 735-743.

Axe, E.L., Walker, S.A., Manifava, M., Chandra, P., Roderick, H.L., Habermann, A., Griffiths, G., and Ktistakis, N.T. (2008). Autophagosome formation from membrane compartments enriched in phosphatidylinositol 3-phosphate and dynamically connected to the endoplasmic reticulum. The Journal of cell biology *182*, 685.

Azevedo, F.A., Carvalho, L.R., Grinberg, L.T., Farfel, J.M., Ferretti, R.E., Leite, R.E., Jacob Filho, W., Lent, R., and Herculano-Houzel, S. (2009). Equal numbers of neuronal and nonneuronal cells make the human brain an isometrically scaled-up primate brain. J Comp Neurol *513*, 532-541.

Baixauli, F., López-Otín, C., and Mittelbrunn, M. (2014). Exosomes and Autophagy: Coordinated Mechanisms for the Maintenance of Cellular Fitness. Frontiers in Immunology *5*.

Bakhti, M., Snaidero, N., Schneider, D., Aggarwal, S., Mobius, W., Janshoff, A., Eckhardt, M., Nave, K.A., and Simons, M. (2013). Loss of electrostatic cell-surface repulsion mediates myelin membrane adhesion and compaction in the central nervous system. Proceedings of the National Academy of Sciences of the United States of America *110*, 3143-3148.

Baraban, M., Koudelka, S., and Lyons, D.A. (2018). Ca (2+) activity signatures of myelin sheath formation and growth in vivo. Nature neuroscience *21*, 19-23.

Baraban, M., Mensch, S., and Lyons, D.A. (2016). Adaptive myelination from fish to man. Brain research *1641*, 149-161.

Barmada, S.J., Serio, A., Arjun, A., Bilican, B., Daub, A., Ando, D.M., Tsvetkov, A., Pleiss, M., Li, X., Peisach, D., *et al.* (2014). Autophagy induction enhances TDP43 turnover and survival in neuronal ALS models. Nature chemical biology *10*, 677-685.

Baron, W., Ozgen, H., Klunder, B., de Jonge, J.C., Nomden, A., Plat, A., Trifilieff, E., de Vries, H., and Hoekstra, D. (2015). The major myelin-resident protein PLP is transported to myelin membranes via a transcytotic mechanism: involvement of sulfatide. Molecular and cellular biology *35*, 288-302.

Barres, B.A., Hart, I.K., Coles, H.S., Burne, J.F., Voyvodic, J.T., Richardson, W.D., and Raff, M.C. (1992). Cell death and control of cell survival in the oligodendrocyte lineage. Cell *70*, 31-46.

Barres, B.A., Jacobson, M.D., Schmid, R., Sendtner, M., and Raff, M.C. (1993). Does oligodendrocyte survival depend on axons? Current biology : CB *3*, 489-497.

Barres, B.A., and Raff, M.C. (1993). Proliferation of oligodendrocyte precursor cells depends on electrical activity in axons. Nature *361*, 258-260.

Baumann, N., and Pham-Dinh, D. (2001). Biology of oligodendrocyte and myelin in the mammalian central nervous system. Physiological reviews *81*, 871-927.

Bengtsson, S.L., Nagy, Z., Skare, S., Forsman, L., Forssberg, H., and Ullen, F. (2005). Extensive piano practicing has regionally specific effects on white matter development. Nature neuroscience *8*, 1148-1150.

Bercury, K.K., and Macklin, W.B. (2015). Dynamics and mechanisms of CNS myelination. Developmental cell *32*, 447-458.

Berg, T.O., Fengsrud, M., Stromhaug, P.E., Berg, T., and Seglen, P.O. (1998). Isolation and characterization of rat liver amphisomes. Evidence for fusion of autophagosomes with both early and late endosomes. J Biol Chem *273*, 21883-21892.

Bergles, D.E., Roberts, J.D., Somogyi, P., and Jahr, C.E. (2000). Glutamatergic synapses on oligodendrocyte precursor cells in the hippocampus. Nature *405*, 187-191.

Betz, U.A., Vosshenrich, C.A., Rajewsky, K., and Muller, W. (1996). Bypass of lethality with mosaic mice generated by Cre-loxP-mediated recombination. Current biology : CB *6*, 1307-1316.

Bin, J.M., Harris, S.N., and Kennedy, T.E. (2016). The oligodendrocyte-specific antibody 'CC1' binds Quaking 7. Journal of neurochemistry *139*, 181-186.

Boggs, J.M. (2006). Myelin basic protein: a multifunctional protein. Cell Mol Life Sci *63*, 1945-1961.

Boyle, K.B., and Randow, F. (2015). Rubicon swaps autophagy for LAP. Nature cell biology *17*, 843-845.

Brand, A.H., and Perrimon, N. (1993). Targeted gene expression as a means of altering cell fates and generating dominant phenotypes. Development (Cambridge, England) *118*, 401-415.

Brocard, J., Warot, X., Wendling, O., Messaddeq, N., Vonesch, J.L., Chambon, P., and Metzger, D. (1997). Spatio-temporally controlled site-specific somatic mutagenesis in the mouse. Proceedings of the National Academy of Sciences of the United States of America *94*, 14559-14563.

Brosius Lutz, A., Chung, W.S., Sloan, S.A., Carson, G.A., Zhou, L., Lovelett, E., Posada, S., Zuchero, J.B., and Barres, B.A. (2017). Schwann cells use TAM receptor-mediated phagocytosis in addition to autophagy to clear myelin in a mouse model of nerve injury. Proceedings of the National Academy of Sciences of the United States of America *114*, E8072-e8080.

Bujalka, H., Koenning, M., Jackson, S., Perreau, V.M., Pope, B., Hay, C.M., Mitew, S., Hill, A.F., Lu, Q.R., Wegner, M., *et al.* (2013). MYRF is a membrane-associated transcription factor that autoproteolytically cleaves to directly activate myelin genes. PLoS biology *11*, e1001625.

Cai, J., Qi, Y., Hu, X., Tan, M., Liu, Z., Zhang, J., Li, Q., Sander, M., and Qiu, M. (2005). Generation of oligodendrocyte precursor cells from mouse dorsal spinal cord independent of Nkx6 regulation and Shh signaling. Neuron *45*, 41-53.

Calver, A.R., Hall, A.C., Yu, W.P., Walsh, F.S., Heath, J.K., Betsholtz, C., and Richardson, W.D. (1998). Oligodendrocyte population dynamics and the role of PDGF in vivo. Neuron *20*, 869-882.

Cantarella, C., Cayre, M., Magalon, K., and Durbec, P. (2008). Intranasal HB-EGF administration favors adult SVZ cell mobilization to demyelinated lesions in mouse corpus callosum. Developmental neurobiology *68*, 223-236.

Castelfranco, A.M., and Hartline, D.K. (2015). The evolution of vertebrate and invertebrate myelin: a theoretical computational study. Journal of computational neuroscience *38*, 521-538.

Chandross, K.J., Cohen, R.I., Paras, P., Gravel, M., Braun, P.E., and Hudson, L.D. (1999). Identification and Characterization of Early Glial Progenitors Using a Transgenic Selection Strategy. The Journal of Neuroscience *19*, 759-774.

Chang, K.J., Redmond, S.A., and Chan, J.R. (2016). Remodeling myelination: implications for mechanisms of neural plasticity. Nature neuroscience *19*, 190-197.

Chang, K.J., Zollinger, D.R., Susuki, K., Sherman, D.L., Makara, M.A., Brophy, P.J., Cooper, E.C., Bennett, V., Mohler, P.J., and Rasband, M.N. (2014). Glial ankyrins facilitate paranodal axoglial junction assembly. Nature neuroscience *17*, 1673-1681.

Charles, P., Hernandez, M.P., Stankoff, B., Aigrot, M.S., Colin, C., Rougon, G., Zalc, B., and Lubetzki, C. (2000). Negative regulation of central nervous system myelination by polysialylated-neural cell adhesion molecule. Proceedings of the National Academy of Sciences of the United States of America *97*, 7585-7590.

Chintawar, S., Cayrol, R., Antel, J., Pandolfo, M., and Prat, A. (2009). Blood-brain barrier promotes differentiation of human fetal neural precursor cells. Stem cells (Dayton, Ohio) *27*, 838-846.

Chomiak, T., and Hu, B. (2009). What is the optimal value of the g-ratio for myelinated fibers in the rat CNS? A theoretical approach. PLoS One *4*, e7754.

Chong, S.Y., Rosenberg, S.S., Fancy, S.P., Zhao, C., Shen, Y.A., Hahn, A.T., McGee, A.W., Xu, X., Zheng, B., Zhang, L.I., *et al.* (2012). Neurite outgrowth inhibitor Nogo-A establishes spatial segregation and extent of oligodendrocyte myelination. Proceedings of the National Academy of Sciences of the United States of America *109*, 1299-1304.

Chow, C.Y., Zhang, Y., Dowling, J.J., Jin, N., Adamska, M., Shiga, K., Szigeti, K., Shy, M.E., Li, J., Zhang, X., *et al.* (2007). Mutation of FIG4 causes neurodegeneration in the pale tremor mouse and patients with CMT4J. Nature *448*, 68-72.

Ciechanover, A., Orian, A., and Schwartz, A.L. (2000). Ubiquitin-mediated proteolysis: biological regulation via destruction. BioEssays : news and reviews in molecular, cellular and developmental biology *22*, 442-451.

Crang, A.J., Gilson, J., and Blakemore, W.F. (1998). The demonstration by transplantation of the very restricted remyelinating potential of post-mitotic oligodendrocytes. Journal of neurocytology *27*, 541-553.

Crawford, A.H., Tripathi, R.B., Foerster, S., McKenzie, I., Kougioumtzidou, E., Grist, M., Richardson, W.D., and Franklin, R.J. (2016). Pre-Existing Mature Oligodendrocytes Do Not Contribute to Remyelination following Toxin-Induced Spinal Cord Demyelination. The American journal of pathology *186*, 511-516.

Czopka, T., Ffrench-Constant, C., and Lyons, D.A. (2013). Individual oligodendrocytes have only a few hours in which to generate new myelin sheaths in vivo. Developmental cell *25*, 599-609.

Dangata, Y.Y., Findlater, G.S., and Kaufman, M.H. (1996). Postnatal development of the optic nerve in (C57BL x CBA)F1 hybrid mice: general changes in morphometric parameters. Journal of anatomy *189 (Pt 1)*, 117-125.

Davison, A.N., and Dobbing, J. (1960). Phospholipid metabolism in nervous tissue. 3. The anatomical distribution of metabolically inert phospholipid in the central nervous system. Biochemical Journal *75*, 571-574.

de Araujo, M.E., Lamberti, G., and Huber, L.A. (2015). Isolation of Early and Late Endosomes by Density Gradient Centrifugation. Cold Spring Harbor protocols *2015*, 1013-1016.

De Biase, L.M., Nishiyama, A., and Bergles, D.E. (2010). Excitability and synaptic communication within the oligodendrocyte lineage. J Neurosci *30*, 3600-3611.

DeBoy, C.A., Zhang, J., Dike, S., Shats, I., Jones, M., Reich, D.S., Mori, S., Nguyen, T., Rothstein, B., Miller, R.H., *et al.* (2007). High resolution diffusion tensor imaging of axonal damage in focal inflammatory and demyelinating lesions in rat spinal cord. Brain : a journal of neurology *130*, 2199-2210.

Dessaud, E., Ribes, V., Balaskas, N., Yang, L.L., Pierani, A., Kicheva, A., Novitch, B.G., Briscoe, J., and Sasai, N. (2010). Dynamic assignment and maintenance of positional identity in the ventral neural tube by the morphogen sonic hedgehog. PLoS biology *8*, e1000382.

Di Malta, C., Fryer, J.D., Settembre, C., and Ballabio, A. (2012). Autophagy in astrocytes: a novel culprit in lysosomal storage disorders. Autophagy *8*, 1871-1872.

Dimou, L., Simon, C., Kirchhoff, F., Takebayashi, H., and Gotz, M. (2008). Progeny of Olig2-expressing progenitors in the gray and white matter of the adult mouse cerebral cortex. J Neurosci *28*, 10434-10442.

Djeddi, A., Michelet, X., Culetto, E., Alberti, A., Barois, N., and Legouis, R. (2012). Induction of autophagy in ESCRT mutants is an adaptive response for cell survival in C. elegans. Journal of cell science *125*, 685-694.

Dong, X., Chen, K., Cuevas-Diaz Duran, R., You, Y., Sloan, S.A., Zhang, Y., Zong, S., Cao, Q., Barres, B.A., and Wu, J.Q. (2015). Comprehensive Identification of Long Non-coding RNAs in Purified Cell Types from the Brain Reveals Functional LncRNA in OPC Fate Determination. PLoS genetics *11*, e1005669.

Ducros, A., Nagy, T., Alamowitch, S., Nibbio, A., Joutel, A., Vahedi, K., Chabriat, H., Iba-Zizen, M.T., Julien, J., Davous, P., *et al.* (1996). Cerebral autosomal dominant arteriopathy with

subcortical infarcts and leukoencephalopathy, genetic homogeneity, and mapping of the locus within a 2-cM interval. American journal of human genetics *58*, 171-181.

Dugas, J.C., Cuellar, T.L., Scholze, A., Ason, B., Ibrahim, A., Emery, B., Zamanian, J.L., Foo, L.C., McManus, M.T., and Barres, B.A. (2010). Dicer1 and miR-219 Are required for normal oligodendrocyte differentiation and myelination. Neuron *65*, 597-611.

Edgar, J.M., McLaughlin, M., Werner, H.B., McCulloch, M.C., Barrie, J.A., Brown, A., Faichney, A.B., Snaidero, N., Nave, K.A., and Griffiths, I.R. (2009). Early ultrastructural defects of axons and axon-glia junctions in mice lacking expression of Cnp1. Glia *57*, 1815-1824.

Edvardson, S., Gerhard, F., Jalas, C., Lachmann, J., Golan, D., Saada, A., Shaag, A., Ungermann, C., and Elpeleg, O. (2015). Hypomyelination and developmental delay associated with VPS11 mutation in Ashkenazi-Jewish patients. Journal of medical genetics *52*, 749-753.

Emery, B., Agalliu, D., Cahoy, J.D., Watkins, T.A., Dugas, J.C., Mulinyawe, S.B., Ibrahim, A., Ligon, K.L., Rowitch, D.H., and Barres, B.A. (2009). Myelin gene regulatory factor is a critical transcriptional regulator required for CNS myelination. Cell *138*, 172-185.

Emery, B., and Dugas, J.C. (2013). Purification of oligodendrocyte lineage cells from mouse cortices by immunopanning. Cold Spring Harbor protocols *2013*, 854-868.

Etienne-Manneville, S., and Hall, A. (2002). Rho GTPases in cell biology. Nature *420*, 629.

Faul, F., Erdfelder, E., Buchner, A., and Lang, A.G. (2009). Statistical power analyses using G*Power 3.1: tests for correlation and regression analyses. Behavior research methods *41*, 1149-1160.

Feldmann, A., Amphornrat, J., Schonherr, M., Winterstein, C., Mobius, W., Ruhwedel, T., Danglot, L., Nave, K.A., Galli, T., Bruns, D., *et al.* (2011). Transport of the major myelin proteolipid protein is directed by VAMP3 and VAMP7. J Neurosci *31*, 5659-5672.

Feldmann, A., Winterstein, C., White, R., Trotter, J., and Kramer-Albers, E.M. (2009). Comprehensive analysis of expression, subcellular localization, and cognate pairing of SNARE proteins in oligodendrocytes. Journal of neuroscience research *87*, 1760-1772.

Fengsrud, M., Erichsen, E.S., Berg, T.O., Raiborg, C., and Seglen, P.O. (2000). Ultrastructural characterization of the delimiting membranes of isolated autophagosomes and amphisomes by freeze-fracture electron microscopy. European journal of cell biology *79*, 871-882.

Ferguson, C.J., Lenk, G.M., and Meisler, M.H. (2009). Defective autophagy in neurons and astrocytes from mice deficient in PI (3, 5) P2. Human molecular genetics *18*, 4868-4878.

Fields, R.D. (2008). White matter in learning, cognition and psychiatric disorders. Trends Neurosci *31*, 361-370.

Filimonenko, M., Isakson, P., Finley, K.D., Anderson, M., Jeong, H., Melia, T.J., Bartlett, B.J., Myers, K.M., Birkeland, H.C., Lamark, T., *et al.* (2010). The selective macroautophagic degradation of aggregated proteins requires the PI3P-binding protein Alfy. Molecular cell *38*, 265-279.

Filimonenko, M., Stuffers, S., Raiborg, C., Yamamoto, A., Malerod, L., Fisher, E.M., Isaacs, A., Brech, A., Stenmark, H., and Simonsen, A. (2007). Functional multivesicular bodies are required for autophagic clearance of protein aggregates associated with neurodegenerative disease. The Journal of cell biology *179*, 485-500.

Fischer, C.A., and Morell, P. (1974). Turnover of proteins in myelin and myelin-like material of mouse brain. Brain research *74*, 51-65.

Flores, A.I., Narayanan, S.P., Morse, E.N., Shick, H.E., Yin, X., Kidd, G., Avila, R.L., Kirschner, D.A., and Macklin, W.B. (2008). Constitutively active Akt induces enhanced myelination in the CNS. J Neurosci *28*, 7174-7183.

Florey, O., Kim, S.E., Sandoval, C.P., Haynes, C.M., and Overholtzer, M. (2011). Autophagy machinery mediates macroendocytic processing and entotic cell death by targeting single membranes. Nature cell biology *13*, 1335-1343.

Florey, O., and Overholtzer, M. (2012). Autophagy proteins in macroendocytic engulfment. Trends in cell biology *22*, 374-380.

Fogarty, M., Richardson, W.D., and Kessaris, N. (2005). A subset of oligodendrocytes generated from radial glia in the dorsal spinal cord. Development (Cambridge, England) *132*, 1951-1959.

Fortun, J., Dunn, W.A., Joy, S., Li, J., and Notterpek, L. (2003). Emerging role for autophagy in the removal of aggresomes in Schwann cells. The Journal of neuroscience *23*, 10672-10680.

Foti, S.B., Chou, A., Moll, A.D., and Roskams, A.J. (2013). HDAC inhibitors dysregulate neural stem cell activity in the postnatal mouse brain. International journal of developmental neuroscience : the official journal of the International Society for Developmental Neuroscience *31*, 434-447.

Fruhbeis, C., Frohlich, D., Kuo, W.P., Amphornrat, J., Thilemann, S., Saab, A.S., Kirchhoff, F., Mobius, W., Goebbels, S., Nave, K.A., *et al.* (2013). Neurotransmitter-triggered transfer of exosomes mediates oligodendrocyte-neuron communication. PLoS biology *11*, e1001604.

Fujimoto, E., Gaynes, B., Brimley, C.J., Chien, C.B., and Bonkowsky, J.L. (2011). Gal80 intersectional regulation of cell-type specific expression in vertebrates. Developmental dynamics : an official publication of the American Association of Anatomists *240*, 2324-2334.

Funfschilling, U., Supplie, L.M., Mahad, D., Boretius, S., Saab, A.S., Edgar, J., Brinkmann, B.G., Kassmann, C.M., Tzvetanova, I.D., Mobius, W., *et al.* (2012). Glycolytic oligodendrocytes maintain myelin and long-term axonal integrity. Nature *485*, 517-521.

Furusho, M., Dupree, J.L., Nave, K.A., and Bansal, R. (2012). Fibroblast growth factor receptor signaling in oligodendrocytes regulates myelin sheath thickness. J Neurosci *32*, 6631-6641.

Furusho, M., Kaga, Y., Ishii, A., Hebert, J.M., and Bansal, R. (2011). Fibroblast growth factor signaling is required for the generation of oligodendrocyte progenitors from the embryonic forebrain. J Neurosci *31*, 5055-5066.

Gan, L., Vargas, M.R., Johnson, D.A., and Johnson, J.A. (2012). Astrocyte-specific overexpression of Nrf2 delays motor pathology and synuclein aggregation throughout the CNS in the alpha-synuclein mutant (A53T) mouse model. J Neurosci *32*, 17775-17787.

Geng, J., and Klionsky, D.J. (2008). The Atg8 and Atg12 ubiquitin-like conjugation systems in macroautophagy. 'Protein modifications: beyond the usual suspects' review series. EMBO reports *9*, 859-864.

Gibson, E.M., Purger, D., Mount, C.W., Goldstein, A.K., Lin, G.L., Wood, L.S., Inema, I., Miller, S.E., Bieri, G., Zuchero, J.B., *et al.* (2014). Neuronal activity promotes oligodendrogenesis and adaptive myelination in the mammalian brain. Science (New York, NY) *344*, 1252304.

Goebbels, S., Oltrogge, J.H., Kemper, R., Heilmann, I., Bormuth, I., Wolfer, S., Wichert, S.P., Mobius, W., Liu, X., Lappe-Siefke, C., *et al.* (2010). Elevated phosphatidylinositol 3,4,5-trisphosphate in glia triggers cell-autonomous membrane wrapping and myelination. J Neurosci *30*, 8953-8964.

Gomez-Sanchez, J.A., Carty, L., Iruarrizaga-Lejarreta, M., Palomo-Irigoyen, M., Varela-Rey, M., Griffith, M., Hantke, J., Macias-Camara, N., Azkargorta, M., Aurrekoetxea, I., *et al.* (2015). Schwann cell autophagy, myelinophagy, initiates myelin clearance from injured nerves. The Journal of cell biology *210*, 153-168.

Gonzalez-Perez, O., and Alvarez-Buylla, A. (2011). Oligodendrogenesis in the subventricular zone and the role of epidermal growth factor. Brain research reviews *67*, 147-156.

Gordon, P.B., and Seglen, P.O. (1988). Prelysosomal convergence of autophagic and endocytic pathways. Biochemical and biophysical research communications *151*, 40-47.

Gossen, M., and Bujard, H. (1992). Tight control of gene expression in mammalian cells by tetracycline-responsive promoters. Proceedings of the National Academy of Sciences of the United States of America *89*, 5547-5551.

Gould, R.M. (1977). Incorporation of glycoproteins into peripheral nerve myelin. The Journal of cell biology *75*, 326-338.

Gould, R.M., and Dawson, R.M. (1976). Incorporation of newly formed lecithin into peripheral nerve myelin. The Journal of cell biology *68*, 480-496.

Griffiths, I., Klugmann, M., Anderson, T., Yool, D., Thomson, C., Schwab, M.H., Schneider, A., Zimmermann, F., McCulloch, M., Nadon, N., *et al.* (1998). Axonal swellings and degeneration in mice lacking the major proteolipid of myelin. Science (New York, NY) *280*, 1610-1613.

Hack, M.A., Saghatelyan, A., de Chevigny, A., Pfeifer, A., Ashery-Padan, R., Lledo, P.M., and Gotz, M. (2005). Neuronal fate determinants of adult olfactory bulb neurogenesis. Nature neuroscience *8*, 865-872.

Hagemeyer, N., Goebbels, S., Papiol, S., Kastner, A., Hofer, S., Begemann, M., Gerwig, U.C., Boretius, S., Wieser, G.L., Ronnenberg, A., *et al.* (2012). A myelin gene causative of a catatonia-depression syndrome upon aging. EMBO Mol Med *4*, 528-539.

Hailey, D.W., Rambold, A.S., Satpute-Krishnan, P., Mitra, K., Sougrat, R., Kim, P.K., and Lippincott-Schwartz, J. (2010). Mitochondria supply membranes for autophagosome biogenesis during starvation. Cell *141*, 656-667.

Hajihosseini, M., Tham, T.N., and Dubois-Dalcq, M. (1996). Origin of oligodendrocytes within the human spinal cord. J Neurosci *16*, 7981-7994.

Hall, A. (1998). Rho GTPases and the Actin Cytoskeleton. Science (New York, NY) *279*, 509-514.

Hamasaki, M., Furuta, N., Matsuda, A., Nezu, A., Yamamoto, A., Fujita, N., Oomori, H., Noda, T., Haraguchi, T., Hiraoka, Y., *et al.* (2013). Autophagosomes form at ER–mitochondria contact sites. Nature *495*, 389.

Hara, T., Nakamura, K., Matsui, M., Yamamoto, A., Nakahara, Y., Suzuki-Migishima, R., Yokoyama, M., Mishima, K., Saito, I., Okano, H., *et al.* (2006). Suppression of basal autophagy in neural cells causes neurodegenerative disease in mice. Nature *441*, 885-889.

Hayashi-Nishino, M., Fujita, N., Noda, T., Yamaguchi, A., Yoshimori, T., and Yamamoto, A. (2009). A subdomain of the endoplasmic reticulum forms a cradle for autophagosome formation. Nature cell biology *11*, 1433.

Hayashi-Nishino, M., Fujita, N., Noda, T., Yamaguchi, A., Yoshimori, T., and Yamamoto, A. (2010). Electron tomography reveals the endoplasmic reticulum as a membrane source for autophagosome formation. Autophagy *6*, 301-303.

Hayashi, S., and McMahon, A.P. (2002). Efficient recombination in diverse tissues by a tamoxifen-inducible form of Cre: a tool for temporally regulated gene activation/inactivation in the mouse. Developmental biology *244*, 305-318.

He, D., Wang, J., Lu, Y., Deng, Y., Zhao, C., Xu, L., Chen, Y., Hu, Y.C., Zhou, W., and Lu, Q.R. (2017a). lncRNA Functional Networks in Oligodendrocytes Reveal Stage-Specific Myelination Control by an lncOL1/Suz12 Complex in the CNS. Neuron *93*, 362-378.

He, Y., Dupree, J., Wang, J., Sandoval, J., Li, J., Liu, H., Shi, Y., Nave, K.A., and Casaccia-Bonnefil, P. (2007a). The transcription factor Yin Yang 1 is essential for oligodendrocyte progenitor differentiation. Neuron *55*, 217-230.

He, Y., Sandoval, J., and Casaccia-Bonnefil, P. (2007b). Events at the transition between cell cycle exit and oligodendrocyte progenitor differentiation: the role of HDAC and YY1. Neuron glia biology *3*, 221-231.

He, Y., She, H., Zhang, T., Xu, H., Cheng, L., Yepes, M., Zhao, Y., and Mao, Z. (2017b). p38 MAPK inhibits autophagy and promotes microglial inflammatory responses by phosphorylating ULK1. The Journal of cell biology.

Herve, D., and Chabriat, H. (2010). CADASIL. Journal of geriatric psychiatry and neurology *23*, 269-276.

Hines, J.H., Ravanelli, A.M., Schwindt, R., Scott, E.K., and Appel, B. (2015). Neuronal activity biases axon selection for myelination in vivo. Nature neuroscience *18*, 683-689.

Hoflich, K.M., Beyer, C., Clarner, T., Schmitz, C., Nyamoya, S., Kipp, M., and Hochstrasser, T. (2016). Acute axonal damage in three different murine models of multiple sclerosis: A comparative approach. Brain research *1650*, 125-133.

Hollenbeck, P.J. (1993). Products of endocytosis and autophagy are retrieved from axons by regulated retrograde organelle transport. The Journal of cell biology *121*, 305-315.

Howng, S.Y., Avila, R.L., Emery, B., Traka, M., Lin, W., Watkins, T., Cook, S., Bronson, R., Davisson, M., Barres, B.A., *et al.* (2010). ZFP191 is required by oligodendrocytes for CNS myelination. Genes & development *24*, 301-311.

Hu, Q.D., Ang, B.T., Karsak, M., Hu, W.P., Cui, X.Y., Duka, T., Takeda, Y., Chia, W., Sankar, N., Ng, Y.K., *et al.* (2003). F3/contactin acts as a functional ligand for Notch during oligodendrocyte maturation. Cell *115*, 163-175.

Hu, Y., and Wilson, G.S. (1997). A Temporary Local Energy Pool Coupled to Neuronal Activity: Fluctuations of Extracellular Lactate Levels in Rat Brain Monitored with Rapid-Response Enzyme-Based Sensor. Journal of neurochemistry *69*, 1484-1490.

Hursh, J.B. (1939). CONDUCTION VELOCITY AND DIAMETER OF NERVE FIBERS. American Journal of Physiology-Legacy Content *127*, 131-139.

Hussien, Y., Podojil, J.R., Robinson, A.P., Lee, A.S., Miller, S.D., and Popko, B. (2015). ER Chaperone BiP/GRP78 Is Required for Myelinating Cell Survival and Provides Protection during Experimental Autoimmune Encephalomyelitis. J Neurosci *35*, 15921-15933.

Jaffe, A.B., and Hall, A. (2005). Rho GTPases: biochemistry and biology. Annual review of cell and developmental biology *21*, 247-269.

Jahn, O., Tenzer, S., and Werner, H.B. (2009). Myelin Proteomics: Molecular Anatomy of an Insulating Sheath. Molecular Neurobiology *40*, 55-72.

Janen, S.B., Chaachouay, H., and Richter-Landsberg, C. (2010). Autophagy is activated by proteasomal inhibition and involved in aggresome clearance in cultured astrocytes. Glia *58*, 1766-1774.

Jang, S.Y., Shin, Y.K., Park, S.Y., Park, J.Y., Lee, H.J., Yoo, Y.H., Kim, J.K., and Park, H.T. (2016). Autophagic myelin destruction by Schwann cells during Wallerian degeneration and segmental demyelination. Glia *64*, 730-742.

Jang, S.Y., Shin, Y.K., Park, S.Y., Park, J.Y., Rha, S.H., Kim, J.K., Lee, H.J., and Park, H.T. (2015). Autophagy is involved in the reduction of myelinating Schwann cell cytoplasm during myelin maturation of the peripheral nerve. PLoS One *10*, e0116624.

Jeffries, M.A., Urbanek, K., Torres, L., Wendell, S.G., Rubio, M.E., and Fyffe-Maricich, S.L. (2016). ERK1/2 Activation in Preexisting Oligodendrocytes of Adult Mice Drives New Myelin Synthesis and Enhanced CNS Function. J Neurosci *36*, 9186-9200.

Jin, F., Dong, B., Georgiou, J., Jiang, Q., Zhang, J., Bharioke, A., Qiu, F., Lommel, S., Feltri, M.L., Wrabetz, L., *et al.* (2011). N-WASp is required for Schwann cell cytoskeletal dynamics, normal myelin gene expression and peripheral nerve myelination. Development (Cambridge, England) *138*, 1329-1337.

Johnson, C.W., Melia, T.J., and Yamamoto, A. (2012). Modulating macroautophagy: a neuronal perspective. Future Medicinal Chemistry *4*, 1715-1731.

Jovicic, A., Roshan, R., Moisoi, N., Pradervand, S., Moser, R., Pillai, B., and Luthi-Carter, R. (2013). Comprehensive expression analyses of neural cell-type-specific miRNAs identify new determinants of the specification and maintenance of neuronal phenotypes. J Neurosci *33*, 5127-5137.

Kang, S.H., Fukaya, M., Yang, J.K., Rothstein, J.D., and Bergles, D.E. (2010). NG2+ CNS glial progenitors remain committed to the oligodendrocyte lineage in postnatal life and following neurodegeneration. Neuron *68*, 668-681.

Keirstead, H.S., and Blakemore, W.F. (1997). Identification of post-mitotic oligodendrocytes incapable of remyelination within the demyelinated adult spinal cord. Journal of neuropathology and experimental neurology *56*, 1191-1201.

Kessaris, N., Fogarty, M., Iannarelli, P., Grist, M., Wegner, M., and Richardson, W.D. (2006). Competing waves of oligodendrocytes in the forebrain and postnatal elimination of an embryonic lineage. Nature neuroscience *9*, 173-179.

Kim, H., Shin, J., Kim, S., Poling, J., Park, H.C., and Appel, B. (2008). Notch-regulated oligodendrocyte specification from radial glia in the spinal cord of zebrafish embryos. Developmental dynamics : an official publication of the American Association of Anatomists *237*, 2081-2089.

Kim, H.J., Cho, M.H., Shim, W.H., Kim, J.K., Jeon, E.Y., Kim, D.H., and Yoon, S.Y. (2017). Deficient autophagy in microglia impairs synaptic pruning and causes social behavioral defects. Molecular psychiatry *22*, 1576-1584.

Kim, H.J., DiBernardo, A.B., Sloane, J.A., Rasband, M.N., Solomon, D., Kosaras, B., Kwak, S.P., and Vartanian, T.K. (2006). WAVE1 is required for oligodendrocyte morphogenesis and normal CNS myelination. J Neurosci *26*, 5849-5859.

Klionsky, D.J., Cuervo, A.M., and Seglen, P.O. (2007). Methods for Monitoring Autophagy from Yeast to Human. Autophagy *3*, 181-206.

Kochl, R., Hu, X.W., Chan, E.Y., and Tooze, S.A. (2006). Microtubules facilitate autophagosome formation and fusion of autophagosomes with endosomes. Traffic (Copenhagen, Denmark) *7*, 129-145.

Komatsu, M., Waguri, S., Chiba, T., Murata, S., Iwata, J.-i., Tanida, I., Ueno, T., Koike, M., Uchiyama, Y., and Kominami, E. (2006). Loss of autophagy in the central nervous system causes neurodegeneration in mice. Nature *441*, 880-884.

Komatsu, M., Waguri, S., Koike, M., Sou, Y.S., Ueno, T., Hara, T., Mizushima, N., Iwata, J., Ezaki, J., Murata, S., *et al.* (2007). Homeostatic levels of p62 control cytoplasmic inclusion body formation in autophagy-deficient mice. Cell *131*, 1149-1163.

Komatsu, M., Waguri, S., Ueno, T., Iwata, J., Murata, S., Tanida, I., Ezaki, J., Mizushima, N., Ohsumi, Y., Uchiyama, Y., *et al.* (2005). Impairment of starvation-induced and constitutive autophagy in Atg7-deficient mice. The Journal of cell biology *169*, 425-434.

Kondiles, B.R., and Horner, P.J. (2017). Myelin plasticity, neural activity, and traumatic neural injury. Developmental neurobiology.

Koudelka, S., Voas, M.G., Almeida, R.G., Baraban, M., Soetaert, J., Meyer, M.P., Talbot, W.S., and Lyons, D.A. (2016). Individual Neuronal Subtypes Exhibit Diversity in CNS Myelination Mediated by Synaptic Vesicle Release. Current biology : CB *26*, 1447-1455.

Krämer-Albers, E.-M., Bretz, N., Tenzer, S., Winterstein, C., Möbius, W., Berger, H., Nave, K.-A., Schild, H., and Trotter, J. (2007). Oligodendrocytes secrete exosomes containing major myelin and stress-protective proteins: Trophic support for axons? PROTEOMICS – Clinical Applications *1*, 1446-1461.

Kukley, M., Capetillo-Zarate, E., and Dietrich, D. (2007). Vesicular glutamate release from axons in white matter. Nature neuroscience *10*, 311-320.

Lafont, F., Verkade, P., Galli, T., Wimmer, C., Louvard, D., and Simons, K. (1999). Raft association of SNAP receptors acting in apical trafficking in Madin-Darby canine kidney cells. Proceedings of the National Academy of Sciences of the United States of America *96*, 3734-3738.

Lappe-Siefke, C., Goebbels, S., Gravel, M., Nicksch, E., Lee, J., Braun, P.E., Griffiths, I.R., and Nave, K.A. (2003). Disruption of Cnp1 uncouples oligodendroglial functions in axonal support and myelination. Nature genetics *33*, 366-374.

Lau, P., Verrier, J.D., Nielsen, J.A., Johnson, K.R., Notterpek, L., and Hudson, L.D. (2008). Identification of dynamically regulated microRNA and mRNA networks in developing oligodendrocytes. J Neurosci *28*, 11720-11730.

Laursen, L.S., Chan, C.W., and Ffrench-Constant, C. (2011). Translation of myelin basic protein mRNA in oligodendrocytes is regulated by integrin activation and hnRNP-K. The Journal of cell biology *192*, 797-811.

Lebrun-Julien, F., Bachmann, L., Norrmen, C., Trotzmuller, M., Kofeler, H., Ruegg, M.A., Hall, M.N., and Suter, U. (2014). Balanced mTORC1 activity in oligodendrocytes is required for accurate CNS myelination. J Neurosci *34*, 8432-8448.

Lee, Y., Morrison, B.M., Li, Y., Lengacher, S., Farah, M.H., Hoffman, P.N., Liu, Y., Tsingalia, A., Jin, L., Zhang, P.W., *et al.* (2012). Oligodendroglia metabolically support axons and contribute to neurodegeneration. Nature *487*, 443-448.

Leone, D.P., Genoud, S.t., Atanasoski, S., Grausenburger, R., Berger, P., Metzger, D., Macklin, W.B., Chambon, P., and Suter, U. (2003). Tamoxifen-inducible glia-specific Cre mice for somatic mutagenesis in oligodendrocytes and Schwann cells. Molecular and Cellular Neuroscience *22*, 430-440.

Li, H., Lu, Y., Smith, H.K., and Richardson, W.D. (2007). Olig1 and Sox10 interact synergistically to drive myelin basic protein transcription in oligodendrocytes. J Neurosci *27*, 14375-14382.

Liang, C.-C., Wang, C., Peng, X., Gan, B., and Guan, J.-L. (2010). Neural-specific Deletion of FIP200 Leads to Cerebellar Degeneration Caused by Increased Neuronal Death and Axon Degeneration. Journal of Biological Chemistry *285*, 3499-3509.

Ligon, K.L., Kesari, S., Kitada, M., Sun, T., Arnett, H.A., Alberta, J.A., Anderson, D.J., Stiles, C.D., and Rowitch, D.H. (2006). Development of NG2 neural progenitor cells requires Olig gene function. Proceedings of the National Academy of Sciences of the United States of America *103*, 7853-7858.

Lin, S.T., Huang, Y., Zhang, L., Heng, M.Y., Ptacek, L.J., and Fu, Y.H. (2013). MicroRNA-23a promotes myelination in the central nervous system. Proceedings of the National Academy of Sciences of the United States of America *110*, 17468-17473.

Liu, A., Li, J., Marin-Husstege, M., Kageyama, R., Fan, Y., Gelinas, C., and Casaccia-Bonnefil, P. (2006). A molecular insight of Hes5-dependent inhibition of myelin gene expression: old partners and new players. The EMBO journal *25*, 4833-4842.

Liu, J., Dietz, K., DeLoyht, J.M., Pedre, X., Kelkar, D., Kaur, J., Vialou, V., Lobo, M.K., Dietz, D.M., Nestler, E.J., *et al.* (2012). Impaired adult myelination in the prefrontal cortex of socially isolated mice. Nature neuroscience *15*, 1621-1623.

Logan, A.M., Mammel, A.E., Robinson, D.C., Chin, A.L., Condon, A.F., and Robinson, F.L. (2017). Schwann cell-specific deletion of the endosomal PI 3-kinase Vps34 leads to delayed radial sorting of axons, arrested myelination, and abnormal ErbB2-ErbB3 tyrosine kinase signaling. Glia *65*, 1452-1470.

Lu, Q.R., Sun, T., Zhu, Z., Ma, N., Garcia, M., Stiles, C.D., and Rowitch, D.H. (2002). Common developmental requirement for Olig function indicates a motor neuron/oligodendrocyte connection. Cell *109*, 75-86.

Lu, Q.R., Yuk, D., Alberta, J.A., Zhu, Z., Pawlitzky, I., Chan, J., McMahon, A.P., Stiles, C.D., and Rowitch, D.H. (2000). Sonic hedgehog--regulated oligodendrocyte lineage genes encoding bHLH proteins in the mammalian central nervous system. Neuron *25*, 317-329.

Luan, H., Peabody, N.C., Vinson, C.R., and White, B.H. (2006). Refined spatial manipulation of neuronal function by combinatorial restriction of transgene expression. Neuron *52*, 425-436.

Lucin, K.M., O'Brien, C.E., Bieri, G., Czirr, E., Mosher, K.I., Abbey, R.J., Mastroeni, D.F., Rogers, J., Spencer, B., Masliah, E., *et al.* (2013). Microglial beclin 1 regulates retromer trafficking and phagocytosis and is impaired in Alzheimer's disease. Neuron *79*, 873-886.

Lyons, D.A., Naylor, S.G., Scholze, A., and Talbot, W.S. (2009). Kif1b is essential for mRNA localization in oligodendrocytes and development of myelinated axons. Nature genetics *41*, 854-858.

Madisen, L., Zwingman, T.A., Sunkin, S.M., Oh, S.W., Zariwala, H.A., Gu, H., Ng, L.L., Palmiter, R.D., Hawrylycz, M.J., Jones, A.R., *et al.* (2010). A robust and high-throughput Cre reporting and characterization system for the whole mouse brain. Nature neuroscience *13*, 133-140.

Madison, D.L., Krueger, W.H., Cheng, D., Trapp, B.D., and Pfeiffer, S.E. (1999). SNARE Complex Proteins, Including the Cognate Pair VAMP-2and Syntaxin-4, Are Expressed in Cultured Oligodendrocytes. Journal of neurochemistry *72*, 988-998.

Madorsky, I., Opalach, K., Waber, A., Verrier, J.D., Solmo, C., Foster, T., Dunn, W.A., Jr., and Notterpek, L. (2009). Intermittent fasting alleviates the neuropathic phenotype in a mouse model of Charcot-Marie-Tooth disease. Neurobiology of disease *34*, 146-154.

Maire, C.L., Wegener, A., Kerninon, C., and Nait Oumesmar, B. (2010). Gain-of-function of Olig transcription factors enhances oligodendrogenesis and myelination. Stem cells (Dayton, Ohio) *28*, 1611-1622.

Makinodan, M., Okuda-Yamamoto, A., Ikawa, D., Toritsuka, M., Takeda, T., Kimoto, S., Tatsumi, K., Okuda, H., Nakamura, Y., Wanaka, A., *et al.* (2013). Oligodendrocyte Plasticity with an Intact Cell Body In Vitro. PLOS ONE *8*, e66124.

Mangin, J.M., Li, P., Scafidi, J., and Gallo, V. (2012). Experience-dependent regulation of NG2 progenitors in the developing barrel cortex. Nature neuroscience *15*, 1192-1194.

Marques, S., Zeisel, A., Codeluppi, S., van Bruggen, D., Mendanha Falcao, A., Xiao, L., Li, H., Haring, M., Hochgerner, H., Romanov, R.A., *et al.* (2016). Oligodendrocyte heterogeneity in the mouse juvenile and adult central nervous system. Science (New York, NY) *352*, 1326-1329.

Martinez, J., Almendinger, J., Oberst, A., Ness, R., Dillon, C.P., Fitzgerald, P., Hengartner, M.O., and Green, D.R. (2011). Microtubule-associated protein 1 light chain 3 alpha (LC3)-associated phagocytosis is required for the efficient clearance of dead cells. Proceedings of the National Academy of Sciences of the United States of America *108*, 17396-17401.

Martinez, J., Cunha, L.D., Park, S., Yang, M., Lu, Q., Orchard, R., Li, Q.Z., Yan, M., Janke, L., Guy, C., *et al.* (2016). Noncanonical autophagy inhibits the autoinflammatory, lupus-like response to dying cells. Nature *533*, 115-119.

Martinez, J., Malireddi, R.K., Lu, Q., Cunha, L.D., Pelletier, S., Gingras, S., Orchard, R., Guan, J.L., Tan, H., Peng, J., *et al.* (2015). Molecular characterization of LC3-associated phagocytosis reveals distinct roles for Rubicon, NOX2 and autophagy proteins. Nature cell biology *17*, 893-906.

McEwan, D.G., Popovic, D., Gubas, A., Terawaki, S., Suzuki, H., Stadel, D., Coxon, F.P., Miranda de Stegmann, D., Bhogaraju, S., Maddi, K., *et al.* (2015). PLEKHM1 regulates autophagosome-lysosome fusion through HOPS complex and LC3/GABARAP proteins. Molecular cell *57*, 39-54.

McKenzie, I.A., Ohayon, D., Li, H., de Faria, J.P., Emery, B., Tohyama, K., and Richardson, W.D. (2014). Motor skill learning requires active central myelination. Science (New York, NY) *346*, 318-322.

Medina D , L., Fraldi, A., Bouche, V., Annunziata, F., Mansueto, G., Spampanato, C., Puri, C., Pignata, A., Martina J , A., Sardiello, M., *et al.* (2011). Transcriptional Activation of Lysosomal Exocytosis Promotes Cellular Clearance. Developmental cell *21*, 421-430.

Mensch, S., Baraban, M., Almeida, R., Czopka, T., Ausborn, J., El Manira, A., and Lyons, D.A. (2015). Synaptic vesicle release regulates myelin sheath number of individual oligodendrocytes in vivo. Nature neuroscience *18*, 628-630.

Mironova, Y.A., Lenk, G.M., Lin, J.P., Lee, S.J., Twiss, J.L., Vaccari, I., Bolino, A., Havton, L.A., Min, S.H., Abrams, C.S., *et al.* (2016). PI(3,5)P2 biosynthesis regulates oligodendrocyte differentiation by intrinsic and extrinsic mechanisms. eLife *5*.

Mizushima, N., Yamamoto, A., Matsui, M., Yoshimori, T., and Ohsumi, Y. (2004). In vivo analysis of autophagy in response to nutrient starvation using transgenic mice expressing a fluorescent autophagosome marker. Molecular biology of the cell *15*, 1101-1111.

Mohseni, S. (2011). Autophagy in insulin-induced hypoglycaemic neuropathy. Pathology *43*, 254-260.

Morell, P., and Quarles, R. (1999). The Myelin Sheath. In Basic Neurochemistry: Molecular, Cellular and Medical Aspects, A.B. Siegel GJ, Albers RW, et al., ed. (Philadelphia: Lippincott-Raven).

Muller, S., Dennemarker, J., and Reinheckel, T. (2012). Specific functions of lysosomal proteases in endocytic and autophagic pathways. Biochimica et biophysica acta *1824*, 34-43.

Najm, F.J., Lager, A.M., Zaremba, A., Wyatt, K., Caprariello, A.V., Factor, D.C., Karl, R.T., Maeda, T., Miller, R.H., and Tesar, P.J. (2013). Transcription factor-mediated reprogramming of fibroblasts to expandable, myelinogenic oligodendrocyte progenitor cells. Nature biotechnology *31*, 426-433.

Nakatani, H., Martin, E., Hassani, H., Clavairoly, A., Maire, C.L., Viadieu, A., Kerninon, C., Delmasure, A., Frah, M., Weber, M., *et al.* (2013). Ascl1/Mash1 promotes brain oligodendrogenesis during myelination and remyelination. J Neurosci *33*, 9752-9768.

Narayanan, S.P., Flores, A.I., Wang, F., and Macklin, W.B. (2009). Akt signals through the mammalian target of rapamycin pathway to regulate CNS myelination. J Neurosci *29*, 6860-6870.

Nawaz, S., Sanchez, P., Schmitt, S., Snaidero, N., Mitkovski, M., Velte, C., Bruckner, B.R., Alexopoulos, I., Czopka, T., Jung, S.Y., *et al.* (2015). Actin filament turnover drives leading edge growth during myelin sheath formation in the central nervous system. Developmental cell *34*, 139-151.

Nery, S., Wichterle, H., and Fishell, G. (2001). Sonic hedgehog contributes to oligodendrocyte specification in the mammalian forebrain. Development (Cambridge, England) *128*, 527-540.

Nguyen, T.N., Padman, B.S., Usher, J., Oorschot, V., Ramm, G., and Lazarou, M. (2016). Atg8 family LC3/GABARAP proteins are crucial for autophagosome-lysosome fusion but not autophagosome formation during PINK1/Parkin mitophagy and starvation. The Journal of cell biology *215*, 857-874.

Nicholson, G., Lenk, G.M., Reddel, S.W., Grant, A.E., Towne, C.F., Ferguson, C.J., Simpson, E., Scheuerle, A., Yasick, M., Hoffman, S., *et al.* (2011). Distinctive genetic and clinical features of CMT4J: a severe neuropathy caused by mutations in the PI(3,5)P(2) phosphatase FIG4. Brain : a journal of neurology *134*, 1959-1971.

Nicks, J., Lee, S., Harris, A., Falk, D.J., Todd, A.G., Arredondo, K., Dunn, W.A., Jr., and Notterpek, L. (2014). Rapamycin improves peripheral nerve myelination while it fails to benefit neuromuscular performance in neuropathic mice. Neurobiology of disease *70c*, 224-236.

Noble, M., Murray, K., Stroobant, P., Waterfield, M.D., and Riddle, P. (1988). Platelet-derived growth factor promotes division and motility and inhibits premature differentiation of the oligodendrocyte/type-2 astrocyte progenitor cell. Nature *333*, 560-562.

Notterpek, L., Shooter, E.M., and Snipes, G.J. (1997). Upregulation of the endosomal-lysosomal pathway in the trembler-J neuropathy. J Neurosci *17*, 4190-4200.

Novak, N., Bar, V., Sabanay, H., Frechter, S., Jaegle, M., Snapper, S.B., Meijer, D., and Peles, E. (2011). N-WASP is required for membrane wrapping and myelination by Schwann cells. The Journal of cell biology *192*, 243-250.

Odagiri, S., Tanji, K., Mori, F., Kakita, A., Takahashi, H., and Wakabayashi, K. (2012). Autophagic adapter protein NBR1 is localized in Lewy bodies and glial cytoplasmic inclusions and is involved in aggregate formation in alpha-synucleinopathy. Acta neuropathologica *124*, 173-186.

Ortega, F., Gascon, S., Masserdotti, G., Deshpande, A., Simon, C., Fischer, J., Dimou, L., Chichung Lie, D., Schroeder, T., and Berninger, B. (2013). Oligodendrogliogenic and neurogenic adult subependymal zone neural stem cells constitute distinct lineages and exhibit differential responsiveness to Wnt signalling. Nature cell biology *15*, 602-613.

Paes de Faria, J., Kessaris, N., Andrew, P., Richardson, W.D., and Li, H. (2014). New Olig1 null mice confirm a non-essential role for Olig1 in oligodendrocyte development. BMC neuroscience *15*, 12.

Pajevic, S., Basser, P.J., and Fields, R.D. (2014). Role of myelin plasticity in oscillations and synchrony of neuronal activity. Neuroscience *276*, 135-147.

Park, H.C., and Appel, B. (2003). Delta-Notch signaling regulates oligodendrocyte specification. Development (Cambridge, England) *130*, 3747-3755.

Parras, C.M., Hunt, C., Sugimori, M., Nakafuku, M., Rowitch, D., and Guillemot, F. (2007). The proneural gene Mash1 specifies an early population of telencephalic oligodendrocytes. J Neurosci *27*, 4233-4242.

Patzig, J., Erwig, M.S., Tenzer, S., Kusch, K., Dibaj, P., Mobius, W., Goebbels, S., Schaeren-Wiemers, N., Nave, K.A., and Werner, H.B. (2016). Septin/anillin filaments scaffold central nervous system myelin to accelerate nerve conduction. eLife *5*.

Pedraza, L., Huang, J.K., and Colman, D. (2009). Disposition of axonal caspr with respect to glial cell membranes: Implications for the process of myelination. Journal of neuroscience research *87*, 3480-3491.

Pellegrino, R.G., and Spencer, P.S. (1985). Schwann cell mitosis in response to regenerating peripheral axons in vivo. Brain research *341*, 16-25.

Pellerin, L., and Magistretti, P.J. (1994). Glutamate uptake into astrocytes stimulates aerobic glycolysis: a mechanism coupling neuronal activity to glucose utilization. Proceedings of the National Academy of Sciences *91*, 10625-10629.

Pfeffer, S.R. (1994). Rab GTPases: master regulators of membrane trafficking. Current Opinion in Cell Biology *6*, 522-526.

Pfeiffer, S.E., Warrington, A.E., and Bansal, R. (1993). The oligodendrocyte and its many cellular processes. Trends in cell biology *3*, 191-197.

Piaton, G., Aigrot, M.S., Williams, A., Moyon, S., Tepavcevic, V., Moutkine, I., Gras, J., Matho, K.S., Schmitt, A., Soellner, H., *et al.* (2011). Class 3 semaphorins influence oligodendrocyte precursor recruitment and remyelination in adult central nervous system. Brain : a journal of neurology *134*, 1156-1167.

Plane, J.M., Andjelkovic, A.V., Keep, R.F., and Parent, J.M. (2010). Intact and injured endothelial cells differentially modulate postnatal murine forebrain neural stem cells. Neurobiology of disease *37*, 218-227.

Pringle, N.P., Mudhar, H.S., Collarini, E.J., and Richardson, W.D. (1992). PDGF receptors in the rat CNS: during late neurogenesis, PDGF alpha-receptor expression appears to be restricted to glial cells of the oligodendrocyte lineage. Development (Cambridge, England) *115*, 535-551.

Pringle, N.P., and Richardson, W.D. (1993). A singularity of PDGF alpha-receptor expression in the dorsoventral axis of the neural tube may define the origin of the oligodendrocyte lineage. Development (Cambridge, England) *117*, 525-533.

Psachoulia, K., Jamen, F., Young, K.M., and Richardson, W.D. (2009). Cell cycle dynamics of NG2 cells in the postnatal and ageing brain. Neuron glia biology *5*, 57-67.

Pukaβ, K., Goldbaum, O., and Richter-Landsberg, C. (2015). Mitochondrial impairment and oxidative stress compromise autophagosomal degradation of alpha-synuclein in oligodendroglial cells. Journal of neurochemistry *135*, 194-205.

Rabadan, M.A., Cayuso, J., Le Dreau, G., Cruz, C., Barzi, M., Pons, S., Briscoe, J., and Marti, E. (2012). Jagged2 controls the generation of motor neuron and oligodendrocyte progenitors in the ventral spinal cord. Cell death and differentiation *19*, 209-219.

Raff, M.C., Lillien, L.E., Richardson, W.D., Burne, J.F., and Noble, M.D. (1988). Platelet-derived growth factor from astrocytes drives the clock that times oligodendrocyte development in culture. Nature *333*, 562-565.

Rangaraju, S., Verrier, J.D., Madorsky, I., Nicks, J., Dunn, W.A., Jr., and Notterpek, L. (2010). Rapamycin activates autophagy and improves myelination in explant cultures from neuropathic mice. J Neurosci *30*, 11388-11397.

Rasband, M.N., Tayler, J., Kaga, Y., Yang, Y., Lappe-Siefke, C., Nave, K.A., and Bansal, R. (2005). CNP is required for maintenance of axon-glia interactions at nodes of Ranvier in the CNS. Glia *50*, 86-90.

Ravikumar, B., Moreau, K., Jahreiss, L., Puri, C., and Rubinsztein, D.C. (2010). Plasma membrane contributes to the formation of pre-autophagosomal structures. Nature cell biology *12*, 747.

Razi, M., Chan, E.Y., and Tooze, S.A. (2009). Early endosomes and endosomal coatomer are required for autophagy. The Journal of cell biology *185*, 305-321.

Readhead, C., Popko, B., Takahashi, N., Shine, H.D., Saavedra, R.A., Sidman, R.L., and Hood, L. (1987). Expression of a myelin basic protein gene in transgenic shiverer mice: correction of the dysmyelinating phenotype. Cell *48*, 703-712.

Redmond, S.A., Mei, F., Eshed-Eisenbach, Y., Osso, L.A., Leshkowitz, D., Shen, Y.A., Kay, J.N., Aurrand-Lions, M., Lyons, D.A., Peles, E., *et al.* (2016). Somatodendritic Expression of JAM2 Inhibits Oligodendrocyte Myelination. Neuron *91*, 824-836.

Relucio, J., Menezes, M.J., Miyagoe-Suzuki, Y., Takeda, S., and Colognato, H. (2012). Laminin regulates postnatal oligodendrocyte production by promoting oligodendrocyte progenitor survival in the subventricular zone. Glia *60*, 1451-1467.

Revelo, N.H., Kamin, D., Truckenbrodt, S., Wong, A.B., Reuter-Jessen, K., Reisinger, E., Moser, T., and Rizzoli, S.O. (2014). A new probe for super-resolution imaging of membranes elucidates trafficking pathways. The Journal of cell biology *205*, 591-606.

Richardson, W.D., Pringle, N., Mosley, M.J., Westermark, B., and Dubois-Dalcq, M. (1988). A role for platelet-derived growth factor in normal gliogenesis in the central nervous system. Cell *53*, 309-319.

Rivers, L.E., Young, K.M., Rizzi, M., Jamen, F., Psachoulia, K., Wade, A., Kessaris, N., and Richardson, W.D. (2008). PDGFRA/NG2 glia generate myelinating oligodendrocytes and piriform projection neurons in adult mice. Nature neuroscience *11*, 1392-1401.

Roth, B.L. (2016). DREADDs for Neuroscientists. Neuron *89*, 683-694.

Rothman, J.E. (1994). Intracellular membrane fusion. Advances in second messenger and phosphoprotein research *29*, 81-96.

Rouach, N., Koulakoff, A., Abudara, V., Willecke, K., and Giaume, C. (2008). Astroglial Metabolic Networks Sustain Hippocampal Synaptic Transmission. Science (New York, NY) *322*, 1551-1555.

Safaiyan, S., Kannaiyan, N., Snaidero, N., Brioschi, S., Biber, K., Yona, S., Edinger, A.L., Jung, S., Rossner, M.J., and Simons, M. (2016). Age-related myelin degradation burdens the clearance function of microglia during aging. Nature neuroscience *19*, 995-998.

Samanta, J., and Kessler, J.A. (2004). Interactions between ID and OLIG proteins mediate the inhibitory effects of BMP4 on oligodendroglial differentiation. Development (Cambridge, England) *131*, 4131-4142.

Savas, J.N., Toyama, B.H., Xu, T., Yates, J.R., and Hetzer, M.W. (2012). Extremely Long-Lived Nuclear Pore Proteins in the Rat Brain. Science (New York, NY) *335*, 942.

Schain, A.J., Hill, R.A., and Grutzendler, J. (2014). Label-free in vivo imaging of myelinated axons in health and disease with spectral confocal reflectance microscopy. Nature medicine *20*, 443-449.

Schardt, A., Brinkmann, B.G., Mitkovski, M., Sereda, M.W., Werner, H.B., and Nave, K.A. (2009). The SNARE protein SNAP-29 interacts with the GTPase Rab3A: Implications for membrane trafficking in myelinating glia. Journal of neuroscience research *87*, 3465-3479.

Schlake, T., and Bode, J. (1994). Use of mutated FLP recognition target (FRT) sites for the exchange of expression cassettes at defined chromosomal loci. Biochemistry *33*, 12746-12751.

Schlegel, A.A., Rudelson, J.J., and Tse, P.U. (2012). White matter structure changes as adults learn a second language. Journal of cognitive neuroscience *24*, 1664-1670.

Schneider, C.A., Rasband, W.S., and Eliceiri, K.W. (2012). NIH Image to ImageJ: 25 years of image analysis. Nature methods *9*, 671-675.

Schneider, S., Gruart, A., Grade, S., Zhang, Y., Kroger, S., Kirchhoff, F., Eichele, G., Delgado Garcia, J.M., and Dimou, L. (2016). Decrease in newly generated oligodendrocytes leads to motor dysfunctions and changed myelin structures that can be rescued by transplanted cells. Glia *64*, 2201-2218.

Scholz, J., Klein, M.C., Behrens, T.E., and Johansen-Berg, H. (2009). Training induces changes in white-matter architecture. Nature neuroscience *12*, 1370-1371.

Schwarz, L., Goldbaum, O., Bergmann, M., Probst-Cousin, S., and Richter-Landsberg, C. (2012). Involvement of macroautophagy in multiple system atrophy and protein aggregate formation in oligodendrocytes. J Mol Neurosci *47*, 256-266.

See, J.M., and Grinspan, J.B. (2009). Sending mixed signals: bone morphogenetic protein in myelination and demyelination. Journal of neuropathology and experimental neurology *68*, 595-604.

Seidl, A.H. (2014). Regulation of conduction time along axons. Neuroscience *276*, 126-134.

Seidl, A.H., Rubel, E.W., and Barria, A. (2014). Differential conduction velocity regulation in ipsilateral and contralateral collaterals innervating brainstem coincidence detector neurons. J Neurosci *34*, 4914-4919.

Settembre, C., Fraldi, A., Medina, D.L., and Ballabio, A. (2013). Signals for the lysosome: a control center for cellular clearance and energy metabolism. Nature reviews Molecular cell biology *14*, 283-296.

Sharma, K., Schmitt, S., Bergner, C.G., Tyanova, S., Kannaiyan, N., Manrique-Hoyos, N., Kongi, K., Cantuti, L., Hanisch, U.K., Philips, M.A., *et al.* (2015). Cell type- and brain region-resolved mouse brain proteome. Nature neuroscience *18*, 1819-1831.

Sher, F., Rossler, R., Brouwer, N., Balasubramaniyan, V., Boddeke, E., and Copray, S. (2008). Differentiation of neural stem cells into oligodendrocytes: involvement of the polycomb group protein Ezh2. Stem cells (Dayton, Ohio) *26*, 2875-2883.

Shibuya, Y., Chang, C.C., Huang, L.H., Bryleva, E.Y., and Chang, T.Y. (2014). Inhibiting ACAT1/SOAT1 in microglia stimulates autophagy-mediated lysosomal proteolysis and increases Abeta1-42 clearance. J Neurosci *34*, 14484-14501.

Siebzehnrubl, F.A., Buslei, R., Eyupoglu, I.Y., Seufert, S., Hahnen, E., and Blumcke, I. (2007). Histone deacetylase inhibitors increase neuronal differentiation in adult forebrain precursor cells. Experimental brain research *176*, 672-678.

Simon, C., Gotz, M., and Dimou, L. (2011). Progenitors in the adult cerebral cortex: cell cycle properties and regulation by physiological stimuli and injury. Glia *59*, 869-881.

Simons, M., Kramer, E.M., Thiele, C., Stoffel, W., and Trotter, J. (2000). Assembly of myelin by association of proteolipid protein with cholesterol- and galactosylceramide-rich membrane domains. The Journal of cell biology *151*, 143-154.

Simpson, P.B., Mehotra, S., Lange, G.D., and Russell, J.T. (1997). High density distribution of endoplasmic reticulum proteins and mitochondria at specialized Ca2+ release sites in oligodendrocyte processes. J Biol Chem *272*, 22654-22661.

Sinclair, J.L., Fischl, M.J., Alexandrova, O., Hebeta, M., Grothe, B., Leibold, C., and Kopp-Scheinpflug, C. (2017). Sound-Evoked Activity Influences Myelination of Brainstem Axons in the Trapezoid Body. J Neurosci *37*, 8239-8255.

Smith, C.M., Mayer, J.A., and Duncan, I.D. (2013). Autophagy promotes oligodendrocyte survival and function following dysmyelination in a long-lived myelin mutant. J Neurosci *33*, 8088-8100.

Smith, M.E. (1968). The turnover of myelin in the adult rat. Biochimica et Biophysica Acta (BBA) - Lipids and Lipid Metabolism *164*, 285-293.

Smith, R.S., and Koles, Z.J. (1970). Myelinated nerve fibers: computed effect of myelin thickness on conduction velocity. The American journal of physiology *219*, 1256-1258.

Snaidero, N., Mobius, W., Czopka, T., Hekking, L.H., Mathisen, C., Verkleij, D., Goebbels, S., Edgar, J., Merkler, D., Lyons, D.A., *et al.* (2014). Myelin membrane wrapping of CNS axons by PI(3,4,5)P3-dependent polarized growth at the inner tongue. Cell *156*, 277-290.

Snaidero, N., and Simons, M. (2014). Myelination at a glance. Journal of cell science *127*, 2999-3004.

Snaidero, N., Velte, C., Myllykoski, M., Raasakka, A., Ignatev, A., Werner, H.B., Erwig, M.S., Mobius, W., Kursula, P., Nave, K.A., *et al.* (2017). Antagonistic Functions of MBP and CNP Establish Cytosolic Channels in CNS Myelin. Cell reports *18*, 314-323.

Song, J.W., Misgeld, T., Kang, H., Knecht, S., Lu, J., Cao, Y., Cotman, S.L., Bishop, D.L., and Lichtman, J.W. (2008). Lysosomal activity associated with developmental axon pruning. J Neurosci *28*, 8993-9001.

Stange-Marten, A., Nabel, A.L., Sinclair, J.L., Fischl, M., Alexandrova, O., Wohlfrom, H., Kopp-Scheinpflug, C., Pecka, M., and Grothe, B. (2017). Input timing for spatial processing is precisely tuned via constant synaptic delays and myelination patterns in the auditory brainstem. Proceedings of the National Academy of Sciences of the United States of America *114*, E4851-e4858.

Steshenko, O., Andrade, D.M., Honigmann, A., Mueller, V., Schneider, F., Sezgin, E., Hell, S.W., Simons, M., and Eggeling, C. (2016). Reorganization of Lipid Diffusion by Myelin Basic Protein as Revealed by STED Nanoscopy. Biophysical journal *110*, 2441-2450.

Stolt, C.C., Lommes, P., Friedrich, R.P., and Wegner, M. (2004). Transcription factors Sox8 and Sox10 perform non-equivalent roles during oligodendrocyte development despite functional redundancy. Development (Cambridge, England) *131*, 2349-2358.

Stolt, C.C., Lommes, P., Sock, E., Chaboissier, M.C., Schedl, A., and Wegner, M. (2003). The Sox9 transcription factor determines glial fate choice in the developing spinal cord. Genes & development *17*, 1677-1689.

Stolt, C.C., Schlierf, A., Lommes, P., Hillgartner, S., Werner, T., Kosian, T., Sock, E., Kessaris, N., Richardson, W.D., Lefebvre, V., *et al.* (2006). SoxD proteins influence multiple stages of oligodendrocyte development and modulate SoxE protein function. Developmental cell *11*, 697-709.

Stolt, C.C., Schmitt, S., Lommes, P., Sock, E., and Wegner, M. (2005). Impact of transcription factor Sox8 on oligodendrocyte specification in the mouse embryonic spinal cord. Developmental biology *281*, 309-317.

Stromhaug, P.E., BERG, T.O., FENGSRUD, M., and SEGLEN, P.O. (1998). Purification and characterization of autophagosomes from rat hepatocytes. Biochemical Journal *335*, 217-224.

Stromhaug, P.E., and Seglen, P.O. (1993). Evidence for acidity of prelysosomal autophagic/endocytic vacuoles (amphisomes). Biochemical Journal *291 (Pt 1)*, 115-121.

Su, P., Zhang, J., Wang, D., Zhao, F., Cao, Z., Aschner, M., and Luo, W. (2016). The role of autophagy in modulation of neuroinflammation in microglia. Neuroscience *319*, 155-167.

Sugimori, M., Nagao, M., Parras, C.M., Nakatani, H., Lebel, M., Guillemot, F., and Nakafuku, M. (2008). Ascl1 is required for oligodendrocyte development in the spinal cord. Development (Cambridge, England) *135*, 1271-1281.

Suster, M.L., Seugnet, L., Bate, M., and Sokolowski, M.B. (2004). Refining GAL4-driven transgene expression in Drosophila with a GAL80 enhancer-trap. Genesis (New York, NY : 2000) *39*, 240-245.

Syed, Y.A., Hand, E., Mobius, W., Zhao, C., Hofer, M., Nave, K.A., and Kotter, M.R. (2011). Inhibition of CNS remyelination by the presence of semaphorin 3A. J Neurosci *31*, 3719-3728.

Takebayashi, H., Yoshida, S., Sugimori, M., Kosako, H., Kominami, R., Nakafuku, M., and Nabeshima, Y. (2000). Dynamic expression of basic helix-loop-helix Olig family members: implication of Olig2 in neuron and oligodendrocyte differentiation and identification of a new member, Olig3. Mechanisms of development *99*, 143-148.

Tang, G., Yue, Z., Talloczy, Z., Hagemann, T., Cho, W., Messing, A., Sulzer, D.L., and Goldman, J.E. (2008). Autophagy induced by Alexander disease-mutant GFAP accumulation is regulated by p38/MAPK and mTOR signaling pathways. Human molecular genetics *17*, 1540-1555.

Tanji, K., Odagiri, S., Maruyama, A., Mori, F., Kakita, A., Takahashi, H., and Wakabayashi, K. (2013). Alteration of autophagosomal proteins in the brain of multiple system atrophy. Neurobiology of disease *49*, 190-198.

Tekki-Kessaris, N., Woodruff, R., Hall, A.C., Gaffield, W., Kimura, S., Stiles, C.D., Rowitch, D.H., and Richardson, W.D. (2001). Hedgehog-dependent oligodendrocyte lineage specification in the telencephalon. Development (Cambridge, England) *128*, 2545-2554.

Thurnherr, T., Benninger, Y., Wu, X., Chrostek, A., Krause, S.M., Nave, K.A., Franklin, R.J., Brakebusch, C., Suter, U., and Relvas, J.B. (2006). Cdc42 and Rac1 signaling are both required

for and act synergistically in the correct formation of myelin sheaths in the CNS. J Neurosci *26*, 10110-10119.

Tognatta, R., Sun, W., Goebbels, S., Nave, K.A., Nishiyama, A., Schoch, S., Dimou, L., and Dietrich, D. (2017). Transient Cnp expression by early progenitors causes Cre-Lox-based reporter lines to map profoundly different fates. Glia *65*, 342-359.

Tomassy, G.S., Berger, D.R., Chen, H.H., Kasthuri, N., Hayworth, K.J., Vercelli, A., Seung, H.S., Lichtman, J.W., and Arlotta, P. (2014). Distinct profiles of myelin distribution along single axons of pyramidal neurons in the neocortex. Science (New York, NY) *344*, 319-324.

Torvund-Jensen, J., Steengaard, J., Reimer, L., Fihl, L.B., and Laursen, L.S. (2014). Transport and translation of MBP mRNA is regulated differently by distinct hnRNP proteins. Journal of cell science *127*, 1550-1564.

Touahri, Y., Escalas, N., Benazeraf, B., Cochard, P., Danesin, C., and Soula, C. (2012). Sulfatase 1 Promotes the Motor Neuron-to-Oligodendrocyte Fate Switch by Activating Shh Signaling in Olig2 Progenitors of the Embryonic Ventral Spinal Cord. The Journal of Neuroscience *32*, 18018.

Toyama, B.H., Savas, J.N., Park, S.K., Harris, M.S., Ingolia, N.T., Yates, J.R., and Hetzer, M.W. (2013). Identification of long-lived proteins reveals exceptional stability of essential cellular structures. Cell *154*, 971-982.

Trapp, B.D., Nishiyama, A., Cheng, D., and Macklin, W. (1997). Differentiation and death of premyelinating oligodendrocytes in developing rodent brain. The Journal of cell biology *137*, 459-468.

Tripathi, R.B., Clarke, L.E., Burzomato, V., Kessaris, N., Anderson, P.N., Attwell, D., and Richardson, W.D. (2011). Dorsally and ventrally derived oligodendrocytes have similar electrical properties but myelinate preferred tracts. J Neurosci *31*, 6809-6819.

Tsai, H.H., Niu, J., Munji, R., Davalos, D., Chang, J., Zhang, H., Tien, A.C., Kuo, C.J., Chan, J.R., Daneman, R., *et al.* (2016). Oligodendrocyte precursors migrate along vasculature in the developing nervous system. Science (New York, NY) *351*, 379-384.

Tyler, W.A., Gangoli, N., Gokina, P., Kim, H.A., Covey, M., Levison, S.W., and Wood, T.L. (2009). Activation of the mammalian target of rapamycin (mTOR) is essential for oligodendrocyte differentiation. J Neurosci *29*, 6367-6378.

Uemura, T., Yamamoto, M., Kametaka, A., Sou, Y.-s., Yabashi, A., Yamada, A., Annoh, H., Kametaka, S., Komatsu, M., and Waguri, S. (2014). A Cluster of Thin Tubular Structures Mediates Transformation of the Endoplasmic Reticulum to Autophagic Isolation Membrane. Molecular and cellular biology *34*, 1695-1706.

Vallstedt, A., Klos, J.M., and Ericson, J. (2005). Multiple dorsoventral origins of oligodendrocyte generation in the spinal cord and hindbrain. Neuron *45*, 55-67.

Vassall, K.A., Bamm, V.V., and Harauz, G. (2015). MyelStones: the executive roles of myelin basic protein in myelin assembly and destabilization in multiple sclerosis. Biochemical Journal *472*, 17-32.

Waelsch, H., Sperry, W.M., and Stoyanoff, V.A. (1940a). LIPID METABOLISM IN BRAIN DURING MYELINATION. Journal of Biological Chemistry *135*, 297-302.

Waelsch, H., Sperry, W.M., and Stoyanoff, V.A. (1940b). A study of the synthesis and deposition of lipids in brain and other tissues with deuterium as an indicator. Journal of Biological Chemistry *135*, 291-296.

Waelsch, H., Sperry, W.M., and Stoyanoff, V.A. (1941). The influence of growth and myelination on the deposition and metabolism of lipids in the brain. The Journal of biological chemistry *140*, 885.

Wahl, S.E., McLane, L.E., Bercury, K.K., Macklin, W.B., and Wood, T.L. (2014). Mammalian target of rapamycin promotes oligodendrocyte differentiation, initiation and extent of CNS myelination. J Neurosci *34*, 4453-4465.

Wake, H., Lee, P.R., and Fields, R.D. (2011). Control of local protein synthesis and initial events in myelination by action potentials. Science (New York, NY) *333*, 1647-1651.

Wang, H., Sun, H.Q., Zhu, X., Zhang, L., Albanesi, J., Levine, B., and Yin, H. (2015). GABARAPs regulate PI4P-dependent autophagosome:lysosome fusion. Proceedings of the National Academy of Sciences of the United States of America *112*, 7015-7020.

Wang, S., Li, B., Qiao, H., Lv, X., Liang, Q., Shi, Z., Xia, W., Ji, F., and Jiao, J. (2014). Autophagy-related gene Atg5 is essential for astrocyte differentiation in the developing mouse cortex. EMBO reports *15*, 1053-1061.

Wang, S., Sdrulla, A.D., diSibio, G., Bush, G., Nofziger, D., Hicks, C., Weinmaster, G., and Barres, B.A. (1998). Notch receptor activation inhibits oligodendrocyte differentiation. Neuron *21*, 63-75.

Warf, B.C., Fok-Seang, J., and Miller, R.H. (1991). Evidence for the ventral origin of oligodendrocyte precursors in the rat spinal cord. J Neurosci *11*, 2477-2488.

Watkins, T.A., Emery, B., Mulinyawe, S., and Barres, B.A. (2008). Distinct Stages of Myelination Regulated by γ-Secretase and Astrocytes in a Rapidly Myelinating CNS Coculture System. Neuron *60*, 555-569.

Waxman, S.G. (1980). Determinants of conduction velocity in myelinated nerve fibers. Muscle & nerve *3*, 141-150.

Weissman, A.M., Shabek, N., and Ciechanover, A. (2011). The predator becomes the prey: regulating the ubiquitin system by ubiquitylation and degradation. Nature reviews Molecular cell biology *12*, 605-620.

White, R., Gonsior, C., Kramer-Albers, E.M., Stohr, N., Huttelmaier, S., and Trotter, J. (2008). Activation of oligodendroglial Fyn kinase enhances translation of mRNAs transported in hnRNP A2-dependent RNA granules. The Journal of cell biology *181*, 579-586.

Wilkins, A., Majed, H., Layfield, R., Compston, A., and Chandran, S. (2003). Oligodendrocytes promote neuronal survival and axonal length by distinct intracellular mechanisms: a novel role for oligodendrocyte-derived glial cell line-derived neurotrophic factor. J Neurosci *23*, 4967-4974.

Wilson, H.C., Scolding, N.J., and Raine, C.S. (2006). Co-expression of PDGF alpha receptor and NG2 by oligodendrocyte precursors in human CNS and multiple sclerosis lesions. Journal of neuroimmunology *176*, 162-173.

Winters, J.J., Ferguson, C.J., Lenk, G.M., Giger-Mateeva, V.I., Shrager, P., Meisler, M.H., and Giger, R.J. (2011). Congenital CNS hypomyelination in the Fig4 null mouse is rescued by neuronal expression of the PI(3,5)P(2) phosphatase Fig4. J Neurosci *31*, 17736-17751.

Winterstein, C., Trotter, J., and Kramer-Albers, E.M. (2008). Distinct endocytic recycling of myelin proteins promotes oligodendroglial membrane remodeling. Journal of cell science *121*, 834-842.

Xiao, L., Ohayon, D., McKenzie, I.A., Sinclair-Wilson, A., Wright, J.L., Fudge, A.D., Emery, B., Li, H., and Richardson, W.D. (2016). Rapid production of new oligodendrocytes is required in the earliest stages of motor-skill learning. Nature neuroscience *19*, 1210-1217.

Yamamoto, A., and Yue, Z. (2014). Autophagy and Its Normal and Pathogenic States in the Brain. Annu Rev Neurosci.

Yang, N., Zuchero, J.B., Ahlenius, H., Marro, S., Ng, Y.H., Vierbuchen, T., Hawkins, J.S., Geissler, R., Barres, B.A., and Wernig, M. (2013). Generation of oligodendroglial cells by direct lineage conversion. Nature biotechnology *31*, 434-439.

Yang, Z., Zhao, T.Z., Zou, Y.J., Zhang, J.H., and Feng, H. (2014). Hypoxia Induces autophagic cell death through hypoxia-inducible factor 1alpha in microglia. PLoS One *9*, e96509.

Ye, F., Chen, Y., Hoang, T., Montgomery, R.L., Zhao, X.H., Bu, H., Hu, T., Taketo, M.M., van Es, J.H., Clevers, H., *et al.* (2009). HDAC1 and HDAC2 regulate oligodendrocyte differentiation by disrupting the beta-catenin-TCF interaction. Nature neuroscience *12*, 829-838.

Yeung, M.S., Zdunek, S., Bergmann, O., Bernard, S., Salehpour, M., Alkass, K., Perl, S., Tisdale, J., Possnert, G., Brundin, L., *et al.* (2014). Dynamics of oligodendrocyte generation and myelination in the human brain. Cell *159*, 766-774.

Young, K.M., Psachoulia, K., Tripathi, R.B., Dunn, S.J., Cossell, L., Attwell, D., Tohyama, K., and Richardson, W.D. (2013). Oligodendrocyte dynamics in the healthy adult CNS: evidence for myelin remodeling. Neuron *77*, 873-885.

Yurlova, L., Kahya, N., Aggarwal, S., Kaiser, H.J., Chiantia, S., Bakhti, M., Pewzner-Jung, Y., Ben-David, O., Futerman, A.H., Brugger, B., *et al.* (2011). Self-segregation of myelin membrane lipids in model membranes. Biophysical journal *101*, 2713-2720.

Zatorre, R.J., Fields, R.D., and Johansen-Berg, H. (2012). Plasticity in gray and white: neuroimaging changes in brain structure during learning. Nature neuroscience *15*, 528-536.

Zaucker, A., Mercurio, S., Sternheim, N., Talbot, W.S., and Marlow, F.L. (2013). notch3 is essential for oligodendrocyte development and vascular integrity in zebrafish. Disease models & mechanisms *6*, 1246-1259.

Zhang, F., Wang, L.P., Brauner, M., Liewald, J.F., Kay, K., Watzke, N., Wood, P.G., Bamberg, E., Nagel, G., Gottschalk, A., *et al.* (2007). Multimodal fast optical interrogation of neural circuitry. Nature *446*, 633-639.

Zhang, J., Lachance, V., Schaffner, A., Li, X., Fedick, A., Kaye, L.E., Liao, J., Rosenfeld, J., Yachelevich, N., Chu, M.L., *et al.* (2016). A Founder Mutation in VPS11 Causes an Autosomal Recessive Leukoencephalopathy Linked to Autophagic Defects. PLoS genetics *12*, e1005848.

Zhang, Y., Chen, K., Sloan, S.A., Bennett, M.L., Scholze, A.R., O'Keeffe, S., Phatnani, H.P., Guarnieri, P., Caneda, C., Ruderisch, N., *et al.* (2014). An RNA-sequencing transcriptome and splicing database of glia, neurons, and vascular cells of the cerebral cortex. J Neurosci *34*, 11929-11947.

Zhao, C., Deng, Y., Liu, L., Yu, K., Zhang, L., Wang, H., He, X., Wang, J., Lu, C., Wu, L.N., *et al.* (2016). Dual regulatory switch through interactions of Tcf7l2/Tcf4 with stage-specific partners propels oligodendroglial maturation. Nature communications *7*, 10883.

Zhao, X., He, X., Han, X., Yu, Y., Ye, F., Chen, Y., Hoang, T., Xu, X., Mi, Q.S., Xin, M., *et al.* (2010). MicroRNA-mediated control of oligodendrocyte differentiation. Neuron *65*, 612-626.

Zhao, X., Wu, J., Zheng, M., Gao, F., and Ju, G. (2012). Specification and maintenance of oligodendrocyte precursor cells from neural progenitor cells: involvement of microRNA-7a. Molecular biology of the cell *23*, 2867-2878.

Zhou, Q., and Anderson, D.J. (2002). The bHLH transcription factors OLIG2 and OLIG1 couple neuronal and glial subtype specification. Cell *109*, 61-73.

Zhou, Q., Wang, S., and Anderson, D.J. (2000). Identification of a novel family of oligodendrocyte lineage-specific basic helix-loop-helix transcription factors. Neuron *25*, 331-343.

Zhu, X., Hill, R.A., Dietrich, D., Komitova, M., Suzuki, R., and Nishiyama, A. (2011). Age-dependent fate and lineage restriction of single NG2 cells. Development (Cambridge, England) *138*, 745-753.

Ziskin, J.L., Nishiyama, A., Rubio, M., Fukaya, M., and Bergles, D.E. (2007). Vesicular release of glutamate from unmyelinated axons in white matter. Nature neuroscience *10*, 321-330.

Zonta, B., Tait, S., Melrose, S., Anderson, H., Harroch, S., Higginson, J., Sherman, D.L., and Brophy, P.J. (2008). Glial and neuronal isoforms of Neurofascin have distinct roles in the assembly of nodes of Ranvier in the central nervous system. The Journal of cell biology *181*, 1169-1177.

Zschocke, J., Zimmermann, N., Berning, B., Ganal, V., Holsboer, F., and Rein, T. (2011). Antidepressant drugs diversely affect autophagy pathways in astrocytes and neurons--dissociation from cholesterol homeostasis. Neuropsychopharmacology *36*, 1754-1768.

Zuchero, J.B., and Barres, B.A. (2015). Glia in mammalian development and disease. Development (Cambridge, England) *142*, 3805-3809.

Zuchero, J.B., Fu, M.M., Sloan, S.A., Ibrahim, A., Olson, A., Zaremba, A., Dugas, J.C., Wienbar, S., Caprariello, A.V., Kantor, C., *et al.* (2015). CNS myelin wrapping is driven by actin disassembly. Developmental cell *34*, 152-167.

APPENDIX I.

Atg7(CNP) cKO mice as a possible model for Multiple Systems Atrophy

I.1 Introduction

Multiple systems atrophy (MSA) is a rare, rapidly progressive neurodegenerative disease that presents clinically with either parkinsonism or cerebellar ataxia, autonomic features, weight loss, neuronal loss and demyelination. The pathological hallmark of this disorder is the appearance of α-synuclein (α-syn)-positive glial cytoplasmic inclusions (GCIs) in oligodendrocytes (OLs) along with astrogliosis (Papapetropoulos et al., 2007; Ubhi et al., 2011). Transgenic models of MSA have been created by heterologously overexpressing α-syn, but the levels of overexpression supersede endogenous levels, namely because it is unclear if α-syn is endogenously expressed in mature OLs. The etiology of this disease remains uncertain (Shults et al., 2005; Stefanova and Wenning, 2015).

Intriguingly, many of the key features of this disease are recapitulated upon the conditional loss of macroautophagy (MA) in the central nervous system (CNS), which causes a rapidly progressing and debilitating phenotype characterized by cerebellar ataxia, astrogliosis, runting, axonal degeneration, and early death (Hara et al., 2006; Komatsu et al., 2006). However, the overt loss of MA gene function in humans, such as that of *ATG5*, leads to a neurodevelopmental disorder that does not resemble MSA (Kim et al., 2016). Nonetheless, considering that the pathological hallmark of MSA is synuclein aggregation in OLs, one cannot help but wonder whether

dysfunction of MA in OLs may contribute to the pathogenesis of the disease. This hypothesis is consistent with data from post-mortem samples suggesting that MA may be dysfunctional in the OLs of MSA patients (Odagiri et al., 2012; Schwarz et al., 2012; Tanji et al., 2013). Moreover, since α-syn has been proposed to impair MA by affecting AP formation and turnover (Tanik et al., 2013; Winslow et al., 2010), these data support a model in which high levels of α-syn in OLs impair MA, which in turn drives the disease.

But what causes the abnormally high levels of α-syn in OLs of MSA patients? Three possible causes have been proposed: abnormally high expression of α-syn, decreased degradation of endogenous α-syn within OLs, or cell-to-cell transmission of α-syn from neurons into OLs (Asi et al., 2014; Miller et al., 2005; Reyes et al., 2014; Ubhi et al., 2011). On the one hand, it is still a matter of debate if mature OLs express α-syn and how much α-syn is expressed in the OLs of MSA patients (Asi et al., 2014; Djelloul et al., 2015; Miller et al., 2005). It has also been shown that OLs are able to take up α-syn from the extracellular milieu (Reyes et al., 2014). On the other hand, studies suggest that α-syn is a substrate of MA (Friedman et al., 2012; Spencer et al., 2009; Webb et al., 2003; Yu et al., 2009), and that MA is impaired in MSA (Odagiri et al., 2012; Schwarz et al., 2012; Tanji et al., 2013). The appearance of GCIs may therefore be indicative of a disruption in protein homeostasis in these highly specialized cells, rather than be the causative element of the disease. Although OL toxicity is observed in mice overexpressing α-syn in an OL-specific manner (Kahle et al., 2002; Shults et al., 2005; Yazawa et al., 2005), given the levels of α-syn overexpression achieved, whether these models reflect what is occurring in disease is in question (Shults et al., 2005; Stefanova and Wenning, 2015). To gain a better understanding of the contribution of MA dysfunction in MSA pathogenesis, we therefore disrupted MA specifically in OLs to determine if this is sufficient to replicate the cardinal symptoms of the disease.

I.2. The Atg7(CNP) cKO mice demonstrate a progressive motor decline

To create our model, we conditionally deleted Atg7, an E1-like ligase essential for LC3 lipidation to the growing autophagosome (AP) membrane, an essential step to initiate MA (Geng and Klionsky, 2008; Komatsu et al., 2005). Cre-mediated deletion in OLs was achieved using a mouse strain in which Cre recombinase is knocked-into the 2',3'-cyclic-nucleotide 3'-phosphodiesterase (*CNP1*) locus (CNP^{Cre}) (Lappe-Siefke et al., 2003). *CNP1* expression begins early in the OL lineage, and thus the resulting Atg7(CNP) cKO mice is predicted to demonstrate a conditional loss of MA at this time. Given the design of the model, the expression of CNP^{Cre} leads to a heterozygous loss of *CNP1* expression. This has been suggested to lead to mild neuroinflammation beginning at 19 months of age, and possible depressive-like symptoms at 24 months age, but no perturbations in motor function (Hagemeyer et al., 2012). To control for these effects, we compared Atg7(CNP) cKO mice with littermates conditionally heterozygous for Atg7 (Atg7(CNP) cHet) in all experiments.

The loss of MA in OLs did not demonstrate a developmental phenotype in OL maturation and overt mouse behavior, as described in detail in Chapter 3 (Figures 3.7-9). Nonetheless, as shown in Chapter 3 Figure 3.10A, we found that Atg7(CNP) cKO mice demonstrate an adult onset premature lethality that begins at 6 months of age. Monitoring of home cage behavior of these mice revealed a dramatic, age-dependent decline in motor function along with the presence of a notable tremor. To quantify this behavior, we performed gait analysis, which revealed an abnormal gait in Atg7(CNP) cKO mice that appeared to worsen with age in female mice (Figure AI.1). In addition to a shorter stride length, stride overlap was diminished, and forepaw and hindpaw base

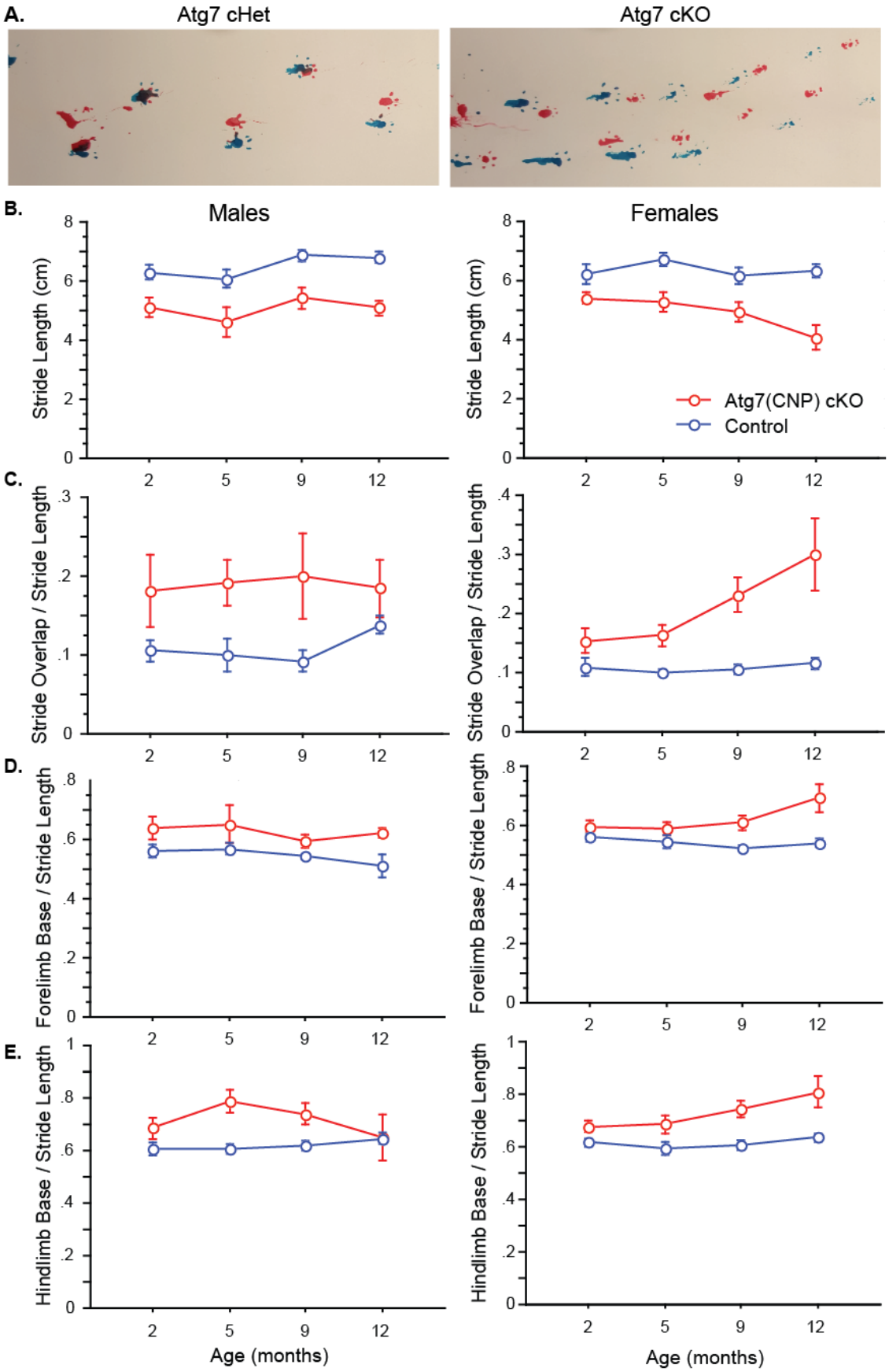
A.
Atg7 cHet
Atg7 cKO
B.
Males
Females
Stride Length (cm)
C.
Stride Overlap / Stride Length
D.
Forelimb Base / Stride Length
E.
Hindlimb Base / Stride Length
Atg7(CNP) cKO
Control
Age (months)

Figure I-1. Gait is altered in Atg7(CNP) cKO mice.
A. Representative tracks from 9-month-old Atg7 cHet and cKO mice. Forelimbs are in red, and hindlimbs are in blue.
B. Stride length, or distance between consecutive steps with the same foot, was measured at 2, 5, 9, and 12 months of age (mo). Repeated Measures-ANOVA (RM-ANOVA) reveals a significant difference for 'genotype,' but not 'age' or an interaction between 'age' and 'genotype' in both male and female mice. Male mice: 'genotype': $F(1,44) = 40.587$, $p < 0.0001$; 'age': $F(3, 44) = 2.1744$, $p = 0.1046$; 'interaction': $F(3,44) = 0.218$, $p = 0.8836$. Female mice: 'genotype': $F(1,67) = 46.607$, $p < 0.0001$; 'age': $F(3, 67) = 2.700$, $p = 0.0526$; 'interaction': $F(3,67) = 1.977$, $p = 0.1257$.
C. Stride overlap, or distance between the fore and hindpaw's pawprint at the same location, was measured at 2, 5, 9, and 12 mo and normalized to stride length to account for the difference reported above. In male mice, RM-ANOVA revealed a significant difference in 'genotype' ($F(1,44) = 11.203$, $p = 0.0017$), but not 'age' ($F(3,44) = 0.111$, $p = 0.9532$) or interaction between 'genotype' and 'age' ($F(3,44) = 0.268$, $p = 0.8483$). In female mice, RM-ANOVA revealed a significant difference in 'genotype' ($F(1,67) = 31.845$, $p < 0.0001$), 'age' ($F(3,67) = 3.781$, $p = 0.0144$), and interaction between 'genotype' and 'age' ($F(3,67) = 2.870$, $p = 0.0428$).
D. Forepaw Base, or distance between each of the forepaws at a given stride, was measured at 2, 5, 9, and 12 mo and normalized to stride length to account for the difference reported above. In male mice, RM-ANOVA revealed a significant difference in 'genotype' ($F(1,44) = 12.289$, $p = 0.0011$), but not 'age' ($F(3,44) = 0.926$, $p = 0.4363$) or interaction between 'genotype' and 'age' ($F(3,44) = 0.253$, $p = 0.8588$). In female mice, RM-ANOVA revealed a significant difference in 'genotype' ($F(1,67) = 22.617$, $p < 0.0001$), but not 'age' ($F(3,67) = 2.045$, $p = 0.1159$), and interaction between 'genotype' and 'age' ($F(3,67) = 2.405$, $p = 0.0750$).
E. Hindpaw Base, or distance between each of the hindpaws at a given stride, was measured at 2, 5, 9, and 12 mo and normalized to stride length to account for the difference reported above. In male mice, RM-ANOVA revealed a significant difference in 'genotype' ($F(1,44) = 8.830$, $p = 0.0048$), but not 'age' ($F(3,44) = 0.635$, $p = 0.5966$) or interaction between 'genotype' and 'age' ($F(3,44) = 1.181$, $p = 0.3278$). In female mice, RM-ANOVA revealed a significant difference in 'genotype' ($F(1,67) = 27.284$, $p < 0.0001$) and 'age' ($F(3,67) = 2.857$, $p = 0.0435$), but not interaction between 'genotype' and 'age' ($F(3,67) = 1.259$, $p = 0.2957$).

were increased in Atg7(CNP) cKO mice. Together, these indicate that Atg7(CNP) cKO mice may have an ataxic gait. Motor dysfunction in Atg7(CNP) cKO mice was further confirmed using the balance beam test, which probes the time required for the mice to cross a narrow beam. We used a 12 mm wide beam for this task. In both male and female Atg7(CNP) cKO mice, there was an age-dependent decline in ability to cross the balance beam not observed in Atg7(CNP) cHet mice (Figure AI.2A). In addition, Atg7(CNP) cKO mice exhibited limb clasping during the tail suspension test, a phenotype suggestive of neurological impairment and perhaps neurodegeneration (DiFiglia et al., 2007; Lalonde and Strazielle, 2011) (Figure AI.2B). Despite the obvious deficits in motor function in these mice, there was no difference in exploratory behavior in the open field test between Atg7(CNP) cHet and cKO littermates (Figure AI.2C), indicating that locomotor behavior was largely normal. Rearing behaviors, however, were impacted, first in female Atg7(CNP) cKOs, then seemingly in both sexes by 16 mo (Figure AI.2D).

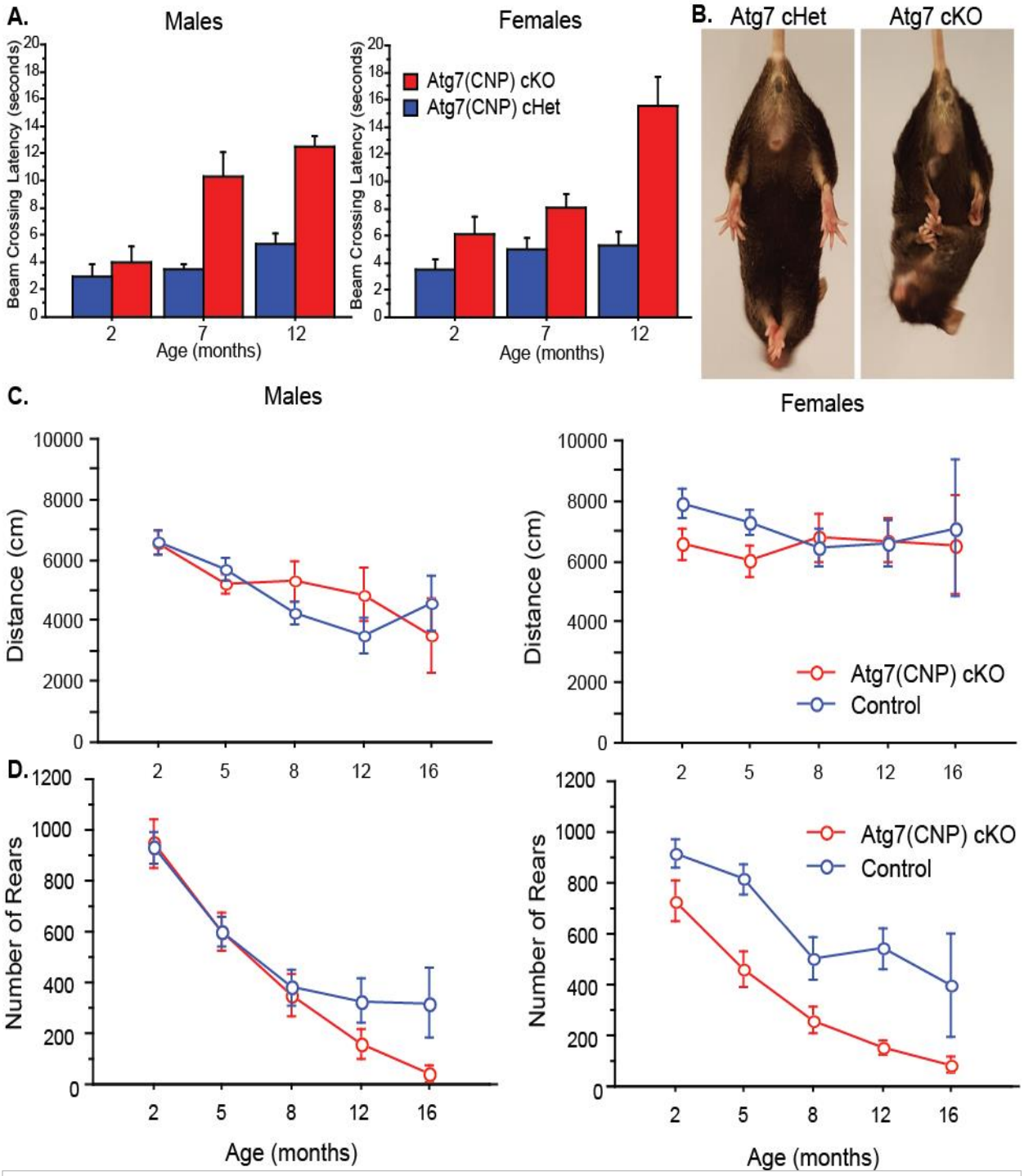

Figure I-2. Motor deficits in Atg7(CNP) cKO mice.
A. Time to cross a narrow balance beam was measured at 2, 7, and 12 months of age (mo). Falling off the beam or crossing the beam in greater than 20 seconds was measured as 20 seconds. In male mice, RM-ANOVA revealed a significant difference in 'genotype' ($F(1,32) = 46.784$, $p < 0.0001$), 'age' ($F(2, 32) = 19.685$, $p < 0.0001$), and interaction between 'genotype' and 'age' ($F(2,32) = 5.255$, $p = 0.0106$). In female mice, RM-ANOVA revealed a significant difference in 'genotype' ($F(1,38) = 29.067$, $p < 0.0001$), 'age' ($F(2,38) = 8.375$, $p = 0.0010$), and interaction between 'genotype' and 'age' ($F(2,38) = 3.971$, $p = 0.0271$).
Continued on next page.

Figure I-2. Continued from previous page
B. At 16 months of age, Atg7(CNP) cKO mice consistently demonstrated limb clasping during the tail suspension test.
C. Open Field analyses of habituated mice indicate that spontaneous locomotor behavior is normal in Atg7(CNP) cKO mice at all ages, as measured by total distance traveled over one hour. In male mice, RM-ANOVA revealed a significant difference by 'age' ($F(4,83) = 7.661$, $p < 0.0001$), but not 'genotype' ($F(1, 83) = 0.201$, $p = 0.6549$) and interaction between 'genotype' and 'age' ($F(4,83) = 1.244$, $p = 0.2988$). In female mice, RM-ANOVA revealed no significant difference in 'genotype' ($F(1,83) = 1.300$, $p = 0.2569$), 'age' ($F(4,83) = 0.385$, $p = 0.8189$), and interaction between 'genotype' and 'age' ($F(4,83) = 0.699$, $p = 0.5943$).
D. Number of rears during one hour of open field analysis. In male mice, RM-ANOVA revealed a significant difference by 'age' ($F(4,83) = 32.275$, $p < 0.0001$), but not 'genotype' ($F(1, 83) = 2.711$, $p = 0.1034$) and interaction between 'genotype' and 'age' ($F(4,83) = 0.989$, $p = 0.4180$). In female mice, RM-ANOVA revealed a significant difference in 'genotype' ($F(1,83) = 29.369$, $p < 0.001$) and 'age' ($F(4,83) = 18.837$, $p < 0.001$), but not interaction between 'genotype' and 'age' ($F(4,83) = 0.697$, $p = 0.5955$).

In summary, in addition to an early loss of life, the loss of MA in OLs leads to an age-dependent motor decline, causing tremors and ataxia. These deficits are reminiscent of the motor dysfunction observed in MSA patients, who can suffer from parkinsonism (MSA-P) or cerebellar ataxia (MSA-C).

I.2. The Atg7(CNP) cKO mice demonstrate autonomic dysfunction

In addition to motor dysfunction, patients with MSA frequently suffer from weight loss and autonomic dysfunction (Papapetropoulos et al., 2007; Ubhi et al., 2011). Weighing mice beginning at 3 weeks of age revealed that both male and female Atg7(CNP) cKO mice weighed significantly less than Atg7(CNP) cHet mice at all ages, but particularly in adulthood (Figure AI.3A). Atg7(CNP) cKO mice also showed signs of autonomic dysfunction: Atg7(CNP) cKO mice struggled to breed and, on the rare occasions that they did, produced significantly smaller litters (Figure AI.3B). As another test of autonomic function, we measured the defecation rate of Atg7(CNP) cKO mice. Interestingly, the mice produced more droppings per hour than their littermate controls, suggesting the presence of gastrointestinal dysfunction (Figure AI.3C). Anecdotally, Atg7(CNP) cKO mice at end stage were frequently found to suffer from

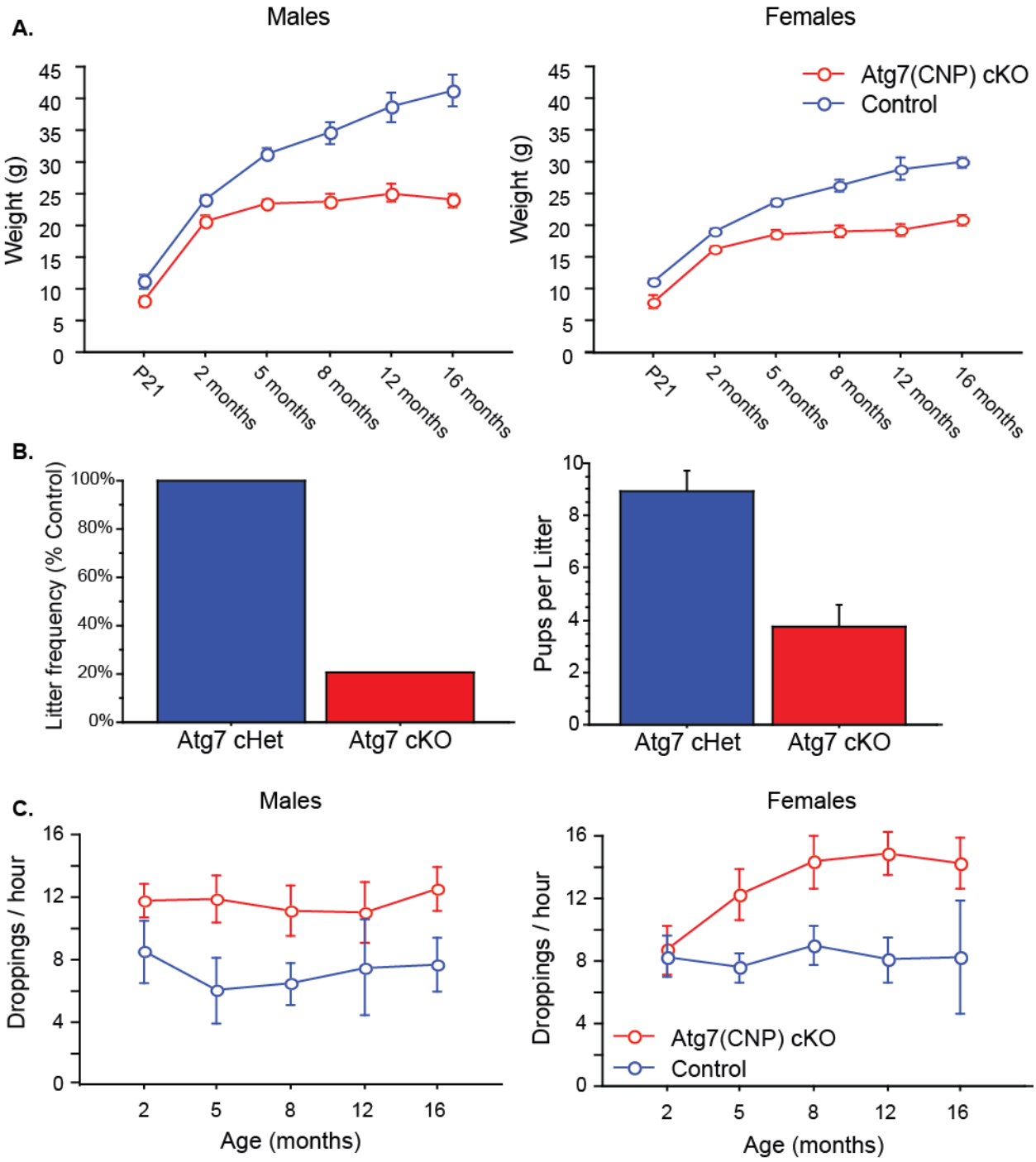

Figure I-3. Atg7(CNP) cKO mice demonstrate autonomic deficits.
A. Body weight was measured at weaning and at 2, 5, 8, 12, and 16 months of age (mo). In male mice, RM-ANOVA revealed a significant difference in 'genotype' ($F(1,103) = 164.357$, $p < 0.0001$), 'age' ($F(5, 103) = 80.979$, $p < 0.0001$), and interaction between 'genotype' and 'age' ($F(5,103) = 10.664$, $p < 0.0001$). In female mice, RM-ANOVA revealed a significant difference in 'genotype' ($F(1,110) = 115.15$, $p < 0.0001$), 'age' ($F(5,110) = 51.678$, $p < 0.0001$), and interaction between 'genotype' and 'age' ($F(5,110) = 5.059$, $p = 0.0003$). B. Droppings produced during one hour in the open field chamber was measured at 2, 5, 8, 12, and 16 mo. In
Continued on next page

Figure I-3. Continued from next page
male mice, RM-ANOVA revealed a significant difference in 'genotype' 'age' ($F(1,60) = 14.795$, $p = 0.0003$), but not 'age' ($F(4, 60) = 0.262$, $p = 0.9011$) and interaction between 'genotype' and 'age' ($F(4,60) = 0.167$, $p = 0.9541$). In female mice, RM-ANOVA revealed a significant difference in 'genotype' ($F(1,83) = 19.174$, $p < 0.0001$), but not 'age' ($F(4,83) = 1.595$, $p = 0..1834$) and interaction between 'genotype' and 'age' ($F(4,83) = 1.315$, $p = 0.2711$).
C. Breeding capacity of Atg7(CNP) cKO mice was evaluated by frequency with which litters were born and the number of pups born per litter. Pups were born from Atg7(CNP) cKO matings at approximately $1/5^{th}$ the frequency as that from Atg7(CNP) cHet matings (both were paired with $Atg7^{flox/flox}$ mice). Litter size from Atg7(CNP) cKO matings was significantly different from that of Atg7(CNP) cHet matings (two tailed unpaired t-test yielded $p = 0.0021$). n = 7 cHet mice, 9 cKO mice

priapism/penile prolapse and were often found to have urinary retention after being sacrificed. Taken together, we can conclude that the loss of MA in OLs causes deficits in weight and autonomic function.

I.3. Atg7(CNP) cKO mice demonstrate the neuropathological indicators of MSA.

We also examined the neuropathology of Atg7(CNP) cKO brains to determine whether the loss of MA in OLs replicates the neuropathological findings in post-mortem brains from MSA patients. We first asked whether Atg7(CNP) cKO brains demonstrate the neuropathological hallmark of MSA: α-syn positive glial cytoplasmic inclusions (GCIs) in OLs. Immunohistochemistry against α-syn in 5-month-old brains revealed punctate structures peppering the white matter tracts of Atg7(CNP) cKO brains, that were confirmed to be perinuclear (Figures AI.4A and AI.4B). Given that there are no neuronal nuclei in white matter, these structures likely signify GCIs, but going forward, we would like to confirm that α-syn is accumulating in OLs by triple-labeling tissue with α-syn, Olig2, and CC1, as OLs are $Olig2^{+}$ $CC1^{+}$ cells. We would also like to confirm the presence of GCI's in OLs by electron microscopy (EM). Immunohistochemistry against protein 62/sequestesome 1 (p62/SQSTM1) revealed not only that p62 accumulated in an age-dependent manner in a variety of white matter tracts in Atg7(CNP) cKO mice, consistent with its role as an

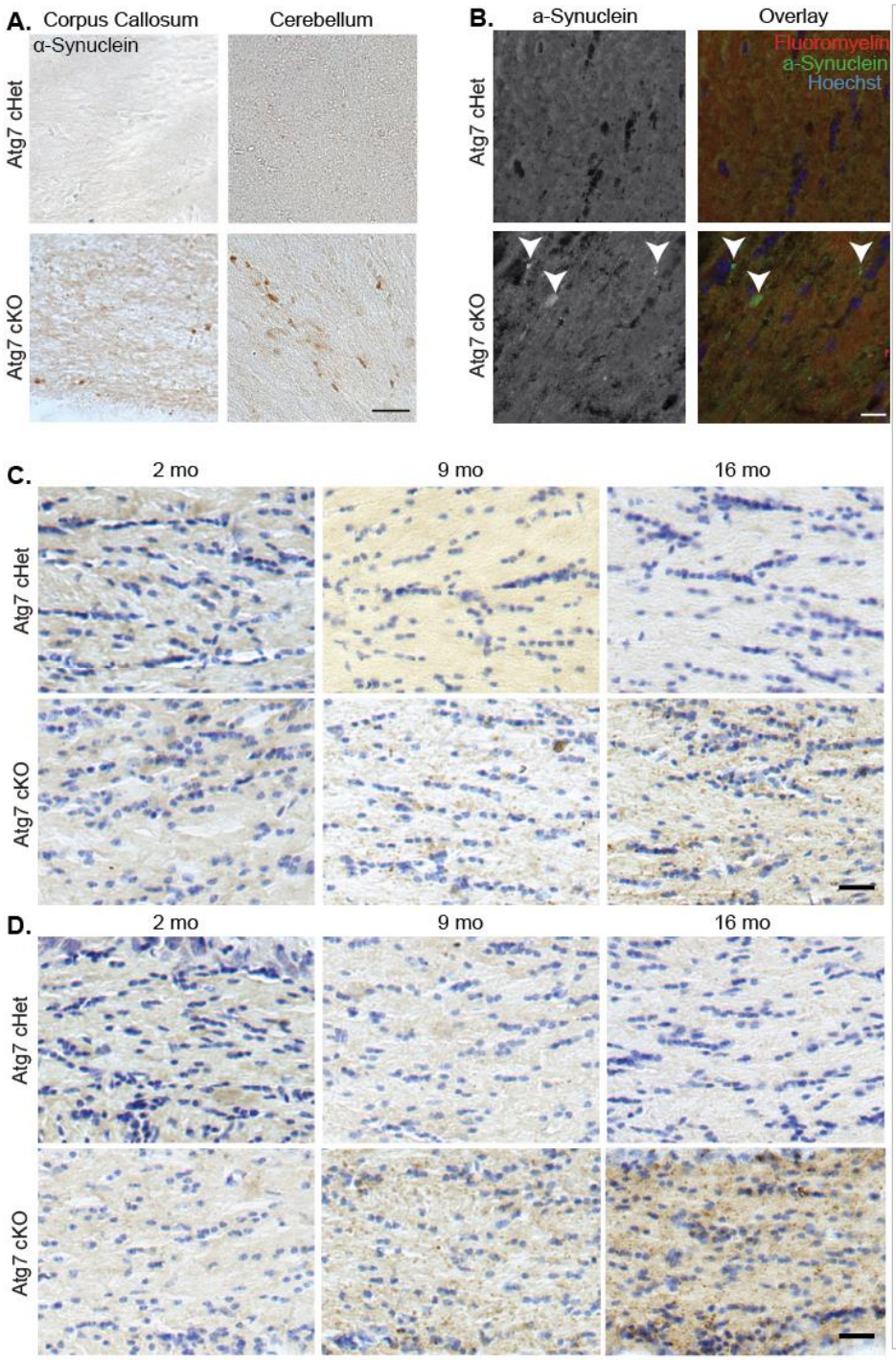

Figure I-4. Accumulation of α-synuclein and p62 in white matter of Atg7(CNP) cKO mice. A. Accumulation of α-synuclein in the corpus callosum and cerebellar white matter of 5-months-old Atg7(CNP) cKO mice. n = 2 / genotype. Scale = 25 μm. B. Perinuclear accumulation of α-synuclein in the corpus callosum 5-months-old Atg7(CNP) cKO mice. Fluoromyelin identifies myelin, and Hoechst identifies nuclei. n = 2 / genotype. Scale = 25 μm. C. and D. Immunostaining for p62 (brown) in (C) anterior commissure and (D) corpus callosum of 2, 9, and 16 mo Atg7(CNP) cHet and cKO mice. There appears to be a time-dependent accumulation of p62 in these white matter tracts. Nissl (blue) identifies nuclei. n = 1 / genotype.

adaptor protein for selective MA (Figures AI.4C and AI.4D), but the accumulation coincided with regions that often have many glial cytoplasmic inclusions in MSA, such as the pons (Figure AI.5A) (Spillantini et al., 1998).

As in many neurodegenerative diseases, signs of neuroinflammation are common in brains of MSA patients. Reactive astrocytosis in the dorsal striatum is a hallmark of MSA, although its etiology is uncertain. Notably, immunohistochemistry against glial fibrillary acid protein (GFAP) in Atg7(CNP) cKO in 5-month-old brain sections reveal reactive astrocytosis in different brain regions including dorsal striatum (Figure AI.5B). In addition, co-immunofluorescence for Iba1 and CD68 revealed the presence of reactive microgliosis (Figure AI.5C). Due to the presence of neuroinflammation and α-syn accumulation in white matter in Atg7(CNP) cKO brains, we concluded that the conditional loss of MA captures many of the neuropathological hallmarks of MSA.

We next determined if neurodegeneration was present in the Atg7(CNP) cKO brains. First, we directly examined axonal health via electron microscopy. At 16 months of age, we found many signs of axonopathy and neurodegeneration in the corpus callosum of Atg7(CNP) cKO brains, including axonal spheroids, axons with electron dense cytoplasm, and myelin sheaths without axons within them (Figure AI.5D). In addition, Nissl staining revealed a disruption of the Purkinje cell layer in the cerebellum of 16 month Atg7(CNP) cKO mice suggestive of Purkinje cell degeneration (Figure AI.5E), consistent with the behavioral changes, and importantly, human pathology (Kume et al., 1991). Taken together, we conclude that the loss of MA in OLs can induce neurodegeneration.

I.4. Discussion

In this study we used mouse genetics to establish that the conditional loss of MA in OLs can be used to model MSA. We found that Atg7(CNP) cKO mice can recapitulate key hallmarks

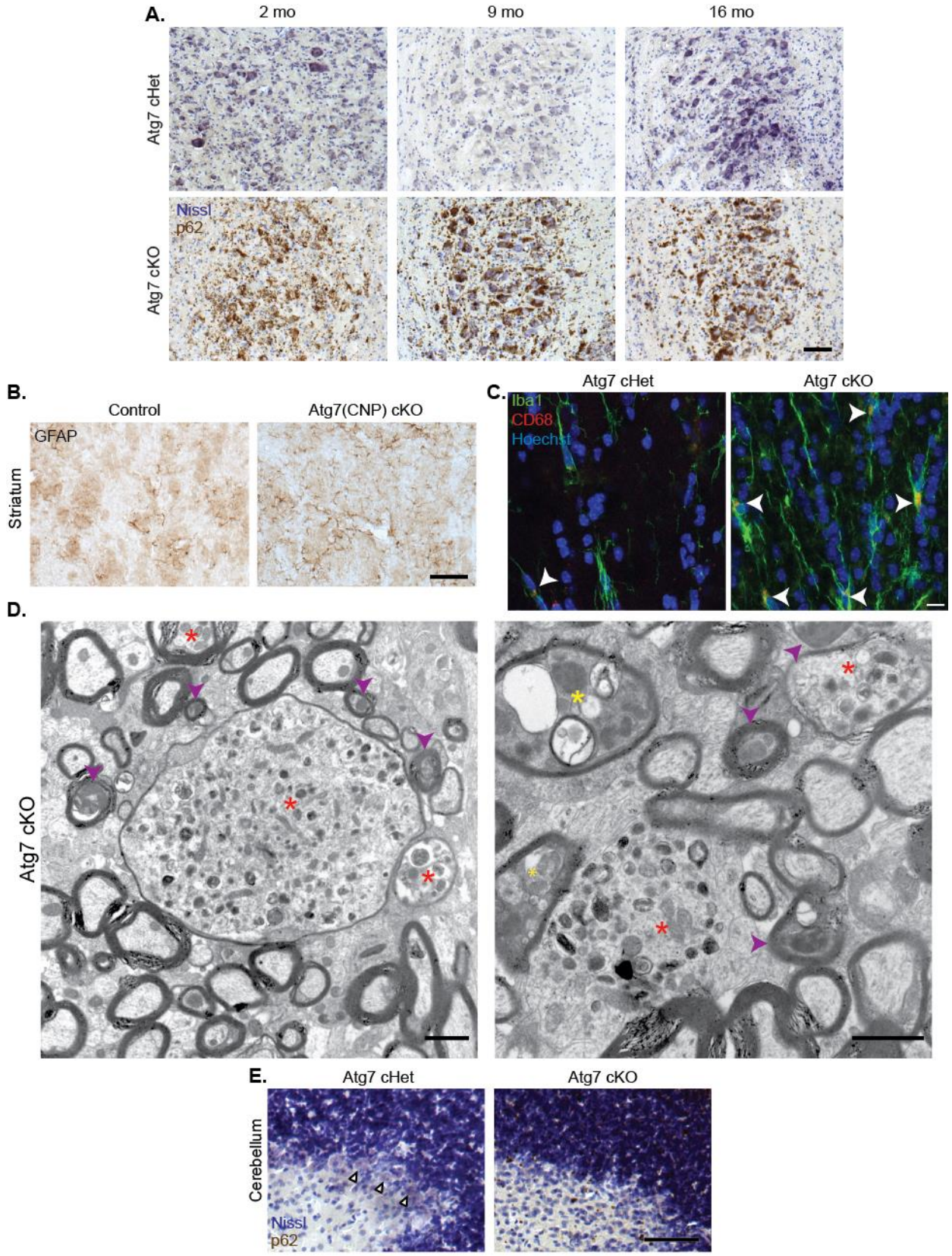
A.
2 mo
9 mo
16 mo
Atg7 cHet
Atg7 cKO
Nissl
p62
B.
Control
Atg7(CNP) cKO
GFAP
Striatum
C.
Atg7 cHet
Atg7 cKO
Iba1
CD68
Hoechst
D.
Atg7 cKO
E.
Atg7 cHet
Atg7 cKO
Cerebellum
Nissl
p62

Figure I-5. Atg7(CNP) cKO mice demonstrate signs of neuroinflammation and neurodegeneration.
A. Immunostaining for p62 (brown) in the pons of 2, 9, and 16 mo Atg7(CNP) cHet and cKO mice. There is dramatic accumulation of p62 in this area, particularly at older ages. Nissl (blue) identifies nuclei. n = 1 / genotype. Scale = 25 μm.
B. GFAP staining is used to identify astrocyte morphology. There is a marked increase in the number of reactive astrocytes in Atg7(CNP) cKO mice at 16 months of age. n = 3 / genotype. Scale = 50 μm.
C. Iba1 staining is used to identify microglial morphology, and CD68 stainign is used to identify activated microglia. There is a remarkable increase in number of reactive microglia in the corpus callosum of 16 mo Atg7(CNP) cKO mice. n = 3 / genotype. Scale = 10 μm.
D. Electron micrographs of Atg7(CNP) cKO corpus callosum. We identified a number of structures suggestive of degenerating axons, including axonal spheroids (red asterisk), vacuolated axons (yellow asterisk), and axons with electron dense cytoplasm (purple arrowheads). n = 3 / genotype. Scale = 1 μm.
E. Nissl staining of 16 mo Atg7(CNP) Het and cKO cerebella to examine the Purkinje cells. Note that the purkinje cell nuclei (round, faint purple nuclei identified by white arrows in the cHet) are missing in the purkinje cell layer of Atg7(CNP) cKO cerebellum. n = 1 / genotype. Scale = 25 μm.

of the disease including motor dysfunction, autonomic dysfunction, and neurodegeneration. Although still preliminary, strikingly, we also uncovered the accumulation of endogenous α-syn in white matter tracks, indicative of α-syn GCIs. These experiments verify that MSA may be caused by a disruption of protein homeostasis within OLs.

These experiments, however, do not resolve two key outstanding questions regarding MSA: From where does the accumulated α-syn in OLs originate, and is α-syn accumulation the causative factor in MSA or a passive indicator of a disruption in protein homeostasis in these highly specialized cells? These questions could not be answered using the previous α-syn-driven transgenic models of MSA (Kahle et al., 2002; Shults et al., 2005; Yazawa et al., 2005), given that the design of the model relies on heterologous overexpression of α-syn. The model we present here however, may finally provide insight into these long sought-after answers in the field.

To determine whether α-syn is exerting a toxicity that is beyond its ability to interfere with MA, one can cross Atg7(CNP) cKO mice with the *Synuclein alpha* (*Snca*) knockout mice (Snca KO) to generate mice lacking Atg7 in OLs and lacking α-syn globally (Atg7(CNP) cKO::Snca KO). As the loss of *Snca* alone demonstrates no remarkable phenotype, the constitutive loss of *Snca* in these mice should not confound any of the readouts used in this study (Abeliovich et al., 2000). Should the loss of α-syn expression have no impact on the Atg7(CNP) cKO phenotype, we

must conclude that in these mice, the accumulation of α-syn has little to no further consequence than the loss of MA alone. The GCIs *per se* may not be pathogenic. Thus, one might conclude that the etiology of MSA relies on disruption of MA-dependent degradation events. However, if there is a significant change in the phenotype of the Atg7(CNP) cKO::Snca KO mice, this would indicate an important contribution of endogenous α-syn in the MSA-like symptomatology of these mice, and thus approaches to alter α-syn levels might be a valid therapeutic approach for this disease.

One of the most fundamental questions in the field of MSA is the origin of the α-syn found in GCIs. The inability to establish whether significant α-syn levels are present in mature OLs for the adult brain has led to a broad range of possibilities. Given the relatively high level of α-syn expression in neurons, studies have suggested that the origin of the α-syn is the neuron, and that α-syn, via cell-to-cell transmission, becomes trapped in OLs leading to this aberrant neuropathological event. Upon the disruption of MA in OLs, we have found that endogenous α-syn accumulates in what appears to be OLs, although further experiments are pending. This observation provides an *in vivo* model to answer this question. To test the hypothesis that the syn we observe originates in the OL, we can create a double conditional KO mouse (d-cKO) for which both *Atg7* and *Snca* are conditionally deleted using CNP^{Cre}. If the deletion of the *Snca* gene specifically in OLs is sufficient to eliminate the presence of α-syn in GCIs, this would be a strong indicator that the Snca observed is not neuronal in origin. Studies monitoring behavior and autonomic function as described above could then ascertain whether the loss of *Snca* in OLs has any impact on phenotype.

By eliminating MA in OLs, we have found a progressive neurodegenerative phenotype with premature lethality that leads to an MSA-like phenotype. Specifically, Atg7(CNP) cKO mice demonstrated many key characteristics of MSA including motor and autonomic dysfunction along

with neuroinflammation and neurodegeneration. Although preliminary, the accumulation of endogenous α-syn perinuclearly in white matter tracts in Atg7(CNP) cKO was suggestive that GCIs were present. These experiments confirm that MSA may be caused by a disruption of protein homeostasis within OLs. Moreover, Atg7(CNP) cKO mice may be a viable model for MSA that can be used to enhance our understanding of the pathology in MSA and open new avenues for drug discovery.

I.5. References

Abeliovich, A., Schmitz, Y., Fariñas, I., Choi-Lundberg, D., Ho, W.-H., Castillo, P.E., Shinsky, N., Verdugo, J.M.G., Armanini, M., Ryan, A., *et al.* (2000). Mice Lacking α-Synuclein Display Functional Deficits in the Nigrostriatal Dopamine System. Neuron *25*, 239-252.

Asi, Y.T., Simpson, J.E., Heath, P.R., Wharton, S.B., Lees, A.J., Revesz, T., Houlden, H., and Holton, J.L. (2014). Alpha-synuclein mRNA expression in oligodendrocytes in MSA. Glia *62*, 964-970.

DiFiglia, M., Sena-Esteves, M., Chase, K., Sapp, E., Pfister, E., Sass, M., Yoder, J., Reeves, P., Pandey, R.K., Rajeev, K.G., *et al.* (2007). Therapeutic silencing of mutant huntingtin with siRNA attenuates striatal and cortical neuropathology and behavioral deficits. Proceedings of the National Academy of Sciences of the United States of America *104*, 17204-17209.

Djelloul, M., Holmqvist, S., Boza-Serrano, A., Azevedo, C., Yeung, M.S., Goldwurm, S., Frisen, J., Deierborg, T., and Roybon, L. (2015). Alpha-Synuclein Expression in the Oligodendrocyte Lineage: an In Vitro and In Vivo Study Using Rodent and Human Models. Stem Cell Reports *5*, 174-184.

Friedman, L.G., Lachenmayer, M.L., Wang, J., He, L., Poulose, S.M., Komatsu, M., Holstein, G.R., and Yue, Z. (2012). Disrupted autophagy leads to dopaminergic axon and dendrite degeneration and promotes presynaptic accumulation of alpha-synuclein and LRRK2 in the brain. J Neurosci *32*, 7585-7593.

Geng, J., and Klionsky, D.J. (2008). The Atg8 and Atg12 ubiquitin-like conjugation systems in macroautophagy. 'Protein modifications: beyond the usual suspects' review series. EMBO reports *9*, 859-864.

Hagemeyer, N., Goebbels, S., Papiol, S., Kastner, A., Hofer, S., Begemann, M., Gerwig, U.C., Boretius, S., Wieser, G.L., Ronnenberg, A., *et al.* (2012). A myelin gene causative of a catatonia-depression syndrome upon aging. EMBO Mol Med *4*, 528-539.

Hara, T., Nakamura, K., Matsui, M., Yamamoto, A., Nakahara, Y., Suzuki-Migishima, R., Yokoyama, M., Mishima, K., Saito, I., Okano, H., *et al.* (2006). Suppression of basal autophagy in neural cells causes neurodegenerative disease in mice. Nature *441*, 885-889.

Kahle, P.J., Neumann, M., Ozmen, L., Muller, V., Jacobsen, H., Spooren, W., Fuss, B., Mallon, B., Macklin, W.B., Fujiwara, H., *et al.* (2002). Hyperphosphorylation and insolubility of alpha-synuclein in transgenic mouse oligodendrocytes. EMBO reports *3*, 583-588.

Kim, M., Sandford, E., Gatica, D., Qiu, Y., Liu, X., Zheng, Y., Schulman, B.A., Xu, J., Semple, I., Ro, S.H., *et al.* (2016). Mutation in ATG5 reduces autophagy and leads to ataxia with developmental delay. eLife *5*.

Komatsu, M., Waguri, S., Chiba, T., Murata, S., Iwata, J.-i., Tanida, I., Ueno, T., Koike, M., Uchiyama, Y., and Kominami, E. (2006). Loss of autophagy in the central nervous system causes neurodegeneration in mice. Nature *441*, 880-884.

Komatsu, M., Waguri, S., Ueno, T., Iwata, J., Murata, S., Tanida, I., Ezaki, J., Mizushima, N., Ohsumi, Y., Uchiyama, Y., *et al.* (2005). Impairment of starvation-induced and constitutive autophagy in Atg7-deficient mice. The Journal of cell biology *169*, 425-434.

Kume, A., Takahashi, A., Hashizume, Y., and Asai, J. (1991). A histometrical and comparative study on Purkinje cell loss and olivary nucleus cell loss in multiple system atrophy. Journal of the neurological sciences *101*, 178-186.

Lalonde, R., and Strazielle, C. (2011). Brain regions and genes affecting limb-clasping responses. Brain research reviews *67*, 252-259.

Miller, D.W., Johnson, J.M., Solano, S.M., Hollingsworth, Z.R., Standaert, D.G., and Young, A.B. (2005). Absence of alpha-synuclein mRNA expression in normal and multiple system atrophy oligodendroglia. J Neural Transm (Vienna) *112*, 1613-1624.

Odagiri, S., Tanji, K., Mori, F., Kakita, A., Takahashi, H., and Wakabayashi, K. (2012). Autophagic adapter protein NBR1 is localized in Lewy bodies and glial cytoplasmic inclusions and is involved in aggregate formation in alpha-synucleinopathy. Acta neuropathologica *124*, 173-186.

Papapetropoulos, S., Tuchman, A., Laufer, D., Papatsoris, A.G., Papapetropoulos, N., and Mash, D.C. (2007). Causes of death in multiple system atrophy. Journal of Neurology, Neurosurgery, and Psychiatry *78*, 327-329.

Reyes, J.F., Rey, N.L., Bousset, L., Melki, R., Brundin, P., and Angot, E. (2014). Alpha-synuclein transfers from neurons to oligodendrocytes. Glia *62*, 387-398.

Schwarz, L., Goldbaum, O., Bergmann, M., Probst-Cousin, S., and Richter-Landsberg, C. (2012). Involvement of macroautophagy in multiple system atrophy and protein aggregate formation in oligodendrocytes. J Mol Neurosci *47*, 256-266.

Shults, C.W., Rockenstein, E., Crews, L., Adame, A., Mante, M., Larrea, G., Hashimoto, M., Song, D., Iwatsubo, T., Tsuboi, K., *et al.* (2005). Neurological and neurodegenerative alterations in a transgenic mouse model expressing human alpha-synuclein under oligodendrocyte promoter: implications for multiple system atrophy. J Neurosci *25*, 10689-10699.

Spencer, B., Potkar, R., Trejo, M., Rockenstein, E., Patrick, C., Gindi, R., Adame, A., Wyss-Coray, T., and Masliah, E. (2009). BECLIN 1 GENE TRANSFER ACTIVATES AUTOPHAGY AND AMELIORATES THE NEURODEGENERATIVE PATHOLOGY IN α-SYNUCLEIN MODELS OF PARKINSON'S AND LEWY BODY DISEASE. The Journal of neuroscience : the official journal of the Society for Neuroscience *29*, 13578-13588.

Spillantini, M.G., Crowther, R.A., Jakes, R., Cairns, N.J., Lantos, P.L., and Goedert, M. (1998). Filamentous alpha-synuclein inclusions link multiple system atrophy with Parkinson's disease and dementia with Lewy bodies. Neuroscience letters *251*, 205-208.

Stefanova, N., and Wenning, G.K. (2015). Animal models of multiple system atrophy. Clinical autonomic research : official journal of the Clinical Autonomic Research Society *25*, 9-17.

Tanik, S.A., Schultheiss, C.E., Volpicelli-Daley, L.A., Brunden, K.R., and Lee, V.M. (2013). Lewy body-like alpha-synuclein aggregates resist degradation and impair macroautophagy. J Biol Chem *288*, 15194-15210.

Tanji, K., Odagiri, S., Maruyama, A., Mori, F., Kakita, A., Takahashi, H., and Wakabayashi, K. (2013). Alteration of autophagosomal proteins in the brain of multiple system atrophy. Neurobiology of disease *49*, 190-198.

Ubhi, K., Low, P., and Masliah, E. (2011). Multiple system atrophy: a clinical and neuropathological perspective. Trends Neurosci *34*, 581-590.

Webb, J.L., Ravikumar, B., Atkins, J., Skepper, J.N., and Rubinsztein, D.C. (2003). α-Synuclein Is Degraded by Both Autophagy and the Proteasome. Journal of Biological Chemistry *278,* 25009-25013.

Winslow, A.R., Chen, C.W., Corrochano, S., Acevedo-Arozena, A., Gordon, D.E., Peden, A.A., Lichtenberg, M., Menzies, F.M., Ravikumar, B., Imarisio, S., *et al.* (2010). alpha-Synuclein impairs macroautophagy: implications for Parkinson's disease. The Journal of cell biology *190,* 1023-1037.

Yazawa, I., Giasson, B.I., Sasaki, R., Zhang, B., Joyce, S., Uryu, K., Trojanowski, J.Q., and Lee, V.M. (2005). Mouse model of multiple system atrophy alpha-synuclein expression in oligodendrocytes causes glial and neuronal degeneration. Neuron *45,* 847-859.

Yu, W.H., Dorado, B., Figueroa, H.Y., Wang, L., Planel, E., Cookson, M.R., Clark, L.N., and Duff, K.E. (2009). Metabolic Activity Determines Efficacy of Macroautophagic Clearance of Pathological Oligomeric α-Synuclein. The American journal of pathology *175,* 736-747.

APPENDIX II.

Multiple Sclerosis and Oligodendroglial Macroautophagy

II.1 Introduction

Multiple sclerosis (MS) is a chronic, immune-mediated inflammatory disease of the CNS (Dendrou et al., 2015; Nylander and Hafler, 2012). The majority of MS patients experience cycles of relapsing and remitting CNS symptoms such as visual disturbances and motor impairments. Most MS cases eventually result in progressive and irreversible neurological dysfunction and failure.

Although the exact cause of MS is unknown, it is widely believed that MS begins with an inflammatory immune-mediated event, in which autoreactive lymphocytes mistake myelin or an associated protein such as myelin oligodendrocyte glycoprotein (MOG) for a pathological antigen (Dendrou et al., 2015; Nylander and Hafler, 2012). As T cells do not enter the CNS unless there is breakdown of the blood brain barrier, usually secondary to neuroinflammation, why T cells are reacting to a CNS antigen is not well understood.

Antigens reach T cells through the major histocompatibility complex (MHC). MHC class I is expressed by all nucleated cells and presents antigens from proteins that were degraded intracellularly. MHC class II, on the other hand, is only expressed by antigen presenting cells (APCs) and presents antigens taken up from the extracellular milieu. The resident APCs of the CNS are microglia (Koning et al., 2013). Interestingly, studies have suggested that macroautophagy (MA) may be important for antigen presentation through both MHC class I and MHC class II (English et al., 2009; Keller and Lunemann, 2017; Li et al., 2010; Munz, 2016;

Strawbridge and Blum, 2007). Oligodendroglial MA may be involved in presentation of myelin autoantigen through MHC Class I, considering that we have demonstrated that myelin degradation is MA-dependent. Alternatively, it is known that microglia phagocytose extracellular whorls of myelin (Safaiyan et al., 2016). As MA is known to be involved in exocytosis, OLs have myelin proteins in their exosomes, and our EM data suggests OLs may exocytose myelin, it is possible that formation of these extracellular myelin whorls is contingent upon MA in OLs (Baixauli et al., 2014; Krämer-Albers et al., 2007). If this is the case, MHC class II presentation of myelin antigens by microglia may depend upon oligodendroglial MA. We therefore asked whether the loss of MA in OLs prevents antigen presentation and the immune response in a mouse model of MS.

II.2 Results

To examine autoimmune evoked demyelination, we performed a pilot study using the experimental autoimmune encephalomyelitis (EAE) model of MS in Atg7(CNP) Het and cKO mice in collaboration with Julian Smith and Dritan Agalliu, who are experts in this technique (Stromnes and Goverman, 2006). Briefly, approximately 8-week-old mice were injected with a 20 amino acid peptide fragment of MOG (MOG_{35-55}), complete Freunds' adjuvant (CFA) and pertussis toxin (PTX). Mice were then scored on a scale from 0 to 5 as described previously (Lengfeld et al., 2017; Stromnes and Goverman, 2006). Interestingly, our preliminary study suggested that loss of MA delayed the onset of clinical phenotype in Atg7(CNP) cKO mice (Figure II-1A). Moreover, the clinical score of Atg7(CNP) cKO mice peaked at a lower score than that of Atg7(CNP) cHet mice (Figure AII.1A). To determine whether the reduced response to EAE was caused by a diminished immune response, we probed sections of REGION spinal cord for infiltration of $CD4^+$ T cells. As there appeared to be fewer $CD4^+$ T cells in spinal cords from

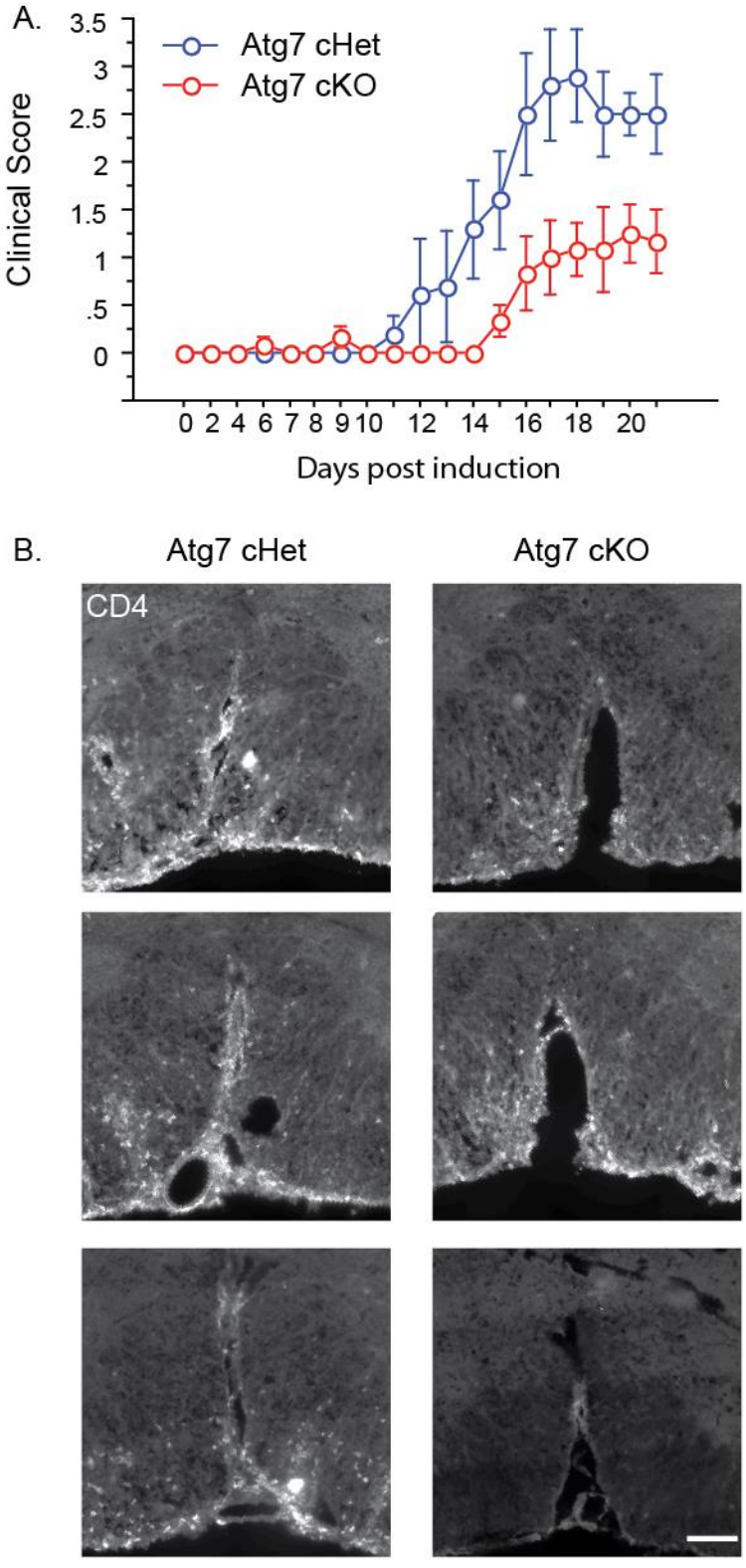

Figure AII.1. Loss of MA in OLs diminishes the clinical and immune response to EAE.
A. 8-week-old mice were assigned a clinical score every other day for one week after induction of EAE and then scored daily thereafter. Atg7(CNP) cKO mice demonstrate a delayed and diminished response. n = 5-6 mice/genotype.
B. CD4 staining of REGION spinal cord of mice sacrificed 21 days after EAE induction. There is less CD4 cell infiltration in Atg7(CNP) cKO mice. Examples from three mice of each genotype are shown.

Atg7(CNP) cKO mice, we believe that the loss of MA in OLs reduced T cell infiltration and the immune response in EAE (Figure AII.1B).

II.3 Discussion

Our preliminary results suggested that the loss of MA in OLs reduces the clinical severity of EAE due to a diminished inflammatory response. We first need to replicate these results and confirm our findings statistically. Why would the loss of MA in OLs diminish the immune response to MOG_{35-55}? Several possibilities come to my mind. First, as mentioned above,

MA in OLs may be necessary for MHC class I presentation of myelin autoantigen. However, as MHC class I regulates the response of $CD8^+$ cytotoxic T cells and the EAE model induces a response in $CD4^+$ T cells, this is likely not mediating the observed effect (Denic et al., 2013; Janeway et al., 2001). Alternatively, perhaps MA-dependent exocytosis of myelin is necessary for microglial phagocytosis of myelin and subsequent MHC class II-dependent autoantigen presentation inducing a $CD4^+$ T cell response. Further experiments are required to determine the validity and molecular mechanism of this possibility. Based on our results that MA in OLs is required for myelin remodeling, our preliminary data may suggest that loss of myelin remodeling alters the structure or composition of myelin in such a way to prevent autoantigenicity of the myelin sheath. This is quite unlikely, however, because (1) the myelin sheath appears grossly normal by EM at 8 weeks of age, and (2) it is doubtful that loss of myelin remodeling would so drastically alter the myelin sheath so shortly after developmental myelination is complete, especially given the long half-lives of the components of the myelin sheath (Fischer and Morell, 1974; Savas et al., 2012; Smith, 1968; Toyama et al., 2013). Lastly, there may have been a diminished CD4 response in Atg7(CNP) cKO mice due to loss of MA in T cells. CNP is known to be expressed in the thymus, so T-cells may be MA-deficient in Atg7(CNP) cKO mice (Chandross et al., 1999). The loss of MA in T cells would be a significant confound to this experiment, especially considering that MA may be necessary for T cell homeostasis and survival (Puleston and Simon, 2014). This confound can be addressed by repeating this experiment using a different Cre line that mediates recombination in OLs but not the thymus or through T cell transfer experiments (Traka et al., 2016).

II.4 Conclusion

In sum, we presented preliminary, yet intriguing, results suggesting that loss of MA in OLs may be protective in a murine model of multiple sclerosis. Many follow-up experiments are required, however, to better understand this phenomenon.

II.5 References

Baixauli, F., López-Otín, C., and Mittelbrunn, M. (2014). Exosomes and Autophagy: Coordinated Mechanisms for the Maintenance of Cellular Fitness. Frontiers in Immunology *5*.

Chandross, K.J., Cohen, R.I., Paras, P., Gravel, M., Braun, P.E., and Hudson, L.D. (1999). Identification and Characterization of Early Glial Progenitors Using a Transgenic Selection Strategy. The Journal of Neuroscience *19*, 759-774.

Dendrou, C.A., Fugger, L., and Friese, M.A. (2015). Immunopathology of multiple sclerosis. Nature reviews Immunology *15*, 545-558.

Denic, A., Wootla, B., and Rodriguez, M. (2013). CD8+ T cells in multiple sclerosis. Expert Opinion on Therapeutic Targets *17*, 1053-1066.

English, L., Chemali, M., Duron, J., Rondeau, C., Laplante, A., Gingras, D., Alexander, D., Leib, D., Norbury, C., Lippe, R., *et al.* (2009). Autophagy enhances the presentation of endogenous viral antigens on MHC class I molecules during HSV-1 infection. Nature immunology *10*, 480-487.

Fischer, C.A., and Morell, P. (1974). Turnover of proteins in myelin and myelin-like material of mouse brain. Brain research *74*, 51-65.

Janeway, C., Travers, P., Walport, M., and Shlomchik, M. (2001). Antigen recognition by T cells. In Immunobiology: The Immune System in Health and Disease (New York: Garland Science).

Keller, C.W., and Lunemann, J.D. (2017). Autophagy and Autophagy-Related Proteins in CNS Autoimmunity. Frontiers in Immunology *8*, 165.

Koning, N., Ilarregui, J.M., García-Vallejo, J.J., and van Kooyk, Y. (2013). Antigen-Presenting Cells in the Central Nervous System. In Multiple Sclerosis Immunology: A Foundation for Current and Future Treatments, T. Yamamura, and B. Gran, eds. (New York, NY: Springer New York), pp. 71-94.

Krämer-Albers, E.-M., Bretz, N., Tenzer, S., Winterstein, C., Möbius, W., Berger, H., Nave, K.-A., Schild, H., and Trotter, J. (2007). Oligodendrocytes secrete exosomes containing major myelin and stress-protective proteins: Trophic support for axons? PROTEOMICS – Clinical Applications *1*, 1446-1461.

Lengfeld, J.E., Lutz, S.E., Smith, J.R., Diaconu, C., Scott, C., Kofman, S.B., Choi, C., Walsh, C.M., Raine, C.S., Agalliu, I., *et al.* (2017). Endothelial Wnt/beta-catenin signaling reduces immune cell infiltration in multiple sclerosis. Proceedings of the National Academy of Sciences of the United States of America *114*, E1168-e1177.

Li, B., Lei, Z., Lichty, B.D., Li, D., Zhang, G.M., Feng, Z.H., Wan, Y., and Huang, B. (2010). Autophagy facilitates major histocompatibility complex class I expression induced by IFN-gamma in B16 melanoma cells. Cancer immunology, immunotherapy : CII *59*, 313-321.

Munz, C. (2016). Autophagy proteins in antigen processing for presentation on MHC molecules. Immunological reviews *272*, 17-27.

Nylander, A., and Hafler, D.A. (2012). Multiple sclerosis. The Journal of clinical investigation *122*, 1180-1188.

Puleston, D.J., and Simon, A.K. (2014). Autophagy in the immune system. Immunology *141*, 1-8.

Safaiyan, S., Kannaiyan, N., Snaidero, N., Brioschi, S., Biber, K., Yona, S., Edinger, A.L., Jung, S., Rossner, M.J., and Simons, M. (2016). Age-related myelin degradation burdens the clearance function of microglia during aging. Nature neuroscience *19*, 995-998.

Savas, J.N., Toyama, B.H., Xu, T., Yates, J.R., and Hetzer, M.W. (2012). Extremely Long-Lived Nuclear Pore Proteins in the Rat Brain. Science (New York, NY) *335*, 942.

Smith, M.E. (1968). The turnover of myelin in the adult rat. Biochimica et Biophysica Acta (BBA) - Lipids and Lipid Metabolism *164*, 285-293.

Strawbridge, A.B., and Blum, J.S. (2007). Autophagy in MHC class II antigen processing. Current opinion in immunology *19*, 87-92.

Stromnes, I.M., and Goverman, J.M. (2006). Active induction of experimental allergic encephalomyelitis. Nature protocols *1*, 1810-1819.

Toyama, B.H., Savas, J.N., Park, S.K., Harris, M.S., Ingolia, N.T., Yates, J.R., and Hetzer, M.W. (2013). Identification of long-lived proteins reveals exceptional stability of essential cellular structures. Cell *154*, 971-982.

Traka, M., Podojil, J.R., McCarthy, D.P., Miller, S.D., and Popko, B. (2016). Oligodendrocyte death results in immune-mediated CNS demyelination. Nature neuroscience *19*, 65-74.